OXIDATION OF DEOXYAMINOSUGARS BY A NEW FLAVIN-DEPENDENT MONOOXYGENASE

By

Ahmad H. Al-Mestarihi

Dissertation

Submitted to the Faculty of the

Graduate School of Vanderbilt University

in partial fulfillment of the requirements

for the degree of

DOCTOR OF PHILOSOPHY

in

Chemistry

December, 2012

Nashville, Tennessee

Approved by:

Professor Brian O. Bachmann

Professor Tina M. Iverson

Professor Michael P. Stone

Professor Richard N. Armstrong

To my late parents Se'da and Hasan

I can't be thankful enough for all the love and support you have given me

TABLE OF CONTENTS

PAGE

ACKNOWLEDGMENTS

This work wouldn't have been possible without the guidance of my advisor and research committee, help from my lab colleagues and staff at Vanderbilt University, and support from my family and friends.

I would like to express my deepest gratitude to my advisor, Prof. Brian Bachmann, for his outstanding guidance, support, and patience, providing me with an excellent atmosphere for conducting research. Prof. Bachmann's support and encouragement exceeded my expectation even with matters outside of research. I would also like to acknowledge the rest of my research committee members, Prof. Tina Iverson, Prof. Michael Stone, and Prof. Richard Armstrong for their excellent support and guidance toward the completion of my PhD at Vanderbilt University.

I have been fortunate to work with several collaborators throughout my research projects, which enriched my experience and knowledge. I would like to thank Prof. Tina Iverson (Vanderbilt University, Nashville, TN) for her willingness to collaborate with our lab on solving the X-ray crystal structure of the nitrososynthase ORF36. Particularly, I would like to thank Prof. Jessica Vey from Prof. Iverson's research group for conducting the crystallography experiments which resulted in a valuable publication. I would also like to thank the research labs of Prof. Michael Burkart (University of California, San Diego, La Jolla, CA) and Prof. Hung-wen Liu (The University of Texas, Austin, TX) for generously providing EvaA-E and RfbB expression constructs, respectively. Many thanks to Prof. Daniel Kahne's research group (Harvard University,

Boston, MA) for supplying the essential synthetic substrate for the nitrososynthase, TDP-L-*epi*-vancosamine, which facilitated our initial biochemical characterization of RubN8 and ORF36.

I would also like to thank all past and present members of the Bachmann lab who I got to know over the last several years. It has been very enjoyable working with all of you and many thanks for your help, support and friendship. Especially I would like to acknowledge a former member of the lab, Dr. Yunfeng Hu, who prepared the ORF36 protein and participated in the initial biochemical characterization of the enzyme.

I am grateful for the funding we received for the research work described in this dissertation from the Office of Naval Research. Their continuous support over the course of several years made the completion of this work possible. The graduate school at Vanderbilt University also provided me with financial support in the form of teaching assistantships and for that I am also grateful.

To all my friends at Vanderbilt University, thank you very much for your friendship and support. You made my life at Vanderbilt a truly memorable experience and your friendships are invaluable to me. To my best friend Prof. Harold Moser, who became like a father to me, following my progress closely providing support and encouragements, I am truly grateful.

Finally, I am very grateful to my big extended family in Jordan, brothers, sisters, nephews and nieces, thank you for your love and support. To my beloved late parents,

who have raised me to be the person I am today, thank you for all the unconditional love, guidance, and support that you have always given me.

LIST OF TABLES

LIST OF FIGURES

LIST OF SCHEMES

LIST OF ABBREVIATIONS

ACP	acyl carrier protein
AMC	rubransarol, 3-amino-4-hydroxy-7-methoxycoumarin
APS	advanced photon source
BVMOs	Baeyer-Villiger monooxygenases
CCK-B	cholecystokinin B
CHF	congestive heart failure
CoA	Coenzyme A
DBT	dibenzothiophene
DHDP	3,4-dihydroxydipicolinate
DMSO	dimethylsulfoxide
DNA	Deoxyribonucleic acid
dTDP	deoxythymidine diphosphate
DTT	dithiothreitol
e.e	enantiomeric excess
EDTA	ethylenediaminetetraacetic acid
ESI	electrospray ionization
FAD	flavin adenine dinucleotide
FMN	flavin mononucleotide
FMOs	flavin-containing monooxygenases
FNOs	microbial N-hydroxylating monooxygenases
FPLC	fast protein liquid chromatography
GirT	Girard's T reagent [(Carboxymethyl)trimethylammonium hydrazine]

GT	glycosyltransferase
HIV	human immunodeficiency virus
HPLC	high performance liquid chromatography
IC_{50}	half maximal inhibitory concentration
IPTG	β–D-1-thiogalactopyranoside
kD	kilo Dalton
KS	ketosynthase
kV	kilovolt
LB	luria broth
LC	liquid chromatography
LC-CAT	life Sciences collaborative access team
MAT	malonyl-CoA:ACP acyltransferase
Mg	milligram
MHz	megahertz
µL	microliter
µM	micromolar
mL	milliliter
mm	millimeter
mM	millimolar
MOE	molecular operating environment
MS	mass spectrometry
MWCO	molecular weight cut-off
NADP	nicotinamide adenine dinucleotide phosphate
NCS	non-crystallographic symmetry

NDP	nucleotide diphosphate
Nm	nanometer
NMR	nuclear magnetic resonance
OD	optical density
PCR	polymerase chain reaction
PDB	protein data bank
PKS	polyketide synthase
PLP	pyridoxal phosphate
PMP	pyridoxamine phosphate
PPi	pyrophosphate
Ppm	parts per million
Psi	pounds per square inch
RNA	ribonucleic acid
ROS	reactive oxygen species
Rpm	rotations per minute
SAM	S-Adenosyl methionine
SAX	strong anion exchange
SDS-PAGE	sodium dodecylsulfide polyacrylamide gel electrophoresis
TCEP	tris(2-carboxyethyl)phosphine
TDP	thymidine diphosphate
TMP	thymidine monophosphate
Tris	tris(hydroxymethyl)aminomethane
UV	ultra violet
V	volt

LIST OF PUBLICATIONS

1. Vey, J.L., Al-Mestarihi, A., Funk, M.A., Bachmann, B.O., and Iverson, T.M. (**2010**) Structure and mechanism of ORF36, an Amino Sugar Oxidizing Enzyme in Everninomicin Biosynthesis. *Biochemistry*, 49(43): 9306-9317.

2. Yunfeng Hu, Ahmad Al-Mestarihi, Catherine L. Grimes, Daniel Kahne and Brian O. Bachmann, A unifying nitrososynthase involved in nitrosugar biosynthesis*, Journal of the American Chemical Society,* 130, 15756-15757 (**2008**)

3. Alexander N.; Bortolus M.; Al-Mestarihi A.; McHaourab H.; Meiler J. (**2008**) De novo high-resolution protein structure determination from sparse spin-labeling EPR data*. Structure* 16, 181–195.

4. Prusakiewicz, JJ, Turman, MV, Vila, A, Ball, HL, Al-Mestarihi, AH, Di Marzo, V, Marnett, LJ Oxidative metabolism of lipoamino acids and vanilloids by lipoxygenases and cyclooxygenases. *Archives of Biochemistry and Biophysi,* 464(2), 260-8, **2007**.

CHAPTER I

INTRODUCTION

Many organisms, such as bacteria, plants and fungi are capable of synthesizing structurally diverse bioactive natural products. The diversity of structure and bioactivity of many of these compounds led to their use in pharmaceutical and agricultural applications.[1] Bacterial natural products often contain sugar moieties attached to their core scaffolds and play significant roles in conferring biological activity. Many of these bioactive sugars are derived from deoxyaminosugar oxidations, the most common of which are deoxynitrosugars.[2]

The recent advances in gene cluster elucidations of several natural products containing these N-oxidized sugars have enabled the proposal of biosynthetic pathways of these important moieties and set the stage for biochemical characterization of the enzymes involved in their biosynthesis. The biosynthetic pathways of deoxyaminosugar moieties in several natural products have been well studied; however, enzymes responsible for the amine oxidation in many deoxynitrosugar-containing and related natural products have not been characterized previous to our investigations.

Given the biological importance of deoxysugar attachments, advances in studying new biosynthetic pathways will provide opportunities for *in vivo* pathway engineering leading to the production of new glycoconjugates with varied biological activities. Particularly, the characterization of the biosynthetic gene(s) for the key oxidation of aminosugars, clearly present the opportunity to increase the sugar

structural diversity of a vast array of glycosides via *in vivo* or *in vitro* pathway manipulation.[2-3] Additionally, discovering new biocatalysts able to perform synthetically difficult enantioselective amine oxidations will have significant implications in the development of alternative synthetic methods.

Biosynthesis of N-oxygenated deoxysugars

Significance of deoxysugars in natural products

Deoxysugars are common structural appendages of many bioactive natural products and are commonly found attached to polyketide scaffolds. Several therapeutically important drugs such as the antibiotic vancomycin and the anticancer agent doxorubicin contain sugars attached to their aglycone cores.[4-5] These sugars play important roles in the biological activity by participating in the interaction between the drug and the cellular target. In some cases, sugars participate in the mode of action of many drugs as they contribute to a variety of processes, including active transmembrane transport, stabilization of protein folding and enzyme inhibition.[4-8]

The most prevalent sugars among sugar-containing bacterial secondary metabolites are deoxysugars, often deoxyaminosugars, the biosyntheses of which have been recently reviewed.[3, 9] Structures of some common deoxysugars are shown in figure I-1.

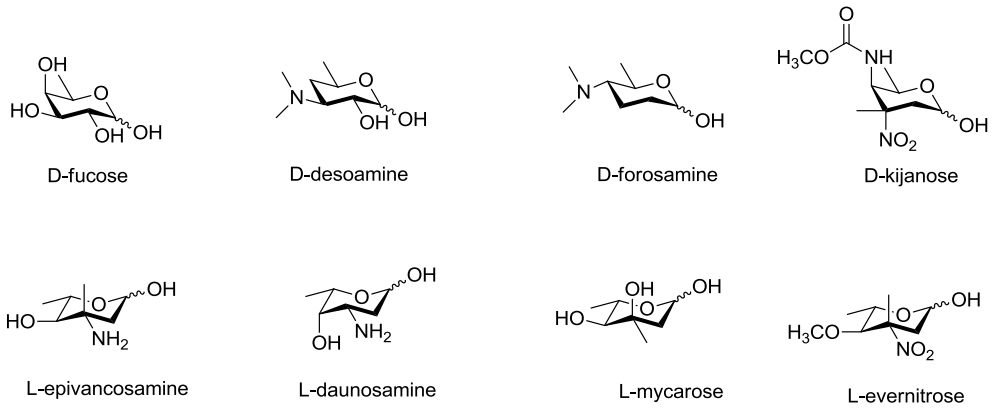

Figure I-1. Examples of some deoxysugars found linked to several natural product scaffolds

Deoxygenation of these sugars proceeds via nucleotide diphosphate (NDP) activation of 6-deoxyhexoses, usually D-glucose. The most common NDP activation is performed by attaching thymidine diphosphate (TDP) at the anomeric carbon of D-glucose-1-phosphate.[3] TDP-activated sugars are the most structurally diverse class of nucleotide sugars found in nature. After NDP-activation, deoxygenation proceeds via a 4-keto-6-deoxy intermediate which is shared among all known deoxysugar pathways.

A less common but very important sugar modification, deoxyaminosugar oxidation to hydroxylamino-, nitroso-, and nitrosugars uniquely extends nature's glycochemical diversity. Natural products containing N-oxidized deoxysugars exhibit a broad range of biological activities including antibacterial, antitumor, antimalarial, anticholesteromic, antiviral, and antidiabetic activities.[2, 10-12] The oxidized congeners of deoxyaminosugars exist in many natural products such as everninomicin, rubradirin and kijanimicin.[13-15] The hydroxylamino-, nitroso-, and nitrosugar variants have been isolated from the fermentation broth of the everninomicin producer *Micromonospora*

carbonecea var. *africana*. It has been shown that the antibacterial activity among these derivatives varied significantly.[16] Modulation of biological activity through enzymatic deoxysugar modification could have significant impact on the development of therapeutically important agents derived from various natural glycoconjugates.

Because of the biological importance of these deoxysugar moieties in various natural products, there has been a growing interest in developing new strategies for altering the deoxysugar appendages of important glycoconjugates either by synthetic or biosynthetic engineering approaches. Biosynthetic engineering strategies require good understanding of the enzymes involved in the deoxysugar modifications and attachment to their corresponding aglycones. The gene clusters of many bioactive compounds containing deoxysugars have been sequenced and deposited into gene data banks, which made functional assignments of the encoded enzymes feasible. This enabled genetic and biochemical characterization of the biosynthetic pathways of several known deoxysugars. Interestingly, studying these pathways showed that several sugar biosynthetic enzymes and glycosyltransferases (GTs), have broad substrate specificity allowing their use both *in vivo* and *in vitro* for altering the sugar moieties in these compounds, a process termed glycodiversification. Several successful glycodiversification studies have been performed on natural product glycoconjugates such as vancomycin and calicheamicin, yielding a new generation of glycorandomized derivatives of altered biological activities.[2, 17-18]

These glycodiversification startegies can be applied for many other natural-product scaffolds utilizing substrate-flexible enzymes to generate libraries of substances for *in vitro* or *in vivo* glycoslation. Enzymes in the deoxysugar pathways can be further manipulated through protein engineering which can result in an expanded pool of glycorandomized derivatives. This new generation of compounds of varied biological activities could lead to the discovery of potentially important drugs to mitigate the daunting threats of human diseases.

Nitrosugar-containing natural products

Deoxynitrosugars are found in many isolated secondary metabolites with diverse scaffolds including spirotetronate antibiotics, ansamycins, and orthosomycins.[13-15] One of the first reported deoxynitrosugar-containing natural products is the orthosomycin antibiotic everninomicin from *Micromonospora carbonacea* var. *africana* which includes a deoxynitrosugar moiety, evernitrose.[15] This nitrosugar is called D-rubranitrose in the polyketide rubradirin isolated from *Streptomyces achromogenes* and is structurally related to D-kijanose from the spirotetronate polyketide antibiotic kijanimycin produced by the Actinomycete *Actinomadura kijaniata*.[14, 19] These compounds possess potent antibacterial activity among other important biological activities. Below is a brief description of these three important nitrosugar-containing natural products with emphasis on the significance of their attached nitrosugar moiety.

Everninomicin

Everninomicin, producd by *Micromonospora carbonacea* var. *africana*, is an oligosaccharide which belongs to the orthosomycin class of antibiotics and possesses potent activity against Gram-positive and Gram-negative bacteria including vancomycin resistant *enterococci*, methicillin resistant *staphylococci*, and penicillin-resistant *streptococci*.[20] The structure of everninomicin is composed of eight deoxysugars including a terminal nitrosugar (L-evernitrose), and acelytated with orsellinic and dichloroisoeverninic acid moieties (Figure I-2).

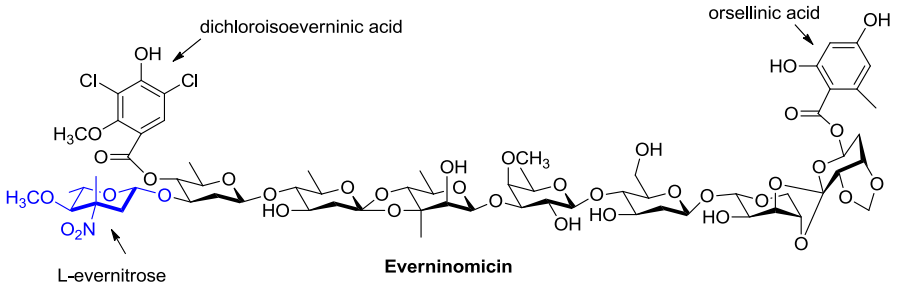

Figure I-2. Chemical structure of everninomicin.

The mechanism of action of everninomicin involves inhibition of protein biosynthesis by binding to the ribosomal protein L16 which affects the function of the 50S ribosomal subunit.[21] Everninomicin was developed through phase III clinical studies when its further development was discontinued in May of 2000 for the stated reason: "the balance between efficacy and safety did not justify further development of the product".[22] However, because of its potent antibacterial activity, researchers have been

interested in its structure diversification to create a number of everninomicin derivatives for structure-activity studies. Only limited chemical derivatization experiments of everninomicin were performed for that purpose, which proved challenging perhaps because of the complexity of the sugar linkages in orthosomycins.[23] This gave rise to the interest of studying the biosynthesis of everninomicin which could potentially lead to the utilization of the natural biocatalysts in its biosynthetic pathway to compliment the chemical synthetic methods in the rational drug design process.

The deoxynitrosugar moiety in everninomicin was shown to be important for the antibacterial activity. For instance, antibacterial activity of the nitrosugar congener against *Staphylococcus aureus* was shown to be 125 fold higher compared to that of the amino-sugar congener.[16] This highlights the significance of studying the enzymes responsible for the N-oxidation of this important deoxysugar moiety. The knowledge that can be gained from understanding this important biochemical transformation could greatly impact current efforts towards everninomicin structure diversification.

Rubradirin

Rubradirin, produced by *Streptomyces achromogenes* var. *rubradiris*, is an ansamycin antibiotic that possesses significant activity against Gram-positive bacteria including multidrug-resistance strains of *Staphylococcus aureus*.[19] The structure of rubradirin is comprised of four distinct moieties; the polyketide scaffold rubransarol, 3-amino-4-hydroxy-7-methoxycoumarin (AMC), the aromatic bridge 3,4-

dihydroxydipicolinate (DHDP), and the nitrosugar D-rubranitrose (2,3,6-trideoxy-3-C-4-O-dimethyl- 3-C-nitro-D-xylo-hexose), (Figure I-3).

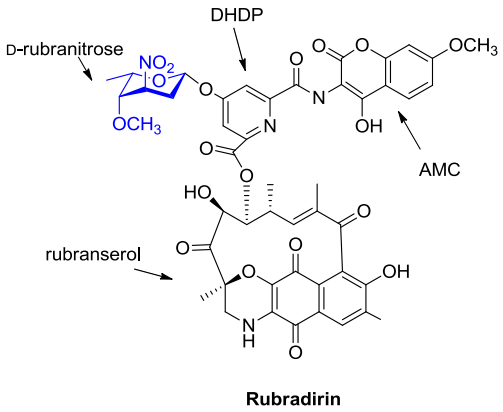

Figure I-3. Chemical structure of rubradirin.

The antibacterial activity of rubradirin involves inhibition of the function of microbial ribosomes by selective prevention of translation chain initiation during protein synthesis. [24] It has also been shown that the aglycone of rubradirin is a potent inhibitor of the human immunodeficiency virus (HIV) reverse transcriptase.[25] The polyketide scaffold rubransarol does not inhibit bacterial RNA polymerase or ribosomal functions on its own, which highlights the importance of the additional structural elements in rubradirin including the deoxynitrosugar moiety.

The gene cluster of rubradirin has been recently sequenced and deposited in the NCBI gene data bank. Functional analysis of this cluster based on sequence homologies, identified the genes responsible for the biosynthesis of the aminosugar precursor of the

nitrosugar D-rubranitrose.[13] The lack of a gene that encodes a C-5 epimerase in the rubradirin gene cluster is consistent with the D-configuration of the nitrosugar moiety. Additionally, a putative oxidase gene, *rubN8*, was also found in the rubradirin gene cluster and proposed to perform N-oxidation of an aminosugar precursor in the biosynthesis of D-rubranitrose.

It is worth noting that only the nitroso congener of rubradrin (protorubradirin) was isolated from the fermentation of the producer *Streptomyces achromogenes* var. *rubradiris* when it was grown in complete darkness. After isolation, protorubradirin readily converted to rubradin upon exposure to ambient light. Based on this observation, it was proposed that the nitroso congener of rubradirin is the true secondary metabolite and that the nitro group is formed through photooxidation.[26]

Kijanimicin

Kijanimicin, produced by *Actinomadura kijaniata*, is a spirotetronate antibiotic and exhibits a broad range of antibacterial activity against Gram-positive bacteria, anaerobes, and the malaria parasite *Plasmodium falciparum*.[14] It has also been shown that derivatives of kijanimicin possess potent activity against human liver and breast cancer cell lines.[27] The structure of kijanimicin includes a pentacyclic polyketide core, linked to four L-digitoxose units and the nitrosugar, 2,3,4,6-tetradeoxy-4-(methylcarbamyl)-3-C-methyl-3-nitro-D-xylo hexopyranose known as D-kijanose (Figure I-4). Kijanimicin derivatives are also known to be produced by other high-GC Gram-

positive bacterial strains (actinomycetes) such as *Streptomyces, Micromonospora*, *Actinomadura*, *Saccharothrix*, and *Verrucosispora*.[14] Most members of this class of compounds exhibit antibacterial and antitumor activities and many possess other biological activities. Examples of these compounds include tetrocarcins and arisostatins, which have been shown to be inducers of apoptosis;[28] chlorothricins, as anticholesterolemic agents;[29] tetronothiodin, a cholecystokinin B (CCK-B) inhibitor;[30] MM46115, an antiviral drug active against parainfluenzae virus 1 and virus 2.[31]

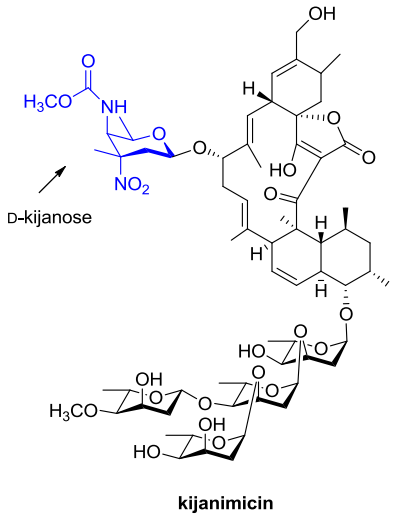

Figure I-4. Chemical structure of kijanimicin.

The deoxysugar moieties that decorate the polyketide core of kijanimicin play an important role in the biological activity of this compound. Although no structure-activity studies yet assed the importance of the D-kijanose sugar, it is likely that this unusually modified deoxynitrosugar is important for biological activity.

Biosynthesis of deoxyaminosugars

Deoxyaminosuagrs are an important class of deoxysugar moieties biosynthesized by a variety of organisms such as plants, fungi and bacteria.[32] Based on gene functional analysis of several natural products possessing N-oxidized deoxysugars, it is largely thought that the precursors of these important moieties are deoxyaminosugars. Therefore, understanding the biosynthetic pathways of these sugar precursors is very helpful in the elucidation of the N-oxidation pathway. Before the introduction of the amine group, the precursor sugar must be in its deoxygenated form. Enzymatic deoxysugar modifications are always carried out on nucleotide activated sugars such as thymidine diphosphate (TDP)-sugars. All known TDP-sugars are derived from glucose-1-phosphate which is converted to TDP-glucose by a thymidilyl transferase and then to TDP-4-keto-6-deoxy-D-glucose by TDP-D-glucose 4,6-dehydratase (Scheme I-1). This provides the entry point for further deoxygenation and other enzymatic modification steps including transamination.[3]

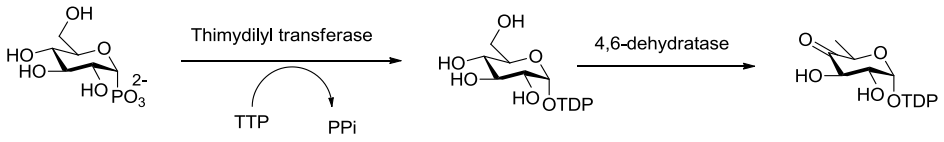

Scheme I-1. Entry point into TDP-deoxysugar secondary metabolism in bacteria.

Deoxyaminosugars are produced from their deoxygenated ketosugar precursors via a transamination reaction carried out by a transaminase or an aminotransferase

which substitutes the keto group with an amino group. These enzymes are usually dependent on pyridoxal phosphate (PLP), a cofactor that reacts with glutamate, which transfers its α-amino group to PLP to make pyridoxamine phosphate (PMP). PMP then transfers its nitrogen to the sugar, forming an aminosugar.[33] Aminotransferase catalysis proceeds via a highly conserved mechanism typically yielding regio- and enantioselective amine installation.[34]

The structure of DesI, an aminotransferase involved in D-desosamine biosynthesis in *Streptomyces venezuelae,* in the presence of PLP and the aminosugar product revealed an external aldimine intermediate in which a lysine residue is in close proximity to both C-4' of PLP and the C-4 atom of the sugar substrate.[35] This residue likely plays a role in mediating the proton transfers that occurs during the transamination yielding a C-4 equatorial amine installation. Unlike DesI, PseC another C-4 aminotransferase from *Helicobacter pylori*, introduces a C-4 axial amino group into a 4-ketosugar.[36] Interestingly, the hexose moiety was found to be rotated by 180° in PseC compared to DesI resulting in this interesting opposite stereochemistry of the amino group.

Biosynthesis of TDP-L-epi-vancosamine

The biosynthesis of TDP-L-epivancosamine (Scheme I-2) is a good example to discuss because this unusual moiety is one of the most modified deoxyaminosgurs found in natural products. Eight enzymatic steps are required for its biosynthesis

starting from glucose. There are two L-epivancosamine sugars linked to the aglycone scaffold in chloroeremomycin, a member of the vancomycin family of glycopeptide antibiotics produced by *Amycolatopsis orientalis*.[37] The biosynthetic gene cluster of chloroeremomycin has been sequenced which facilitated the *in vitro* studies of TDP-L-epivancosamine bisosynthesis.[38] In these studies, five enzymes from the chloroeremomycin pathway, EvaA-E, have been shown to be involved in its biosynthesis starting from TDP-6-deoxy-4-keto-D-glucose.[39] These five enzymes were shown to perform C-2 deoxygenation by EvaA, C-3 amination and methylation by EvaB and EvaC respectively, C-5 epimerization by EvaD, and C-4 ketoreduction by EvaE (Scheme I-2).

To reconstitute the biosynthesis of TDP-L-epivancosamine *in vitro*, the TDP-glucose 4,6-dehydratse (RfbB) from the rhamnose biosynthetic pathway, was used to generate the entry sugar TDP-4-keto-6-deoxy-α-D-glucose.[40] The RfbB activity requires nicotinamide adenine dinucleotide phosphate ($NADP^+$) which is bound to the enzyme. It was shown that the dehydration by EvaA, 2,3-dehydratase, produces the unstable TDP-linked 3,4-dioxo-6-deoxy sugar which is susceptible to TDP elimination with 1,2-olefin formation.[39] The 3-amino group is formed upon the activity of the aminotransferase, EvaB, a PLP dependent enzyme. It was also shown that the activity of this enzyme is enhanced by the inclusion of 1 mM glutamine in the assay. The C-3 methylation step is carried out by the activity of EvaC, a SAM dependent methyltransferase. This methylation is followed by the activity of the C-5 epimerase EvaD which results in a change of the sugar configuration from D to L. The final step of TDP-L-epivancosamine biosynthesis is the activity of the NADPH-dependent C-4 ketoreductase, EvaE, which

reduces the keto group on C-4 to a hydroxyl group. TDP-L-epivancosamine is then attached to the aglycone scaffold of chloroeromomycin by a glycosyltransferase.

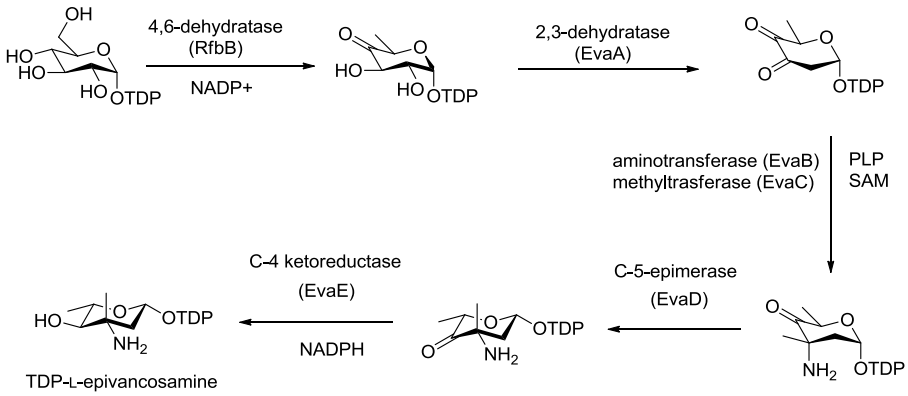

Scheme I-2. Biosynthesis of TDP-L-*epi*-vancosamine.

Comparative genomics of the nitro sugar functionality

The availability of gene cluster data of many isolated natural products provided the opportunity to analyze genes based on sequence and propose functions prior to carrying out biochemical characterization of the encoded enzymes. Sequence based analysis alone is insufficient for identifying/discovering a precise biosynthetic gene especially for large gene clusters that may contain up to 100 genes. However, multiple gene clusters of related compounds can be analyzed via a comparative genomic approach which can substantially simplify identifying genes of interest. Comparative genomic analysis[41] was performed on the related orthosomycins everninomicin and avilamycin which is described below.[42]

Avilamicin is another orthosomycin oligosaccharide structurally very similar to everninomicin but lacks the nitrosugar moiety (Figure I-5).[43] It is produced by *Streptomyces viridochromogenes* and consists of heptasaccharide deoxysugar chain and one PKS-derived dichloroisoeveninic acid moiety. Another structural difference between the two oligosaccharides is the presence of the orsellenic acid moiety at C5 of the deoxysugar ring H of everninomicin which is replaced by an acetyl group in avilamycin.

Like everninomicin, avilamycin was shown to be active against many Gram-positive bacteria, including emerging problem organisms, such as vancomycin-resistant enterococci, methicillin-resistant staphylococci, and penicillin-resistant pneumococci. The mode of action of avilamycin is similar to that of everninomicin, which involves inhibition of protein biosynthesis by binding to the 50S ribosomal subunit of the bacterial ribosomes.[44]

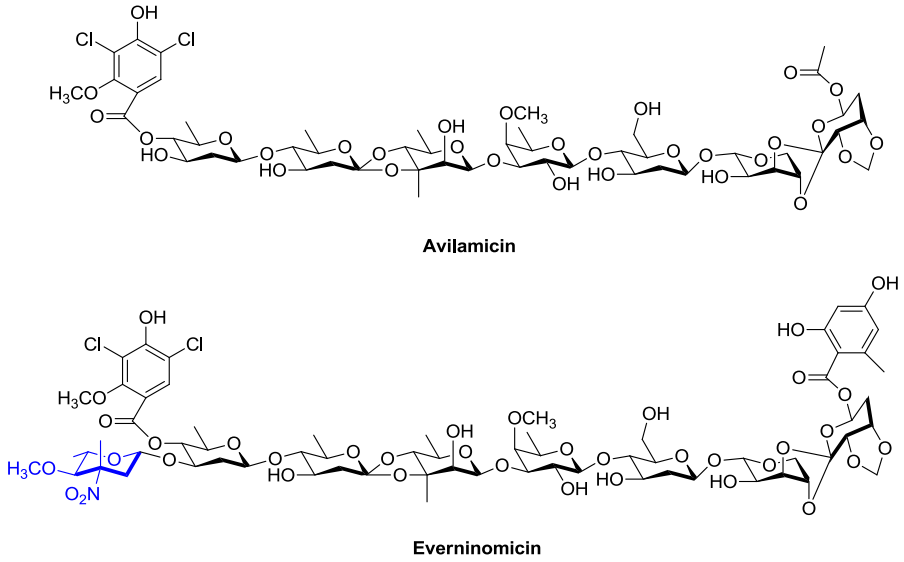

Figure I-5: Chemical structures of everninomicin and avilamycin.

There are two gene clusters described for avilamicin in the public domain (AVIL, AVIA) and two for everninomicin (EVER, EVEA) representing four different producers. By comparing these four clusters and applying simple subtractive analysis, genes that are likely to be involved in the nitrosugar biosynthesis could be proposed. This approach led to the identification of nine candidate genes for the nitrosugar biosynthesis present in the two everninomicin producers; *Micromonospora carbonacae var. aurantiaca* and *Micromonospora carbonacea* var. *africana,* while absent in the two avilamycin producers; *Streptomyces viridochromogenes* and *Streptomyces mobaraensis* (Table I-1).[45]

Table I-1. Possible biosynthetic genes for L-evernitrose. Nine genes present in the everninomicin gene clusters (EVEA and EVER) but absent in the avilamycin gene clusters (AVIL, AVIA). Orf36/42 gene pair (shown in red) from EVEA, EVER clusters, respectively, is the likely N-oxidase in the biosynthesis of the nitrosugar moiety.

EVEA genes	EVER genes	Putative encoded enzymes
Orf37	*Orf43*	(C3 aminotransferase)
Orf40	*Orf46*	(C4 ketoreductase)
Orf39	*Orf45*	(C5 epimerase)
Orf38	*Orf44*	(C3 methytransferase)
Orf35	*Orf21*	(glycosyltransferase)
Orf36	*Orf42*	(flavin-dependent oxidase)
Orf19	*Orf4*	(copper-dependent oxidase)
Orf18	*Orf3*	(RNA methyltransferase)
Orf41	*Orf47*	(C4 O-methlytransferase)

Sequence homology analysis of these genes, allowed the identification of five encoded enzymes involved in the biosynthesis of the aminosugar precursor that shared high sequence similarity and identity with their counterparts in the well characterized TDP-L-epivancosamine's biosynthetic pathway.[39] The nitrosugar L-evernitrose is structurally very similar to TDP-L-epivancosamine with the difference being the N-oxidation on C-3 and the C4 O-methylation in L-evernitrose. Among the genes shared between the two pathways were genes that encode a C-3-aminotransferase, C-3 methyltransferase, C-5-epimerase and C-4-ketoreductase. The *orf35/21* gene pair was found to share sequence homology with genes encoding glycosyltransferases and hence is possibly responsible for the glycoslation of L-evernitrose. The *orf41/47* gene pair shares sequence homology with C4 O-methyltransferases likely responsible for introducing the methoxy group at C4 of the nitrosugar, a functionality that is replaced with a hydroxyl in TDP-L-epivancosamine. The sequence homology analyses excluded two of these nine genes as candidates for the biosynthesis of evernitrose. Namely, the *orf18/3* gene pair which has reasonable homology to RNA-methyltransferase genes and the *Orf19/4* gene pair homologous to copper-dependent oxidase genes involved in primary metabolism. The only remaining and likely oxidase responsible for the oxidation of the aminosugar among these nine gene pairs is *orf36/42*. The encoded proteins of these genes have moderate sequence homology with the flavin dependent monooxygenase dibenzothiophene oxidase DszC which has been shown to oxidize a sulfide group to a sulfone via a sulfoxide intermediate.[46] ORF36 also shares moderate sequence similarity (~ 25%) with the acyl-CoA dehydrogenase family of enzymes. Acyl-

CoA dehydrogenases are flavin-dependent enzymes and are used as a structural model for class-D flavin-dependent monooxygenases.

Proposed deoxysugar N-oxidation pathway

As mentioned above, the oxidase proposed to form the nitrosugar congener from the deoxyaminosugar precursor in the everninomicin pathway is ORF36 from *Micromonospora carbonacea* var. *africana*. This putative flavin-dependent enzyme shares high sequence identity and similarity with other homologues in the biosynthetic pathways of nitrosugar-containing natural products such as RubN8 from the rubradirin pathway and KijD3 from the kijanimicin pathway. All of these putative N-oxidases share moderate homology with the flavin-dependent dibenzothiophene oxidase DszC which oxidizes dibenzothiophene (DBT) to DBT sulfone ($DBTO_2$) as shown in scheme I-3. This two-step oxidation requires the flavin mononucleotide (FMN) and the NADPH cofactors as well as an external flavin reductase to provide reduced flavin which mediates the monooxygenation catalysis. Reduced flavin is known to react with molecular oxygen to form the C4a-hydroperoxyflavin, a reactive oxygen species that is responsible for the electrophilic oxidation of the substrate.[47] The oxygenation step results in the incorporation of one oxygen atom into the substrate, usually as a hydroxyl group, and the formation of the C4a-hydroxyflavin. The hydroxyflavin readily loses a water molecule and is recycled to participate in further rounds of oxidations.

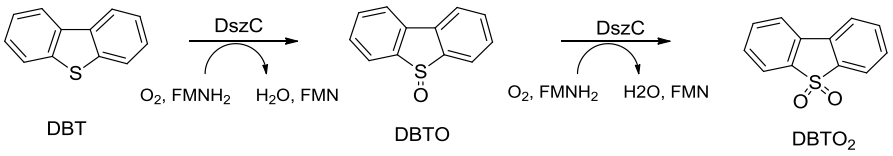

Schem I-3. Oxidation of dibenzothiophene by DszC.

The oxidation mechanism for the aminosugars by the putative flavin-dependent oxidases could be envisioned in a similar manner whereby the reduced flavin is provided by the function of an external flavin reductase. Monooxygenation mediated by C4a-hydroperoxyflavin results in the formation of a hydroxylamine intermediate and consequently, similar flavin-dependent oxidation steps result in the production of further oxidized intermediates perhaps via the nitroso and ultimately the nitro functionality.

Anthracyclines and deoxyaminosugar oxidation

A brief history of anthracycline drugs

Anthracyclines are another class of natural products with deoxysugar moieties attached to their tetracyclic polyketide cores. Some anthracycline compounds are considered the most effective anticancer drugs and possess a wide range of activity against several types of human cancers.[48-50] The first discovered anthracyclines were doxorubicin and daunorubicin when they were isolated from *Streptomyces peucetius* in early 1960s.[5, 51] The tetracyclic structure of doxorubicin and daunorubicin includes quinone-hydroquinone groups represented by rings C-B (Figure I-6). The sugar moiety in

these two compounds is 3-amino-2,3,6-trideoxy-L-fucose, also known as daunosamine. Doxorubicin and daunorubicin share the same tetracyclic core with the difference of a hydroxyl group on C-13 in doxorubicin. This small structural difference has significant effect on the spectrum of the anticancer activity of doxorubicin vs. daunarubicin. For example doxorubicin and some of its analogs were found to have less acute toxicity, cause less cardiomyopathy, and in general more potent anticancer activity.[52] Additionally, daunorubicin shows activity in acute lymphoblastic or myeloblastic leukemias[53] whereas doxorubicin is more active against breast cancer, childhood solid tumors, soft tissue sarcomas, and aggressive lymphomas.[54]

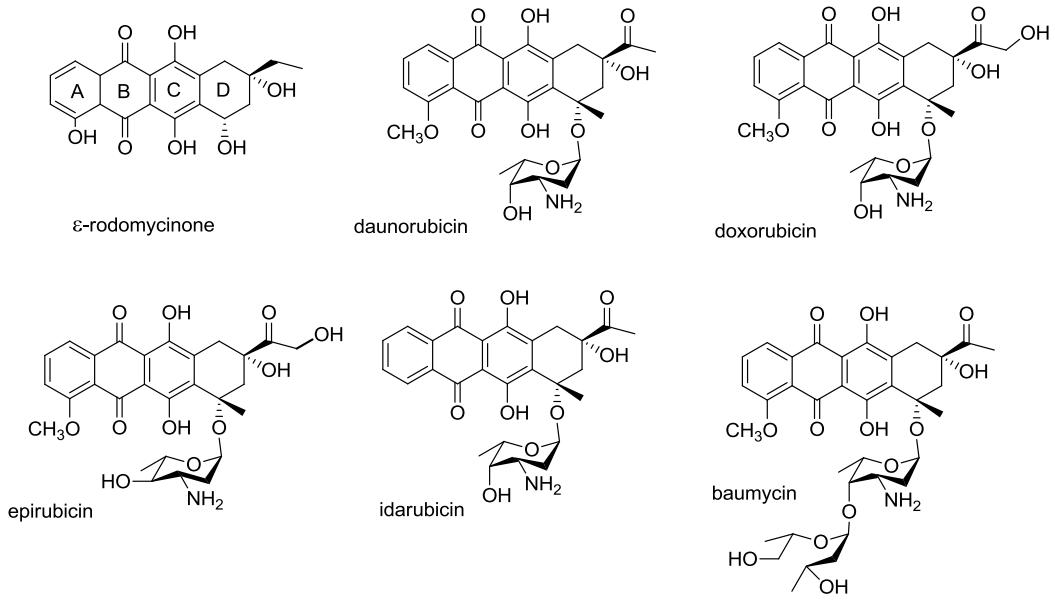

Figure I-6. Chemical structure of some anthracyclines.

The use of doxorubicin and daunorubicin in clinic is facing some challenges such as the development of resistance in tumor cells or toxicity in healthy tissues, resulting in

some cases in chronic cardiomyopathy and congestive heart failure (CHF) among other side effects. Therefore, there is a need for improved anthracycline analogs with varied pharmacokinetics for the treatment of different types of cancer. Hundreds of new doxorubicin and daunorubicin analogs were synthesized but only few of them made it to clinical development and approval.[52] Among the best approved analogues were epirubicin[55-58] and idarubicin[59-61], alternatives to doxorubicin and daunorubicin, respectively. The only difference between epirubicin and doxorubicin is the epimerization at C-4' of daunosamine changing the orientation of the hydroxyl from the axial in doxorubicin to the equatorial in epirubicin. Interestingly, this minor structural difference resulted in significant changes in the pharmacokinetic properties which led to improvements in distribution volume and total body clearance.[53] The idarubicin analogue of daunorubicin is made from the removal of the 4-methoxy group in ring-D and was shown to possess broader spectrum of anticancer activity. It was speculated that this improved activity may be attributed to increased lipophilicty and stabilization of the drug-topoisomerase-DNA ternary complex.[62] Other approved anthracyclin analogues include pirarubicin, aclacinomycin A (aclarubicin), [63-64] and mitoxantrone[65-67] (a substituted aglyconic anthraquinone).

Biosynthesis of baumycin

Baumycin is an another anthracycline compound derived from daunorubicin and has been shown to exhibit high efficacy against gram-positive bacteria and certain cancer cell lines such as leukemia cells (L1210). The structure of baumycin includes a

non-sugar acetal moiety attached at C-4' position of the daunosamine sugar (Figure I-6).[68-71]

In *Streptomyces peucetius*, the polyketide core in baumycin is produced by a Type II polyketide synthase (PKS). The first 3-carbons of the 21-carbon decaketide chain are synthesized from the incorporation of a single propinyl starter unit from propinyl-CoA followed be 9 iterative condensations of malonyl extender units.[72] The minimal PKS proteins that catalyze the formation of this long chain polyketide are an acyl carrier protein (ACP), ketosynthase (KS) and a malonyl-CoA:ACP acyltransferase (MAT).[73] The polyketide chain is converted to 12-deoxyalkalonic acid catalyzed by the dps gene cluster which includes DpsE, an NADPH dependent 9-ketoreductase, and cyclases DpsF and DpsY that catalyze the formation of ring D and C, respectively. The subsequent polyketide modifications are catalyzed by the dnr gene cluster which includes C-12 oxygenase, a SAM dependent alkalonic acid methyltransferase, ring A cyclase, C-7 ketoreductase, and a C-11 hydroxylase.[74] This series of polyketide modifications yields ε-rhodomycinone (Figure I-6), the precursor for doxorubicin and daunorubicin. The daunosamine sugar is then attached by DnrS, a glycosyltransferase followed by additional modifications on the tetracyclic core to yield daunorubicin[75], which is a precursor for doxorubicin and baumycin. The biosynthesis of the actal moiety at C-4' position of the daunosamine sugar is unclear; however, based on gene cluster analysis; a possible pathway is proposed and discussed below.

Deoxysugar genes in anthracyclines

The biosynthetic genes of the deoxysugar L-danosamine in doxorubicin, daunorubicin and baumycin were assigned based on sequence homologies with other sugar modifying enzymes and further studied by gene manipulation. It was shown that the minimal enzymes required for L-daunosamine biosynthesis and attachment are encoded by the *dnm*LMJVUTS genes.[76] These genes were cloned into the heterologous host *Streptomyces lividans* and the resultant recombinant strain was fed with the aglycone ε-rhodomycinone. Scheme I-4 illustrates the enzymatic steps required for the biosynthesis of TDP-L-daunosamine starting from D-glucose-1-phosphate. The DnmL enzyme is highly homologous to the well-known glucose-1-phosphate thymidylyltransferases which catalyze the conversion of D-glucose-1-phosphate into TDP-D-glucose.[77] This sugar is converted to TDP-6-deoxy-4-keto-D-glucose catalyzed by DnmM, a TDP-D-glucose 4,6-dehydratase. The 4-keto sugar is then further dehydrated by DnmT, a 2,3-dehydratase to yield the 3,4-dioxo-6-deoxysugar nucleotide which can be transaminated by DnmJ, a C-3 aminotransferase. At this stage, the sugar can undergo epimerization by DnmU, a C-5 epimerase resulting in configuration change from D- to L-deoxysugar. The last sugar modification before glycoslation appears to be catalyzed by DnmV, a 4-ketoreductase, which yields the TDP-L-daunosamine, the sugar donor substrate of DnmS, a glycosyltransferase. It was also shown that the aglycon of DnmS is ε-rhodomycinone, a precursor for the anthracyclines doxorubicin and daunorubicin.

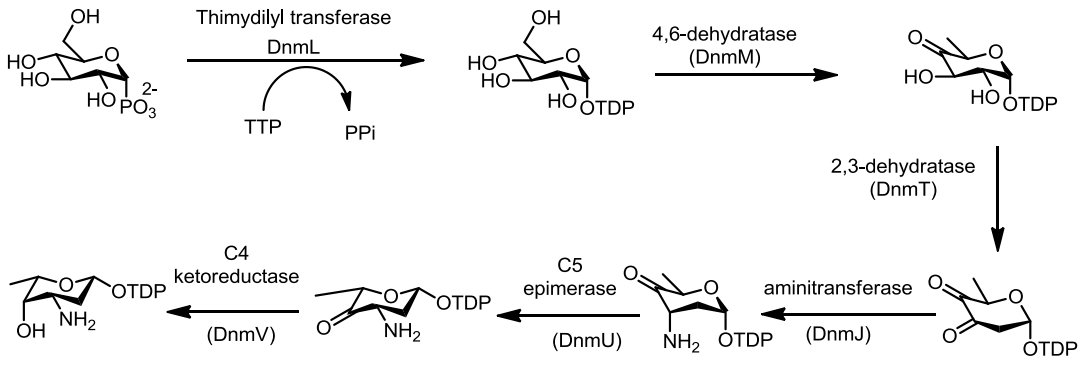

Scheme I-4: biosynthesis of TDP-L-daunosamine.

Further analysis of the *Streptomyces peucetius* anthracycline gene cluster reveals the presence of additional sugar modifying/attachment enzymes. These enzymes include DnrH, a glycosyltransferase, and DnmZ, a flavoprotein homologous to ORF36 from the everninomicin pathway. The deoxysugar gene *dnrx* which encodes a C3 SAM-dependent methyltransferase was also found in the cluster. The C3-methyltransferase is not required for the biosynthesis of L-daunosamine because this sugar lacks C3 methylation. Interestingly, DnrX shares high sequence similarity with the C3 methyltransferase, ORF38, from the putative deoxynitrosugar L-evernitrose's pathway (66% identity, 76% similarity). DnrX is also homologous to EvaC from the TDP-L-epivancosamine pathway (66% identity, 78% similarity).

The presence of these extra deoxysugar genes suggests that their encoded enzymes catalyze sugar modification/attachment steps for a second deoxysugar. To date, no anthracycline compound with two deoxysugar appendages has been isolated from the anthracycline producer *Streptomyces peucetius,* which gives rise to the importance of elucidating the biosynthetic route of the non-sugar acetal moiety in

baumycin. One possibility could be that the formation of this unusual moiety is a result of terminal deoxysugar degradation whereby the sugar undergoes a C-C bond cleavage, perhaps combined with other chemical/enzymatic steps. To resolve this intriguing mystery, it is essential to biochemically confirm the putative roles of these additional deoxysugar enzymes. The glycosyltransferase DnrH and the C-4 ketoreductase DnrX have well known and characterized homologues in other deoxysugar pathways hence, their characterization seems less attractive. Elucidation of the function of the putative flavin-dependent enzyme DnmZ however, seems more interesting considering its homology to ORF36, RubN8, and KijD3 proposed to be involved in deoxyaminosugar oxidation.

The putative role of the flavoenzyme DnmZ

As mentioned above, DnmZ shares high sequence homology with the proposed flavin-dependent enzymes ORF36, RubN8 and KijD3 proposed to be involved in deoxyaminosugar oxidation. For example, DnmZ shares 70% sequence similarity with ORF36 (59% Identity). This suggests that all of these enzymes likely catalyze a similar deoxyaminosugar oxidation reaction. Given the fact that there are no deoxysugar moieties with N-oxidation in any of the anthracycline derivatives produced by *Streptomyces peucetius* isolated to date, proposing a role for DnmZ seems difficult; however, one scenario can be envisioned whereby DnmZ catalyzes a deoxyaminosugar oxidation similar to that proposed for its homologues, whereby the resulting sugar

moiety undergoes further enzymatic or chemical transformations either before or after glycoslation.

The biosynthetic origin of the terminal non-sugar acetal moiety in baumycin is unclear but one possible route for its formation is through enzymatic or chemical modifications of a deoxysugar precursor. The presence of extra sugar genes in the anthracycline gene cluster of *Streptomyces peucetius* supports this hypothesis.[78] The C-3 methyltransferase DnrX is likely involved in the production of the TDP-deoxyaminosugar substrate of the putative DnmZ enzyme. One pathway of this substrate could be proposed in which the DnrX activity follows the transamination by DnmJ forming the C-3 methylated sugar. This methylation step provides a diversion from the L-daunosamine pathway and maybe a key requirement for subsequent deoxyaminosugar oxidation activity. This is consistent with the methylation at C-3 in the deoxynitrosugars L-evernitrose, D-rubranose, and L-kijanose.[13-14, 42] The subsequent steps to produce the DnmZ substrate could be carried out by the C-5 epimerase DnmU and a C-4 ketoreductase yielding TDP-L-epivancosamine, a substrate precursor proposed for the ORF36 homologue. Amine oxidation of this sugar by DnmZ could set the stage for other enzymatic or chemical transformations to ultimately form baumycin (Scheme I-5)

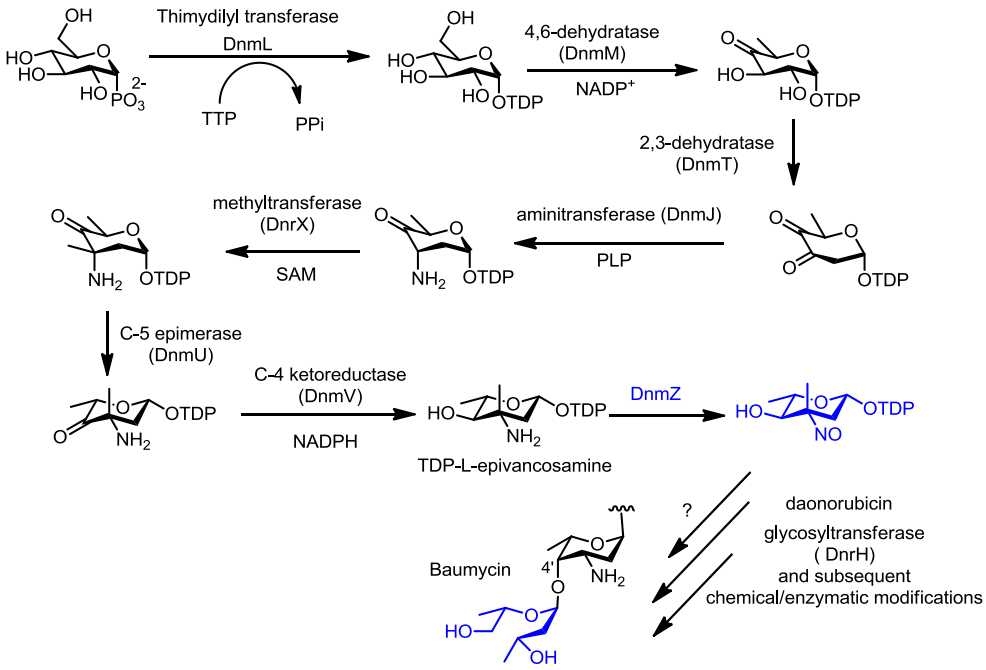

SchemI-5. Proposed pathway of late-step baumycin biosynthesis including the role of DnmZ.

Flavoprotein monooxygenases

As discussed earlier and based on sequence homologies, the enzyme responsible for the formation of the nitro functionality in nitrosugar-containing natural products is likely a flavin-dependent monooxygenase. Enzymes of this family are capable of efficient and specific insertion of one or more oxygen atoms into an organic substrate, a reaction not easy to perform via traditional chemical syntheses.[79] Although many chemical catalysts have been designed to address the difficulty of oxygenation reactions, the exquisite specificity and efficiency of monooxygenases remain unmatched. The discovery and characterization of a new flavin-dependent monooxygenase, will extend our knowledge of important biosynthetic pathways, support the current efforts of natural product structure diversification, as well as introduce new efficient biocatalysts

to perform difficult oxygenation reactions. Below is a brief background on flavoproteins with emphasis on flavin-dependent monooxygenases.

Biochemistry of flavoproteins

Flavin exists in nature in three principle forms; riboflavin (vitamin B2), flavin mononucleotide (FMN), and flavin adenine dinucleotide (FAD) as shown in figure I-7.[80] The FMN and FAD forms are the prosthetic groups for flavoproteins, and there are well characterized mechanisms for their interconversions. Flavins have bright yellow color, like most flavoproteins, and a characteristic UV-absorption that changes significantly depending on the oxidation state of the flavin. This unique spectrophotpmetric property allowed the study of the catalysis of many flavoproteins. Flavins undergo one electron reduction to give stable semiquinone radicals allowing them to mediate between the common two electron oxidations (e.g $NAD(P)^+$/NAD(P)H) and one electron oxidations carried out by heme or iron-sulfur cluster proteins.

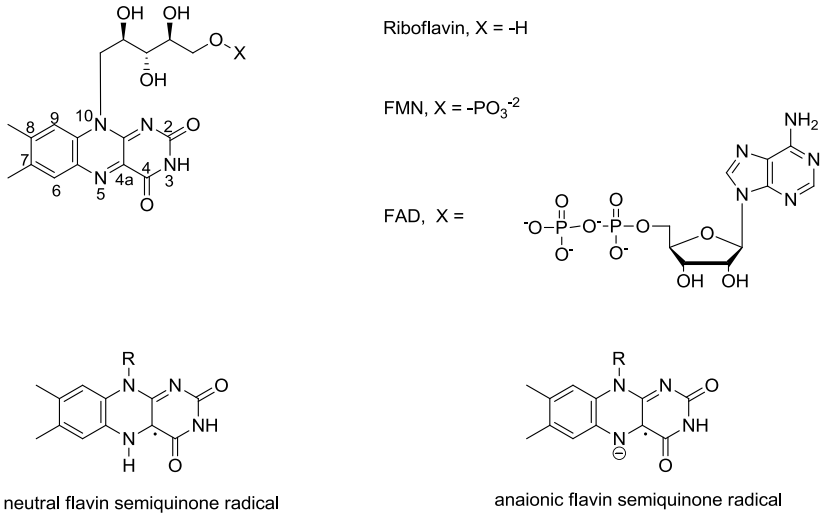

Figure I-7. Chemical structures of several flavin species.

In free solution, a mixture of oxidized and reduced flavin exists in an equilibrium in which a certain amount of radical is formed. At pH 7, only about 5% flavin semiquinone radical is stabilized for a 1:1 mixture of oxidized and reduced flavin. The semiquinone radical can exist in a neutral or anionic form (Figure I-7). Binding to the enzyme can provide up to 100% semiquinone radical stabilization. For the flavin-dependent oxidases, the bound reduced anionic flavin reacts with molecular oxygen to yield a caged radical pair of neutral flavin radical and superoxide (Scheme I-6). This radical pair can react in several pathways. The two radicals can collapse to form the C4a hydroperoxide anion which upon protonation forms the electrophilic C4a-hydroperoxide, a species that is involved in hydroxylation reactions. The peroxide species can undergo hydroperoxide elimination to regenerate oxidized flavin. Oxidized flavin can also be formed via a second one-electron transfer from the radical pair. A third route of the radical pair is the dissociation to its free components, flavin radical

and superoxide. In the oxygenation mechanism, the C4a-hydroperoxide can act as an electrophile such as in aromatic hydroxylations[81], or when deprotonated, as a nucleophile such as in Baeyer-Villiger monooxygenases.[82]

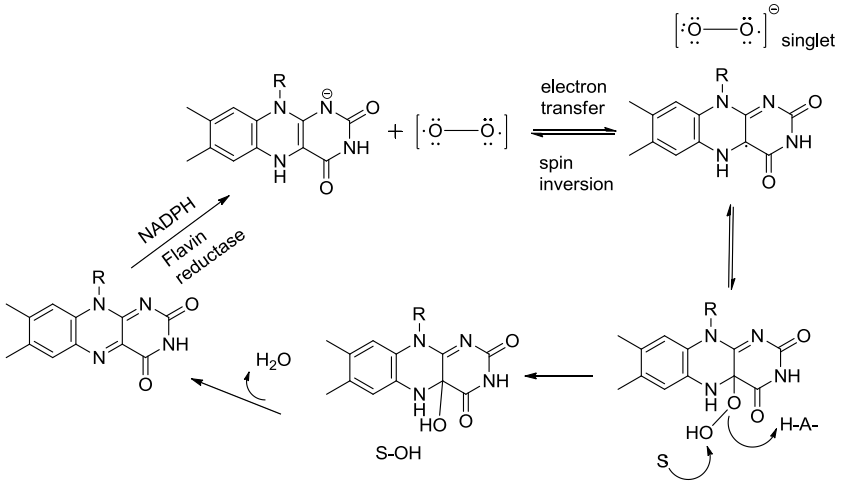

Scheme I-6. General mechanism of oxygenation reactions catalyzed by external flavoprotein monooxygenases.

The monooxygenase family

Besides flavoprotein monooxygenases, a number of other different types of enzymes have evolved in nature to carry out monooxygenation reactions. The cytochrome P450 family of monooxygenases is one of the best characterized monooxygenases. These are heme-containing enzymes and occur in relatively abundant isoforms. The catalytic mechanism of P450 monooxygenases is tightly coupled to substrate binding.[80] Upon binding of the substrate, the heme cofactor can be reduced by gaining electrons from reduced flavin. The flavin is typicaly reduced by an external flavin reductase that accepts electrons form the NADPH coenzyme. The reduced heme is

then used to complete the monooxygenation of the substrate. Cytochrome P450 monooxygenases are cabaple of hydroxylating carbon atoms regioselectively, which has been shown to be of great value to modify sterols and steroids.

Other classes of monooxygenases include non-heme monooxygenases[83] and copper-dependent monooxygenases.[84] A few new types of monooxygenases have been discovered in recent years that do not contain the aforementioned cofactors including the polyketide monooxygenase ActVA-Orf6, involved in actinorhodin biosynthesis in *Streptomyces coelicolor*.[81] Another example is the quinol monooxygenase YgiN, from *Escherichia coli* which oxidizes multiringed aromatic substrates without the participation of any cofactor.[85] Aclacinomycin-10-hydroxylase, involved in anthracycline biosynthesis in *Streptomyces purpurascens*, is another rare type of monooxygenases as it depends on S-adenosyl-l-methionine as a cofactor.[86] Flavin-dependent monooxygenases are perhaps the most ubiquitous of monooxygenases. They perform a wide range of monooxygenation reactions with high regio- and/or enantioselectivity. A brief background on flavin-dependent monooxygenases is disussed below.

Flavoprotein monooxygenase catalysis

Flavoprotein monooxygenases are a broad group of enzymes which share similar properties and mechanistic features.[87] One common property of these enzymes is the use of NADH or NADPH to supply the reduced flavin which reacts with molecular oxygen to form C4a-peroxide required for oxygenation of the substrate. When protonated, the C4a-peroxide is a potent electrophile and can participate in hydroxylation reactions such

as aromatic hydroxylations.[81] The flavin peroxide anion can also react as a nucleophile and is employed by a second subgroup of monooxygenases an example of which is cyclohexanone monooxygenase.[88] These two subgroups of monooxygenases share common but distinctive properties. In most electrophilic monooxygenases, there is an exquisite control mechanism to ensure that the NAD(P)H cofactor is only used when the substrate is bound to the enzyme for oxygenation.[80] Substrate binding is required for rapid reduction of flavin by NAD(P)H. For the nucleophilic monooxygenases, substrate binding is usually not required for flavin reduction but the C4a-peroxide formed upon reaction with O_2 stabilized by the protein is only reactive in the presence of the substrate for oxygen transfer.[89] In contrary, the C4a-hydroperoxide in electrophilic monooxygenases is very unstable in the absence of the substrate.

One of the most well studied electrophilic monoxygenases is *p*-hydroxybenzoate hydroxylase and its basic mechanism appears to be followed by most members of this class.[90] These enzymes can be studied spectrophotometrically exploiting the flavin absorbance and fluorescence properties.[91] The mechanism of *p*-hydroxybenzoate hydroxylase monooxygenation starts with forming the flavin-NADPH-substrate ternary complex resulting in a long-wavelength-absorbing charge transfer between the NADPH as a donor and oxidized flavin as an acceptor (Scheme I-7). The next step is the reduction of the flavin cofactor which is also accompanied by significant change in absorbance and fluorescence causing another long wavelength charge transfer in which reduced flavin is the donor and $NADP^+$ is the acceptor. The $NADP^+$ species is then released forming the enzyme-reduced flavin-substrate complex. The resulting anionic

reduced flavin can then react with molecular oxygen forming the enzyme-C4a-hydroperoxide-substrate intermediate complex. This intermediate has distinctive spectrum with a wavelength maximum at 380 nm which is formed with a pseudo first order constant directly proportional to the oxygen concentration. Oxygen transfer from the hydroperoxyflavin can then take place resulting in a complex of enzyme C4a-hydroxyflavin and the non-aromatic metastable dienone (intermediate III). The following step is the re-aromatization to form intermediate III that includes the more stable hydroxylated product, a step that occurs at sufficiently slow rate that allows the determination of K_6. The final step is the dehydration of the C4a-hydroxyflavin to recycle the oxidized enzyme ready for the next round of catalysis.

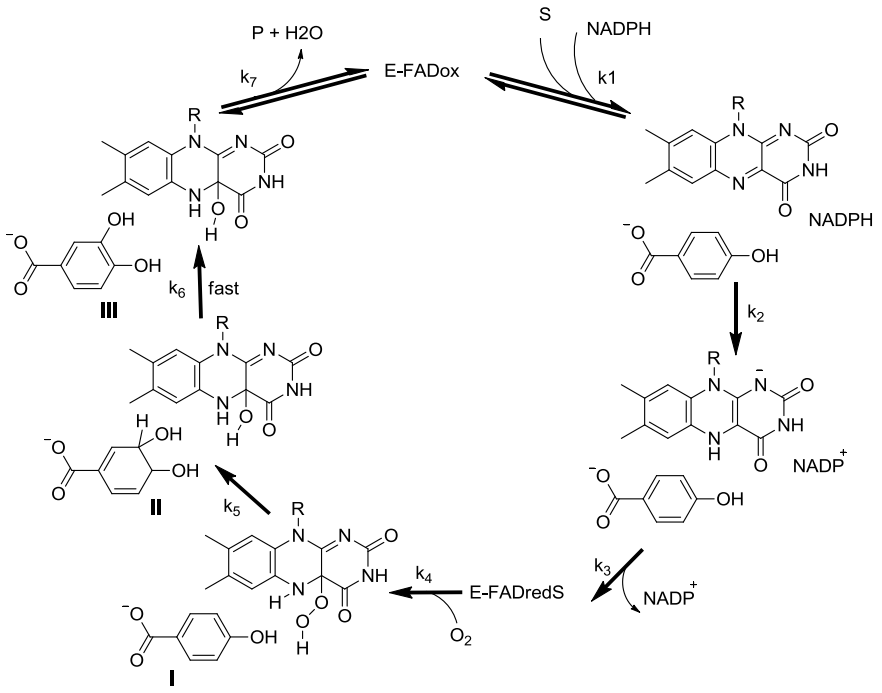

Scheme I-7 . Reaction mechanism of p-hydroxybenzoate monooxygenase.

For p-hydroxybenzoate hydroxylase, it has been found that the flavin exisits in two different conformations: one is mostly buried in the protein core and ideally positioned for hydroxylation and the other is partially solvent exposed and suitable for reduction by NADPH.[92] The mobility of the flavin cofactor has been also confirmed in the structural studies of the related phenol hydroxylase.[93]

In nucleophilic monooxygenation, O_2 reacts with reduced flavin to form the flavin peroxide. This is the nucleophilic flavin-oxygen intermediate that participates in the oxygen transfer to the substrate as in Baeyer-Villiger monooxygenases.[82, 94] In cyclohexanone monooxygenase, the flavin C4a-peroxide formed after the reaction of reduced flavin with molecular oxygen can be slowly protonated to yield the C4a-hydroperoxyflavin, or it can react with cyclohexanone as a nucleophile to form the

Criege intermediate which rearranges to form ε-carbolactam.[95] The resulting hydroxyflavin undergoes elimination of water regenerating the oxidized flavin for next cycle of catalysis.[96-97] The $NADP^+$ species must be bound during the reaction to protect the reactive C4a-hydroperoxide.

Classifications of Flavoprotein monooxygenases

Several hundred flavoenzymes have been characterized to date.[98-99] Most of these enzymes contain a non-covalently bound flavin in the form of FMN or FAD but there are some enzymes that bind the flavin cofactor covalently. Examples of flavin covalently bound enzymes include vanillyl-alcohol oxidase which contains FAD bound to a histidine residue.[100] In *p*-cresol methyl hydroxylase, the FAD is linked to a tyrosine residue. It has been shown that this covalent linkage is beneficial for catalysis in the case of vanillyl-alcohol oxidase.[101] For all internal or external flavoprotein monooxygnases however, the flavin cofactor is not covalently linked to the enzyme.

Classification of the big family of flavoenzymes has been established based on different criteria such as the types of reactions they catalyze, cofactor requirements, sequence homology and structural folds. More recently, external flavoprotein monooxygenases have been classified by following similar criteria mentioned above. They were divided into six different subclasses A-F as shown in table I-2. These subclasses were discriminated based on sequence similarty, specific structural motifs, types of reactions and cofactor requirements. Structures of some prototype flavin-dependent monoxygenases are shown in figure I-8.[79]

Table I-2 classification of external flavoprotein monooxygenases.[79]

Class	Reactions	Cofactor	Coenzyme	Structural fold
A	Hydroxylation, epoxidation	FAD	NAD(P)H	1 FAD/NAD(P)-binding domain
B	Baeyer–Villiger, N-oxidation	FAD	NADPH	2 FAD/NAD(P)-binding domains, 1 helical domain
C	Light emission, S-oxidation, Baeyer–Villiger	–	FMN NAD(P)H	TIM barrel
D	Hydroxylation	–	FAD NAD(P)H	Acyl-CoA dehydrogenase (model)
E	Epoxidation	–	FAD NAD(P)H	1 FAD/NAD(P)-binding domain
F	Halogenation	–	FAD NAD(P)H	1 FAD/NAD(P)-binding domain 1 helical domain

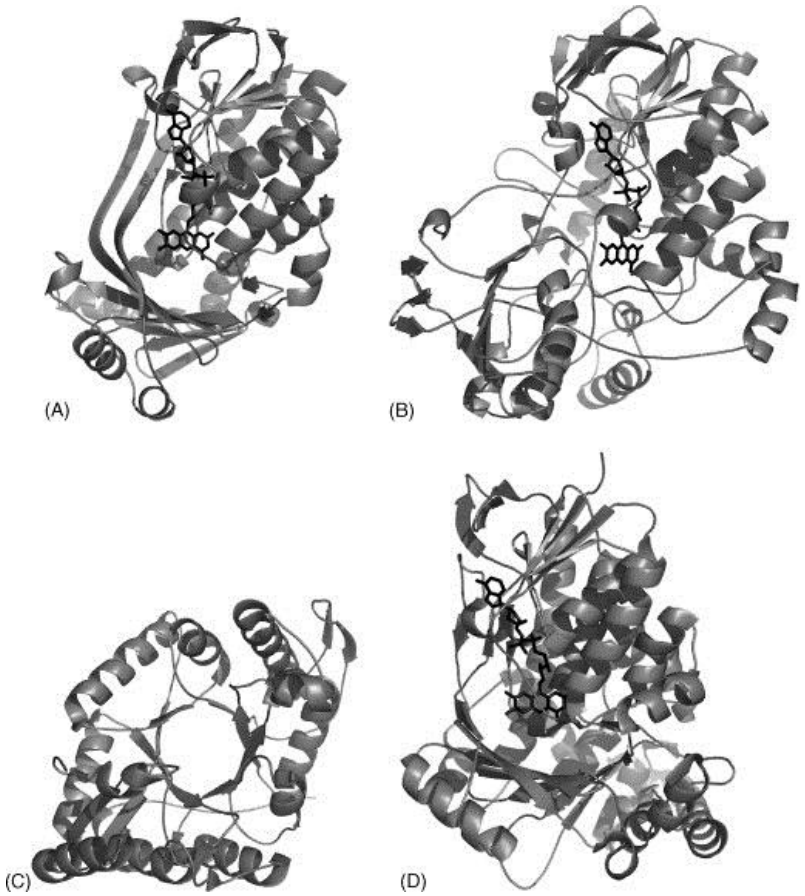

Figure I-8.[79] Structures of several prototype flavoprotein monooxygenases. The FAD cofactor is shown in sticks. (A) Class A: 4-hydroxybenzoate 3-monooxygenase from Pseudomonas fluorescence (B) Class B: phenylacetone monooxygenase from Thermobifida fusca (C) Class C: alkanesulfonate monooxygenase from Escherichia coli (no FMN cofactor was crystallized with the enzyme). (D) Class F: tryptophan 7-halogenase from Pseudomonas fluorescens.

Class A

Enzymes of this subclass are encoded by a single gene and contain a tightly bound FAD cofactor. Reduction of the FAD cofactor depends on the NADH or NADPH coenzyme with immediate release of the $NADP^+$ species after reduction. Class A flavoprotein monooxygenases are structurally composed of a dinucleotide binding domain adopting the Rossman fold[102] for the binding of the FAD cofactor.

Class A flavoprotein monooxygenases are known to catalyze epioxidation reactions. Squalene monooxygenase, a well-known example, is a key enzyme in the commited pathway for cholesterol biosynthesis which catalyzes the epioxidation of squalene across a C-C double bond to yield oxidosqualene.[103] The activity of this enzyme is dependent on NADPH-cytochrome p450 reductase for reducing equivalents.

The recently characterized Baeyer-Villiger enzyme MtOIV represents an atypical class A monooxygenase. This enzyme catalyzes the key-frame modifying step in the biosynthesis of mithramycin, an anticancer drug and calcium lowering agent. MtOIV cleaves a carbon-carbon bond essential for the conversion of the biologically inactive premithramycin B into the active drug mithramycin.[104] Unlike most members of this class, MtOIV uses a peroxyflavin intermediate as its oxygenating species instead of the electrophilic hydroperoxyflavin typically used in class A flavoprotein monooxygenases. Another flavoprotein epioxidase that belongs to this subclass is zeaxanthin epoxidase specific for carotenoids with 3-hydroxyl-β-cyclohexenyl ring. This enzyme requires NADPH and ferrodoxin-like reductives for activity.[105]

The crystal structures of enzymes of this subclass show motifs for the FAD binding region that resembles the β-α-β (Rossman fold) that binds the ADP moiety of FAD. There is no distinct domain for binding of the NADPH coenzyme consistent with its transient complex formation for the reduction of the flavin and rapid release as $NADP^+$. Recent structural characterization of 4-hydroxybenzoate 3-monooxygenase (Figure I-8), a member of this subclass, showed an additional finger-print sequence containing a

highly conserved DG motif involved in binding of both pyrophosphate moieties of NADPH and FAD.[106]

Class B

Enzymes of class B flavoprotein monooxygenases are encoded by a single gene and bind tightly to the FAD cofactor. They commonly depend on the NADPH coenzyme as reducing equivalents and keep the NADPH/$NADP^+$ species bound during catalysis. Their structure is composed of two dinucleotide binding domains adopting the Rossman fold for the binding of both FAD and NADPH. All members of this class are single component FAD-containing monooxygenases with specificity for NADPH.

Class B flavoprotein monooxygenases are also called multifunctional monooxygenases because they are able to oxidize both carbon and hetero atoms. This class of enzymes can also be divided into three sequence related subfamilies: flavin-containing monooxygenases[107] (FMOs), microbial N-hydroxylating monooxygenases[108] (FNOs), and Baeyer-Villiger monooxygenases[82] (type I BVMOs).

Flavin-containing monooxygenases were originally named mixed function monooxygenases.[109] They are known to play an important role in detoxification of drugs and foreign molecules in humans complementing the activities of cytochrome p450 enzymes. This subclass catalyzes monooxygenation of carbon bond-reactive heteroatoms such as sulfur, nitrogen, phosphorous, selenium and iodine.

N-hydroxylating monooxygenases catalyze the N-hydroxylation of primary amines and hence, play an important role in the biosynthesis of bacterial siderophores. They have sequence homology with flavin-containing monooxygenases and require NADPH and FAD for activity. Unlike flavin-containing monooxygenases, N-hydroxylating monooxygenases show lower affinity for FAD which hindered mechanistic studies of their catalysis. Ornithine hydroxylase (PvdA) catalyzes the hydroxylation of the side chain primary amine of ornithine in the initial step of the biosynthesis of the *Pseudomonas aeruginosa* siderophore pyoverdin.[108] Kinetic studies of this enzyme showed that binding of the substrate target is not required to trigger reduction of the flavin by NADPH.[110]

Class B Bayer-Villiger monooxygenases (BVMOs), catalyze an atypical oxygenation reaction converting a ketone or an aldehyde to ester or lactone.[111] One of the first studied enzymes of this family is cyclohexanone monooxygenase, from *actinobacter* sp. NCBBI 9871.[112] This enzyme performs Baeyer-Villiger oxidations on a wide variety of cyclic ketones with exquisite regio- and enantioselectivity. Bayer-Villiger monooxygenases can be identified based on the presence of two Rossman fold domains for FAD and NADPH binding. It was shown that phenylacetone monooxygenase, a well-characterized Baeyer-Villiger monooxygenase and member of this subfamily, has dinucleotide binding domains flanked by two helical domains which are unique for this type of monooxygenases.[113]

Class C

This class belongs to multicomponent monooxygenases and commonly encoded by multiple genes for the monooxygenase and the reductase components. Class C flavoprotein monooxygenases use FMN as a cofactor which is reduced by the reductase component using NADPH or NADH for reducing equivalents. The general structural core for the monooxygenase component displays a TIM-barrel fold.[114]

The most well-known examples of this class are bacterial lucifrases which are enzymes that emit light upon oxidation of long-chain aliphatic aldehydes.[115] Luciferases contain two heterodimeric subunits; one is the oxygenase component and the other is used for the reductase activity. Other examples of this class include 2,5-diketocamphane 1,2-monooxygenase, a type II Baeyer-Villiger monooxygenase.[116] The oxygenase component of this enzyme consists of two subunits for FMN binding similar to luciferases.

Another example is alkanesulfonate monooxygenase.[117] Structural studies of this enzyme revealed that it has a TIM-barrel fold where the monooxygenation catalysis proceedes via the formation of an FMN-monooxygenase-reductase complex.[118] One more example of this series is dibenzothiophene monooxygenase (DszC).[119] This enzyme is involved in desulfunization of benziothiophenes. It was recently shown that DszC is able to utilize either FMNH(2) or FADH(2) when coupled with a flavin reductase that reduces either FMN or FAD.[120] As discussed above, this enzyme shares moderate

homology with the flavin-dependent monooxygenase proposed to catalyze the oxidation of deoxyaminosugars.

Class D

This class of flavoprotein monooxygenases is typically encoded by two genes; one is for the monooxygenase and the other is for the flavin reductase component. The reductase component uses FAD as a cofactor and NADH or NADPH as a coenzyme. These enzymes are structurally homologous to acyl-CoA dehydrogenases and are mostly α-helical proteins.

Members of this class are typically active on regioselective hydroxylation of aromatic substrates. The prototype is 4-hydroxyphenylacetate 3-monooxygenase (Figure I-8) which catalyzes the conversion of 4-hydroxyphenylacetate to 3,4-dihydroxyphenylacetate.[121] The oxygenase component (HpaB) introduces a hydroxyl group into the benzene ring of 4-hydroxyphenylacetate using molecular oxygen and reduced flavin, while the reductase component (HpaC) provides free reduced flavins for HpaB.[122-123] Another example is 2,4,6-trichlorophenol monooxygenase which catalyzes sequential dechlorinations by oxidative and hydrolytic reactions.[124] The acyl-CoA dehydrogenase is a sequence related model for class D flavoprotein monooxygenases which catalyzes fatty acid β-oxidation in the mitochondria of cells.[125]

Class E

Class E flavoprotein monooxygenases are also encoded by two genes; the first gene encodes the monooxygenase component, and the second encodes the reductase component. They use reduced FAD cofactor generated from the reductase activity to mediate the monooxygenation catalysis. The reductase component can use either NADH or NADPH as reducing equivalents. No structures are available for enzymes of this subclass however, sequenece analysis indicate the presence of Rossman fold for dinucleotide binding and suggest that they evolved from class A flavoprotein monooxygenases.

Class E flavoprotein monooxygenases are relatively rare. Styrene monooxygenase from *Pseudomonas putida* is one of the few known enzymes of this class.[126] This enzyme oxidizes styrene in an enantioselective manner to form (S)-styrene epoxide with an *e.e.* of 99%. Mechanistic studies of this enzyme suggested that the reduced flavin does not have to be actively delivered by the reductase to the monooxygenase and the monooxygenase component can stabilize the peroxyflavin after binding reduced FAD and reacting with molecular oxygen.[127]

Class F

Class F flavoprotein monooxygenases are also encoded by two genes one for the monooxygenese and one for the reductase components. This class of enzymes uses reduced FAD generated by the reductase component which uses NADPH or NADH as

coenzyme for reducing equivalents. The general structural fold for FAD binding in this enzyme class is the Rossman fold.

The prototype for class F flavoprotein monooxygenases is tryptophan 7-halogenase from *Pseudomonas fluorescens*.[128] Monooxygenation by this enzyme, and related halogenases, proceed via the formation of the C4a-hydroperoxyflavin intermediate which reacts with the chloride ion to form HOCl. In the catalysis of tryptophan 7-halogenase, this highly reactive nucleophile will travel through a 10 Å tunnel to reach and halogenate the bound tryptophan substrate regioselectively.[129] In this respect, the chloride ion and not the substrate to be halogenated, is regarded as the substrate for monooxygenation.

Dissertation Statement

Deoxynitrosugar moieties are included in many isolated natural products and known to play significant roles in conferring biological activity. These unusual sugars are distributed among various scaffolds including spirotetronate antibiotics, ansamycins, and orthosomycins. Examples of natural products containing deoxynitrosugars include everninomicin, rubradirin, and kijanimicin for which the biosynthetic gene clusters have been recently sequenced. These recent advances in gene cluster data have enabled the proposal of biosynthetic pathways for the aminosugar N-oxidation to generate hydroxylamino-, nitroso- and nitro-sugars. Prior to our investigations, there was no biochemical data available for the enzymes responsible for this key oxidation to yield

these important deoxysugar modifications. We have targeted the producers of everninomicin, rubradirin and baumycin to identify and biochemically characterize the enzyme(s) responsible for their deoxyaminosugar oxidations.

Chapter II describes the initial biochemical characterization of the new nitrososynthase ORF36, a flavin-dependent monooxygenase, from the everninomicin biosynthetic pathway and its homologue RubN8, from the rubradirin biosynthetic pathway which reveals their roles as flavin-dependent monooxygenases in the deoxysugar N-oxidation pathway. Chapter III details additional biochemical characterization of ORF36 including solving its 3-D structure by X-ray crystallography and studying its substrate specificity towards several deoxyaminosugar intermediates. This chapter also describes ^{18}O-incorporation experiments aimed at the investigation of the mechanistic details of the nitrososynthase catalysis. Chapter IV discusses the role of the DnmZ, a nitrososynthase homologue, from the baumycin biosynthetic pathway. The surprising role of this flavin-dependent nitrososynthase in a deoxysugar C-C bond cleavage and its confirmed role of deoxyaminosugar oxidation are also discussed.

In summary, this work details the biochemical characterization of three flavin-dependent nitrososynthase homologues revealing a new and important deoxysugar N-oxidation pathway for a vast array of deoxysugar-containing natural products. The surprising retro-aldol activity of the nitrososynthase enzyme explains a once not understood pathway in the biosynthesis of baumycin-like compounds and provides new opportunities for utilizing this important biocatalyist in organic chemical synthesis.

References

1. Méndez, C.; Salas, J. A., Altering the glycosylation pattern of bioactive compounds. *Trends in Biotechnology* **2001,** *19* (11), 449-456.

2. Timmons, S. C.; Thorson, J. S., Increasing carbohydrate diversity via amine oxidation: aminosugar, hydroxyaminosugar, nitrososugar, and nitrosugar biosynthesis in bacteria. *Current Opinion in Chemical Biology* **2008,** *12* (3), 297-305.

3. Thibodeaux, C. J.; Melancon, C. E., 3rd; Liu, H. W., Natural-product sugar biosynthesis and enzymatic glycodiversification. *Angewandte Chemie* **2008,** *47* (51), 9814-59.

4. Printsevskaya, S. S.; Solovieva, S. E.; Olsufyeva, E. N.; Mirchink, E. P.; Isakova, E. B.; De Clercq, E.; Balzarini, J.; Preobrazhenskaya, M. N., Structure-activity relationship studies of a series of antiviral and antibacterial aglycon derivatives of the glycopeptide antibiotics vancomycin, eremomycin, and dechloroeremomycin. *Journal of Medicinal Chemistry* **2005,** *48* (11), 3885-3890.

5. Aubel-Sadron, G.; Londos-Gagliardi, D., Daunorubicin and doxorubicin, anthracycline antibiotics, a physicochemical and biological review. *Biochimie* **1984,** *66* (5), 333-52.

6. Frederick, C. A.; Williams, L. D.; Ughetto, G.; van der Marel, G. A.; van Boom, J. H.; Rich, A.; Wang, A. H., Structural comparison of anticancer drug-DNA complexes: adriamycin and daunomycin. *Biochemistry* **1990,** *29* (10), 2538-49.

7. Kaplan, J.; Korty, B. D.; Axelsen, P. H.; Loll, P. J., The role of sugar residues in molecular recognition by vancomycin. *Journal of Medicinal Chemistry* **2001,** *44* (11), 1837-40.

8. Weymouth-Wilson, A. C., The role of carbohydrates in biologically active natural products. *Natural Product Reports* **1997,** *14* (2), 99-110.

9. Thibodeaux, C. J.; Melancon, C. E.; Liu, H. W., Unusual sugar biosynthesis and natural product glycodiversification. *Nature* **2007,** *446* (7139), 1008-16.

10. Shimosaka, A.; Kawai, H.; Hayakawa, Y.; Komeshima, N.; Nakagawa, M.; Seto, H.; Otake, N., Arugomycin, a new anthracycline antibiotic. III. Biological activities of arugomycin and its analogues obtained by chemical degradation and modification. *The Journal of Antibiotics* **1987,** *40* (9), 1283-91.

11. Zein, N.; Sinha, A. M.; McGahren, W. J.; Ellestad, G. A., Calicheamicin gamma 1I: an antitumor antibiotic that cleaves double-stranded DNA site specifically. *Science* **1988,** *240* (4856), 1198-201.

12. Kind, R.; Hutter, K.; Zeeck, A.; Schmidt-Base, K.; Egert, E., Viriplanin A, a new anthracycline antibiotic of the nogalamycin group. II. The structure of a novel hydroxyamino sugar from reduced viriplanin A. *The Journal of Antibiotics* **1989,** *42* (1), 7-13.

13. Kim, C. G.; Lamichhane, J.; Song, K. I.; Nguyen, V. D.; Kim, D. H.; Jeong, T. S.; Kang, S. H.; Kim, K. W.; Maharjan, J.; Hong, Y. S.; Kang, J. S.; Yoo, J. C.; Lee, J. J.; Oh, T. J.; Liou, K.; Sohng, J. K., Biosynthesis of rubradirin as an ansamycin antibiotic from Streptomyces achromogenes var. rubradiris NRRL3061. *Archives of Microbiology* **2008,** *189* (5), 463-73.

14. Zhang, H.; White-Phillip, J. A.; Melancon, C. E., 3rd; Kwon, H. J.; Yu, W. L.; Liu, H. W., Elucidation of the kijanimicin gene cluster: insights into the biosynthesis of spirotetronate antibiotics and nitrosugars. *Journal of the American Chemical Society* **2007,** *129* (47), 14670-83.

15. Wagman, G. H.; Luedemann, G. M.; Weinstein, M. J., Fermentation and Isolation of Everninomicin. *Antimicrobial Agents Chemotherapy (Bethesda)* **1964,** *10*, 33-7.

16. Marshall, S. A.; Jones, R. N.; Erwin, M. E., Antimicrobial activity of SCH27899 (Ziracin), a novel everninomicin derivative, tested against Streptococcus spp.: disk diffusion/etest method evaluations and quality control guidelines. The Quality Control Study Group. *Diagnostic Microbiology and Infectious Disease* **1999,** *33* (1), 19-25.

17. Oh, T. J.; Kim, D. H.; Kang, S. Y.; Yamaguchi, T.; Sohng, J. K., Enzymatic synthesis of vancomycin derivatives using galactosyltransferase and sialyltransferase. *The Journal of Antibiotics* **2011,** *64* (1), 103-9.

18. Zhang, C.; Griffith, B. R.; Fu, Q.; Albermann, C.; Fu, X.; Lee, I. K.; Li, L.; Thorson, J. S., Exploiting the reversibility of natural product glycosyltransferase-catalyzed reactions. *Science* **2006,** *313* (5791), 1291-4.

19. Bhuyan, B. K.; Owen, S. P.; Dietz, A., Rubradirin, a New Antibiotic. I. Fermentation and Biological Properties. *Antimicrobial Agents Chemotherapy (Bethesda)* **1964,** *10*, 91-6.

20. Chu, M.; Mierzwa, R.; Jenkins, J.; Chan, T. M.; Das, P.; Pramanik, B.; Patel, M.; Gullo, V., Isolation and characterization of novel oligosaccharides related to Ziracin. *Journal of Natural Products* **2002,** *65* (11), 1588-93.

21. McNicholas, P. M.; Najarian, D. J.; Mann, P. A.; Hesk, D.; Hare, R. S.; Shaw, K. J.; Black, T. A., Evernimicin binds exclusively to the 50S ribosomal subunit and inhibits translation in cell-free systems derived from both gram-positive and gram-negative bacteria. *Antimicrobial Agents and Chemotherapy* **2000,** *44* (5), 1121-6.

22. Poulet, F. M.; Veneziale, R.; Vancutsem, P. M.; Losco, P.; Treinen, K.; Morrissey, R. E., Ziracin-induced congenital urogenital malformations in female rats. *Toxicologic Pathology* **2005,** *33* (3), 320-8.

23. Ganguly, A. K.; Girijavallabhan, V. M.; Miller, G. H.; Sarre, O. Z., Chemical modification of everninomicins. *The Journal of Antibiotics* **1982,** *35* (5), 561-70.

24. Reusser, F., Rubradirin, an inhibitor of ribosomal polypeptide biosynthesis. *Biochemistry* **1973,** *12* (6), 1136-42.

25. Russer F, B. B., Tarpley WG, Althaus IW, Zapotocky BA, Rubradirin derivatives for treatment of HIV infection. *Patent Cooperation Treaty W08808707* **1988**.

26. Bannister, B.; Zapotocky, B. A., Protorubradirin, an antibiotic containing a C-nitroso-sugar fragment, is the true secondary metabolite produced by Streptomyces achromogenes var. rubradiris. Rubradirin, described earlier, is its photo-oxidation product. *The Journal of Antibiotics* **1992,** *45* (8), 1313-24.

27. Wei, R. B.; Xi, T.; Li, J.; Wang, P.; Li, F. C.; Lin, Y. C.; Qin, S., Lobophorin C and D, new kijanimicin derivatives from a marine sponge-associated actinomycetal strain AZS17. *Marine Drugs* **2011,** *9* (3), 359-68.

28. Hara, T.; Omura-Minamisawa, M.; Chao, C.; Nakagami, Y.; Ito, M.; Inoue, T., Bcl-2 inhibitors potentiate the cytotoxic effects of radiation in Bcl-2 overexpressing radioresistant tumor cells. *International Journal of Radiation Oncology, Biology, Physics* **2005,** *61* (2), 517-28.

29. Kawashima, A.; Nakamura, Y.; Ohta, Y.; Akama, T.; Yamagishi, M.; Hanada, K., New cholesterol biosynthesis inhibitors MC-031 (O-demethylchlorothricin), -032 (O-demethylhydroxychlorothricin), -033 and -034. *The Journal of Antibiotics* **1992,** *45* (2), 207-12.

30. Ohtsuka, T.; Kotaki, H.; Nakayama, N.; Itezono, Y.; Shimma, N.; Kudoh, T.; Kuwahara, T.; Arisawa, M.; Yokose, K.; Seto, H., Tetronothiodin, a novel cholecystokinin type-B receptor antagonist produced by Streptomyces sp. NR0489. II. Isolation, characterization and biological activities. *The Journal of Antibiotics* **1993,** *46* (1), 11-7.

31. Ashton, R. J.; Kenig, M. D.; Luk, K.; Planterose, D. N.; Scott-Wood, G., MM 46115, a new antiviral antibiotic from Actinomadura pelletieri. Characteristics of the producing cultures, fermentation, isolation, physico-chemical and biological properties. *The Journal of Antibiotics* **1990,** *43* (11), 1387-93.

32. White-Phillip, J.; Thibodeaux, C. J.; Liu, H., Enzymatic synthesis of TDP-deoxysugars. *Methods in Enzymology* **2009,** *459*, 521-544.

33. Lehninger, A. L.; Nelson, D. L.; Cox, M. M., *Lehninger Principles of Biochemistry*. WH Freeman & Co: 2005; Vol. 1.

34. Iwasaki, A.; Matsumoto, K.; Hasegawa, J.; Yasohara, Y., A novel transaminase, (R)-amine:pyruvate aminotransferase, from Arthrobacter sp. KNK168 (FERM BP-5228): purification, characterization, and gene cloning. *Applied Microbiology and Biotechnology* **2012,** *93* (4), 1563-73.

35. Burgie, E. S.; Holden, H. M., Molecular architecture of DesI: a key enzyme in the biosynthesis of desosamine. *Biochemistry* **2007,** *46* (31), 8999-9006.

36. Schoenhofen, I. C.; Lunin, V. V.; Julien, J. P.; Li, Y.; Ajamian, E.; Matte, A.; Cygler, M.; Brisson, J. R.; Aubry, A.; Logan, S. M.; Bhatia, S.; Wakarchuk, W. W.; Young, N. M., Structural and functional characterization of PseC, an aminotransferase involved in the biosynthesis of pseudaminic acid, an essential flagellar

modification in Helicobacter pylori. *The Journal of Biological Chemistry* **2006,** *281* (13), 8907-16.

37. Schafer, M.; Schneider, T. R.; Sheldrick, G. M., Crystal structure of vancomycin. *Structure* **1996,** *4* (12), 1509-15.

38. van Wageningen, A. M.; Kirkpatrick, P. N.; Williams, D. H.; Harris, B. R.; Kershaw, J. K.; Lennard, N. J.; Jones, M.; Jones, S. J.; Solenberg, P. J., Sequencing and analysis of genes involved in the biosynthesis of a vancomycin group antibiotic. *Chemistry & Biology* **1998,** *5* (3), 155-62.

39. Chen, H.; Thomas, M. G.; Hubbard, B. K.; Losey, H. C.; Walsh, C. T.; Burkart, M. D., Deoxysugars in glycopeptide antibiotics: enzymatic synthesis of TDP-L-epivancosamine in chloroeremomycin biosynthesis. *Proceedings of the National Academy of Sciences of the United States of America* **2000,** *97* (22), 11942-7.

40. Marolda, C. L.; Valvano, M. A., Genetic analysis of the dTDP-rhamnose biosynthesis region of the Escherichia coli VW187 (O7:K1) rfb gene cluster: identification of functional homologs of rfbB and rfbA in the rff cluster and correct location of the rffE gene. *Journal of Bacteriology* **1995,** *177* (19), 5539-46.

41. Zhu, H.; Choi, H. K.; Cook, D. R.; Shoemaker, R. C., Bridging model and crop legumes through comparative genomics. *Plant Physiology* **2005,** *137* (4), 1189-1196.

42. Hosted, T.; Horan, A.; Wang, T., Everninomicin biosynthetic genes. *WO Patent* WO/2001/051,639: **2001**.

43. Weitnauer, G.; Muhlenweg, A.; Trefzer, A.; Hoffmeister, D.; Sussmuth, R. D.; Jung, G.; Welzel, K.; Vente, A.; Girreser, U.; Bechthold, A., Biosynthesis of the orthosomycin antibiotic avilamycin A: deductions from the molecular analysis of the avi biosynthetic gene cluster of Streptomyces viridochromogenes Tu57 and production of new antibiotics. *Chemistry & Biology* **2001,** *8* (6), 569-81.

44. Gaisser, S.; Trefzer, A.; Stockert, S.; Kirschning, A.; Bechthold, A., Cloning of an avilamycin biosynthetic gene cluster from Streptomyces viridochromogenes Tu57. *Journal of Bacteriology* **1997,** *179* (20), 6271-8.

45. Farnet, C.; Zazopoulos, E.; Staffa, A., Compositions and methods for identifying and distinguishing orthosomycin biosynthetic loci. *WO Patent* WO/2002/079,505: *2002*.

46. da Silva Madeira, L.; Ferreira-Leitao, V. S.; da Silva Bon, E. P., Dibenzothiophene oxidation by horseradish peroxidase in organic media: effect of the DBT:H2O2 molar ratio and H2O2 addition mode. *Chemosphere* **2008,** *71* (1), 189-94.

47. Lo, H.; Reeves, R. E., Purification and properties of NADPH:flavin oxidoreductase from Entamoeba histolytica. *Molecular and Biochemical Parasitology* **1980,** *2* (1), 23-30.

48. Mazue, G.; Iatropoulos, M.; Imondi, A.; Castellino, S.; Brughera, M.; Podesta, A.; Dellatorre, P.; Moneta, D., Anthracyclines - a review of general and special toxicity studies. *International Journal of Oncology* **1995,** *7* (4), 713-26.

49. Bryant, J.; Picot, J.; Levitt, G.; Sullivan, I.; Baxter, L.; Clegg, A., Cardioprotection against the toxic effects of anthracyclines given to children with cancer: a systematic review. *Health Technology Assessment* **2007,** *11* (27), iii, ix-x, 1-84.

50. Kaye, S.; Merry, S., Tumour cell resistance to anthracyclines--a review. *Cancer Chemotherapy and Pharmacology* **1985,** *14* (2), 96-103.

51. Trouet, A.; Deprez-De Campeneere, D., Daunorubicin-DNA and doxorubicin-DNA. A review of experimental and clinical data. *Cancer Chemotherapy and Pharmacology* **1979,** *2* (1), 77-9.

52. Weiss, R. B., *The anthracyclines: will we ever find a better doxorubicin?*, **1992**; p 670.

53. Minotti, G.; Menna, P.; Salvatorelli, E.; Cairo, G.; Gianni, L., Anthracyclines: molecular advances and pharmacologic developments in antitumor activity and cardiotoxicity. *Pharmacological Reviews* **2004,** *56* (2), 185-229.

54. Lopes, M. A.; Meisel, A.; Dirnagl, U.; Carvalho, F. D.; Bastos Mde, L., Doxorubicin induces biphasic neurotoxicity to rat cortical neurons. *Neurotoxicology* **2008,** *29* (2), 286-93.

55. Coukell, A. J.; Faulds, D., Epirubicin. An updated review of its pharmacodynamic and pharmacokinetic properties and therapeutic efficacy in the management of breast cancer. *Drugs* **1997,** *53* (3), 453-82.

56. Ormrod, D.; Holm, K.; Goa, K.; Spencer, C., Epirubicin: a review of its efficacy as adjuvant therapy and in the treatment of metastatic disease in breast cancer. *Drugs & Aging* **1999,** *15* (5), 389-416.

57. Onrust, S. V.; Wiseman, L. R.; Goa, K. L., Epirubicin: a review of its intravesical use in superficial bladder cancer. *Drugs & Aging* **1999,** *15* (4), 307-33.

58. Khasraw, M.; Bell, R.; Dang, C., Epirubicin: is it like doxorubicin in breast cancer? A clinical review. *Breast* **2012,** *21* (2), 142-9.

59. Hollingshead, L. M.; Faulds, D., Idarubicin. A review of its pharmacodynamic and pharmacokinetic properties, and therapeutic potential in the chemotherapy of cancer. *Drugs* **1991,** *42* (4), 690-719.

60. Crivellari, D.; Lombardi, D.; Spazzapan, S.; Veronesi, A.; Toffoli, G., New oral drugs in older patients: a review of idarubicin in elderly patients. *Critical Reviews in Oncology/Hematology* **2004,** *49* (2), 153-63.

61. Buckley, M. M.; Lamb, H. M., Oral idarubicin. A review of its pharmacological properties and clinical efficacy in the treatment of haematological malignancies and advanced breast cancer. *Drugs & Aging* **1997,** *11* (1), 61-86.

62. Binaschi, M.; Farinosi, R.; Borgnetto, M. E.; Capranico, G., In vivo site specificity and human isoenzyme selectivity of two topoisomerase II-poisoning anthracyclines. *Cancer Research* **2000,** *60* (14), 3770-6.

63. Ota, K., Clinical review of aclacinomycin A in Japan. *Drugs under Experimental and Clinical Research* **1985,** *11* (1), 17-21.

64. Oka, S., A review of clinical studies on aclacinomycin A--phase I and preliminary phase II evaluation of ACM. *The Science Reports of the Research Institutes, Tohoku University. Ser. C, Medicine. Tohoku Daigaku* **1978,** *25* (3-4), 37-49.

65. Smith, I. E., Mitoxantrone (novantrone): a review of experimental and early clinical studies. *Cancer Treatment Reviews* **1983,** *10* (2), 103-15.

66. Bowles, D. W.; Flaig, T. W., Mitoxantrone-associated acute myelogenous leukemia in a patient with high-risk adenocarcinoma of the prostate: a case report and brief review. *Cancer Investigation* **2006,** *24* (5), 517-20.

67. Ehninger, G.; Schuler, U.; Proksch, B.; Zeller, K. P.; Blanz, J., Pharmacokinetics and metabolism of mitoxantrone. A review. *Clinical Pharmacokinetics* **1990,** *18* (5), 365-80.

68. Yoshimoto, A.; Johdo, O.; Fujii, S.; Kubo, K.; Nishida, H.; Okamoto, R.; Takeuchi, T., Anthracycline metabolites from baumycin-producing Streptomyces sp. D788. I. Isolation of antibiotic-blocked mutants and their characterization. *The Journal of Antibiotics* **1992,** *45* (8), 1255-67.

69. Yoshimoto, A.; Fujii, S.; Johdo, O.; Kubo, K.; Nishida, H.; Okamoto, R.; Takeuchi, T., Anthracycline metabolites from baumycin-producing Streptomyces sp. D788. II. New anthracycline metabolites produced by a blocked mutant strain RPM-5. *The Journal of Antibiotics* **1993,** *46* (1), 56-64.

70. Yoshimoto, A.; Johdo, O.; Nishida, H.; Okamoto, R.; Takeuchi, T., Anthracycline metabolites from baumycin-producing Streptomyces sp. D788. III. New anthracycline metabolites produced by blocked mutants 4L-660 and YDK-18. *The Journal of Antibiotics* **1993,** *46* (11), 1758-61.

71. Matsuzawa, Y.; Yoshimoto, A.; Kouno, K.; Oki, T., Baumycin analogs isolated from Actinomadura sp. *The Journal of Antibiotics* **1981,** *34* (6), 774-6.

72. Hutchinson, C. R., Biosynthetic Studies of Daunorubicin and Tetracenomycin C. *Chemical Reviews* **1997,** *97* (7), 2525-2536.

73. Meurer, G.; Gerlitz, M.; Wendt-Pienkowski, E.; Vining, L. C.; Rohr, J.; Hutchinson, C. R., Iterative type II polyketide synthases, cyclases and ketoreductases exhibit context-dependent behavior in the biosynthesis of linear and angular decapolyketides. *Chemistry & Biology* **1997,** *4* (6), 433-43.

74. Cragg, G. M.; Kingston, D. G. I.; Newman, D. J., *Anticancer Agents from Natural Products*. CRC Press: 2011.

75. Otten, S. L.; Liu, X.; Ferguson, J.; Hutchinson, C. R., Cloning and characterization of the Streptomyces peucetius dnrQS genes encoding a daunosamine biosynthesis enzyme and a glycosyl transferase involved in daunorubicin biosynthesis. *Journal of Bacteriology* **1995,** *177* (22), 6688-6692.

76. Olano, C.; Lomovskaya, N.; Fonstein, L.; Roll, J. T.; Hutchinson, C. R., A two-plasmid system for the glycosylation of polyketide antibiotics: bioconversion of epsilon-rhodomycinone to rhodomycin D. *Chemistry & Biology* **1999,** *6* (12), 845-55.

77. LINDQUIST, L.; KAISER, R.; REEVES, P. R.; LINDBERG, A. A., Purification, characterization and HPLC assay of Salmonella glucose-1-phosphate thymidylyltransferase from the cloned rfbA gene. *European Journal of Biochemistry* **1993,** *211* (3), 763-770.

78. Lomovskaya, N.; Doi-Katayama, Y.; Filippini, S.; Nastro, C.; Fonstein, L.; Gallo, M.; Colombo, A. L.; Hutchinson, C. R., The Streptomyces peucetius dpsY and dnrX genes govern early and late steps of daunorubicin and doxorubicin biosynthesis. *Journal of Bacteriology* **1998,** *180* (9), 2379-86.

79. van Berkel, W. J.; Kamerbeek, N. M.; Fraaije, M. W., Flavoprotein monooxygenases, a diverse class of oxidative biocatalysts. *Journal of Biotechnology* **2006,** *124* (4), 670-89.

80. Massey, V., The chemical and biological versatility of riboflavin. *Biochemical Society Transactions* **2000,** *28* (4), 283-96.

81. Valton, J.; Fontecave, M.; Douki, T.; Kendrew, S. G.; Niviere, V., An aromatic hydroxylation reaction catalyzed by a two-component FMN-dependent Monooxygenase. The ActVA-ActVB system from Streptomyces coelicolor. *The Journal of Biological Chemistry* **2006,** *281* (1), 27-35.

82. Torres Pazmino, D. E.; Dudek, H. M.; Fraaije, M. W., Baeyer-Villiger monooxygenases: recent advances and future challenges. *Current Opinion in Chemical Biology* **2010,** *14* (2), 138-44.

83. Seo, M. J.; Zhu, D.; Endo, S.; Ikeda, H.; Cane, D. E., Genome mining in Streptomyces. Elucidation of the role of Baeyer-Villiger monooxygenases and non-heme iron-dependent dehydrogenase/oxygenases in the final steps of the biosynthesis of pentalenolactone and neopentalenolactone. *Biochemistry* **2011,** *50* (10), 1739-54.

84. Balasubramanian, R.; Smith, S. M.; Rawat, S.; Yatsunyk, L. A.; Stemmler, T. L.; Rosenzweig, A. C., Oxidation of methane by a biological dicopper centre. *Nature* **2010,** *465* (7294), 115-9.

85. Adams, M. A.; Jia, Z., Structural and biochemical evidence for an enzymatic quinone redox cycle in Escherichia coli: identification of a novel quinol monooxygenase. *The Journal of Biological Chemistry* **2005,** *280* (9), 8358-63.

86. Jansson, A.; Koskiniemi, H.; Erola, A.; Wang, J.; Mantsala, P.; Schneider, G.; Niemi, J., Aclacinomycin 10-hydroxylase is a novel substrate-assisted hydroxylase requiring S-adenosyl-L-methionine as cofactor. *The Journal of Biological Chemistry* **2005,** *280* (5), 3636-44.

87. Joosten, V.; van Berkel, W. J. H., Flavoenzymes. *Current Opinion in Chemical Biology* **2007,** *11* (2), 195-202.

88. Opperman, D. J.; Reetz, M. T., Towards practical Baeyer-Villiger-monooxygenases: design of cyclohexanone monooxygenase mutants with enhanced oxidative stability. *Chembiochem : a European Journal of Chemical Biology* **2010,** *11* (18), 2589-96.

89. Hastings, J. W.; Balny, C.; Peuch, C. L.; Douzou, P., Spectral properties of an oxygenated luciferase-flavin intermediate isolated by low-temperature chromatography. *Proceedings of the National Academy of Sciences of the United States of America* **1973,** *70* (12 Pt 1-2), 3468-72.

90. Frederick, K. K.; Palfey, B. A., Kinetics of proton-linked flavin conformational changes in p-hydroxybenzoate hydroxylase. *Biochemistry* **2005,** *44* (40), 13304-14.

91. Macheroux, P., UV-visible spectroscopy as a tool to study flavoproteins. *METHODS IN MOLECULAR BIOLOGY-CLIFTON THEN TOTOWA*- **1999,** *131*, 1-8.

92. Ortiz-Maldonado, M.; Ballou, D. P.; Massey, V., A rate-limiting conformational change of the flavin in p-hydroxybenzoate hydroxylase is necessary for ligand exchange and catalysis: studies with 8-mercapto- and 8-hydroxy-flavins. *Biochemistry* **2001,** *40* (4), 1091-101.

93. Enroth, C., High-resolution structure of phenol hydroxylase and correction of sequence errors. *Acta crystallographica. Section D, Biological Crystallography* **2003,** *59* (Pt 9), 1597-602.

94. Torres Pazmino, D. E.; Riebel, A.; de Lange, J.; Rudroff, F.; Mihovilovic, M. D.; Fraaije, M. W., Efficient biooxidations catalyzed by a new generation of self-sufficient Baeyer-Villiger monooxygenases. *Chembiochem : a European Journal of Chemical Biology* **2009,** *10* (16), 2595-8.

95. Cheesman, M. J.; Kneller, M. B.; Kelly, E. J.; Thompson, S. J.; Yeung, C. K.; Eaton, D. L.; Rettie, A. E., Purification and characterization of hexahistidine-tagged cyclohexanone monooxygenase expressed in Saccharomyces cerevisiae and Escherichia coli. *Protein Expression and Purification* **2001,** *21* (1), 81-6.

96. Mirza, I. A.; Yachnin, B. J.; Wang, S.; Grosse, S.; Bergeron, H.; Imura, A.; Iwaki, H.; Hasegawa, Y.; Lau, P. C.; Berghuis, A. M., Crystal structures of cyclohexanone monooxygenase reveal complex domain movements and a sliding cofactor. *Journal of the American Chemical Society* **2009,** *131* (25), 8848-54.

97. Mihovilovic, M. D.; Rudroff, F.; Winninger, A.; Schneider, T.; Schulz, F.; Reetz, M. T., Microbial Baeyer-Villiger oxidation: stereopreference and substrate acceptance of cyclohexanone monooxygenase mutants prepared by directed evolution. *Organic Letters* **2006,** *8* (6), 1221-4.

98. Joosten, V.; van Berkel, W. J., Flavoenzymes. *Current Opinion in Chemical Biology* **2007,** *11* (2), 195-202.

99. Mattevi, A., To be or not to be an oxidase: challenging the oxygen reactivity of flavoenzymes. *Trends in Biochemical Sciences* **2006,** *31* (5), 276-83.

100. Furukawa, H.; Wieser, M.; Morita, H.; Sugio, T.; Nagasawa, T., Purification and characterization of vanillyl-alcohol oxidase from Byssochlamys fulva V107. *Journal of Bioscience and Bioengineering* **1999,** *87* (3), 285-90.

101. Southan, C.; DeWolf, W. E., Jr.; Kruse, L. I., Inactivation of dopamine beta-hydroxylase by p-cresol: evidence for a second, minor site of covalent modification at tyrosine 357. *Biochimica et Biophysica Acta* **1990,** *1037* (2), 256-8.

102. Petsko, G. A.; Ringe, D., *Protein Structure and Function*. Sinauer Associates Inc: 2004.

103. Laden, B. P.; Tang, Y.; Porter, T. D., Cloning, heterologous expression, and enzymological characterization of human squalene monooxygenase. *Archives of Biochemistry and Biophysics* **2000,** *374* (2), 381-8.

104. Beam, M. P.; Bosserman, M. A.; Noinaj, N.; Wehenkel, M.; Rohr, J., Crystal Structure of Baeyer− Villiger Monooxygenase MtmOIV, the Key Enzyme of the Mithramycin Biosynthetic Pathway. *Biochemistry* **2009,** *48* (21), 4476-4487.

105. Hieber, A. D.; Bugos, R. C.; Yamamoto, H. Y., Plant lipocalins: violaxanthin de-epoxidase and zeaxanthin epoxidase. *Biochimica et Biophysica acta* **2000,** *1482* (1-2), 84-91.

106. Eppink, M. H.; Schreuder, H. A.; Van Berkel, W. J., Identification of a novel conserved sequence motif in flavoprotein hydroxylases with a putative dual function in FAD/NAD(P)H binding. *Protein Science : a Publication of the Protein Society* **1997,** *6* (11), 2454-8.

107. Phillips, I. R.; Shephard, E. A., Flavin-containing monooxygenases: mutations, disease and drug response. *Trends in Pharmacological Sciences* **2008,** *29* (6), 294-301.

108. Olucha, J.; Lamb, A. L., Mechanistic and structural studies of the N-hydroxylating flavoprotein monooxygenases. *Bioorganic Chemistry* **2011,** *39* (5-6), 171-7.

109. Ziegler, D. M., An overview of the mechanism, substrate specificities, and structure of FMOs. *Drug Metabolism Reviews* **2002,** *34* (3), 503-11.

110. Meneely, K. M.; Barr, E. W.; Bollinger, J. M., Jr.; Lamb, A. L., Kinetic mechanism of ornithine hydroxylase (PvdA) from Pseudomonas aeruginosa: substrate

triggering of O2 addition but not flavin reduction. *Biochemistry* **2009,** *48* (20), 4371-6.

111. Fraaije, M. W.; Kamerbeek, N. M.; van Berkel, W. J.; Janssen, D. B., Identification of a Baeyer-Villiger monooxygenase sequence motif. *FEBS Lett* **2002,** *518* (1-3), 43-7.

112. Donoghue, N. A.; Norris, D. B.; Trudgill, P. W., The purification and properties of cyclohexanone oxygenase from Nocardia globerula CL1 and Acinetobacter NCIB 9871. *European Journal of Biochemistry / FEBS* **1976,** *63* (1), 175-92.

113. Torres Pazmino, D. E.; Baas, B. J.; Janssen, D. B.; Fraaije, M. W., Kinetic mechanism of phenylacetone monooxygenase from Thermobifida fusca. *Biochemistry* **2008,** *47* (13), 4082-93.

114. Wierenga, R., The TIM-barrel fold: a versatile framework for efficient enzymes. *FEBS Letters* **2001,** *492* (3), 193-198.

115. Villa, R.; Willetts, A., Oxidations by microbial NADH plus FMN-dependent luciferases from< i> Photobacterium phosphoreum</i> and< i> Vibrio fischeri</i>. *Journal of Molecular Catalysis B: Enzymatic* **1997,** *2* (4), 193-197.

116. McGhie, E. J.; Littlechild, J. A., The purification and crystallisation of 2,5-diketocamphane 1,2-monooxygenase and 3,6-diketocamphane 1,6-monooxygenase from Pseudomonas putida NCIMB 10007. *Biochemical Society Transactions* **1996,** *24* (1), 29S.

117. Eichhorn, E.; van der Ploeg, J. R.; Leisinger, T., Characterization of a two-component alkanesulfonate monooxygenase from Escherichia coli. *The Journal of Biological Chemistry* **1999,** *274* (38), 26639-46.

118. Eichhorn, E.; Davey, C. A.; Sargent, D. F.; Leisinger, T.; Richmond, T. J., Crystal structure of Escherichia coli alkanesulfonate monooxygenase SsuD. *Journal of Molecular Biology* **2002,** *324* (3), 457-68.

119. Ohshiro, T.; Izumi, Y., Purification, characterization and crystallization of enzymes for dibenzothiophene desulfurization. *Bioseparation* **2000,** *9* (3), 185-8.

120. Li, J.; Feng, J.; Li, Q.; Ma, C.; Yu, B.; Gao, C.; Wu, G.; Xu, P., Both FMNH2 and FADH2 can be utilized by the dibenzothiophene monooxygenase from a desulfurizing bacterium Mycobacterium goodii X7B. *Bioresource Technology* **2009,** *100* (9), 2594-2599.

121. Galan, B.; Diaz, E.; Prieto, M. A.; Garcia, J. L., Functional analysis of the small component of the 4-hydroxyphenylacetate 3-monooxygenase of Escherichia coli W: a prototype of a new Flavin:NAD(P)H reductase subfamily. *Journal of Bacteriology* **2000,** *182* (3), 627-36.

122. Kim, S. H.; Hisano, T.; Takeda, K.; Iwasaki, W.; Ebihara, A.; Miki, K., Crystal structure of the oxygenase component (HpaB) of the 4-hydroxyphenylacetate 3-monooxygenase from Thermus thermophilus HB8. *The Journal of Biological Chemistry* **2007,** *282* (45), 33107-17.

123. Buttner, D.; Lorenz, C.; Weber, E.; Bonas, U., Targeting of two effector protein classes to the type III secretion system by a HpaC- and HpaB-dependent protein complex from Xanthomonas campestris pv. vesicatoria. *Molecular Microbiology* **2006,** *59* (2), 513-27.

124. Xun, L.; Webster, C. M., A monooxygenase catalyzes sequential dechlorinations of 2, 4, 6-trichlorophenol by oxidative and hydrolytic reactions. *Journal of Biological Chemistry* **2004,** *279* (8), 6696-6700.

125. Pace, C. P.; Stankovich, M. T., Oxidation-reduction properties of short-chain acyl-CoA dehydrogenase: effects of substrate analogs. *Archives of Biochemistry and Biophysics* **1994,** *313* (2), 261-6.

126. Di Gennaro, P.; Colmegna, A.; Galli, E.; Sello, G.; Pelizzoni, F.; Bestetti, G., A new biocatalyst for production of optically pure aryl epoxides by styrene monooxygenase from Pseudomonas fluorescens ST. *Applied and Environmental Microbiology* **1999,** *65* (6), 2794-7.

127. Schaus, S. E.; Brandes, B. D.; Larrow, J. F.; Tokunaga, M.; Hansen, K. B.; Gould, A. E.; Michael, E.; Jacobsen, E. N., Highly selective hydrolytic kinetic resolution of terminal epoxides catalyzed by chiral (salen) CoIII complexes. Practical synthesis of enantioenriched terminal epoxides and 1, 2-diols. *Journal of the American Chemical Society* **2002,** *124* (7), 1307-1315.

128. Keller, S.; Wage, T.; Hohaus, K.; Holzer, M.; Eichhorn, E.; van Pee, K. H., Purification and Partial Characterization of Tryptophan 7-Halogenase (PrnA) from Pseudomonas fluorescens *Angewandte Chemie* **2000,** *39* (13), 2300-2302.

129. Dong, C.; Flecks, S.; Unversucht, S.; Haupt, C.; Van Pee, K. H.; Naismith, J. H., Tryptophan 7-halogenase (PrnA) structure suggests a mechanism for regioselective chlorination. *Science* **2005,** *309* (5744), 2216-2219.

CHAPTER II

BIOCHEMICAL CHARACTERIZATION OF A NEW FLAVIN-DEPENDENT NITROSOSYNTHASE IN THE BIOSYNTHETIC PATHWAYS OF EVERNINOMICIN AND RUBRADIRIN

Introduction

Many bioactive bacterial natural products are appended to highly modified deoxysugar moities that are often important for their biological activities. These deoxysugar appendages are typically biosynthesized in the form of nucleotide diphosphate (NDP) sugars before the attachment to their corresponding aglycones by the activity of glycosyltransferases. Thymidine diphosphate (TDP)-activated sugars are the most structurally diverse class of nucleotide sugars found in nature.[1] Deoxygenation of these sugars proceeds via a 4-keto-6-deoxy intermediate, catalyzed by a 4,6-dehydratase, which provides the entry point into TDP-deoxysugar secondary metabolism in bacteria.[2] Deoxyaminosugars are among the most prevalent sugars in sugar-containing bacterial secondary metabolites.

The recent advances in gene cluster elucidations of glycoslated natural products facilitated the studies of several deoxyaminosugar pathways. Biosynthesis of deoxyaminosugars includes genes encoding dehydratases, isomerases, aminotransferases, methyltransferases, and glycosyltransferases.[3] The biosynthesis of TDP-L-epivancosamine (Scheme I-2) is one of the well-studied deoxyaminosugar pathways. Five enzymes from the biosynthetic pathway of chloroeremomycin produced

by *Amycolatopsis orientalis*, have been shown to be involved in its biosynthesis starting from TDP-6-deoxy-4-keto-D-glucose. These enzymes were shown to perform C-2 deoxygenation by EvaA, C-3 amination and methylation by EvaB and EvaC respectively, C-5 epimerization by EvaD, and C-4 ketoreduction by EvaE.[4]

Oxidized congeners of deoxyaminosugars also exist in many natural products such as everninomicin from *Micromonospora carbonacea* var. *Africana* and var. *aurantiaca*, rubradirin from *Streptomyces achromogenes* var. *rubradiris*, and kijanimycin from *Actinomycete Actinomadura kijaniata* (Figure II-1).[5-7] Hydroxyamino-, nitroso-, and nitrosugar derivatives of everninomicin have been isolated from the fermentation of some of its producers.[8] It was shown that the N-oxidation of deoxyaminosugars leads to significant change in the antibacterial activity of the parent molecule. For example, the antibacterial activity against *Staphylococcus aureus* was 125 fold greater for the nitro- vs. the amino-sugar variant of everninomicin.[9] This underlines the significance of studying the biosynthetic pathway of this important deoxsugar modification. The knowledge that will be gained from understanding this important N-oxidation reaction will impact current efforts towards natural product structure diversification, as well as introduce new biosynthetic enzymes to be utilized for otherwise difficult to perform oxidation reactions.

The oligosaccharide everninomicin belongs to the orthosomycin class of antibiotics and possesses potent activity against Gram-positive and Gram-negative bacteria including vancomycin resistant *enterococci*, methicillin resistant *staphylococci*,

and penicillin-resistant *streptococci*.[10] The structure of everninomicin is composed of eight deoxysugars including a terminal nitrosugar, orsellinic and dichloroisoeverninic acid moieties. The nitrosugar in everninomicin is called 2,3,6-trideoxy-3-C-methyl-4-O-methyl-3-nitro-L-ribo-aldohexo-pyranose or evernitrose which is structurally related to D-rubranitrose present in the polyketide rubradirin and to D-kijanose in the spirotetronate polyketide antibiotic kijanimicin shown in figure II-1.

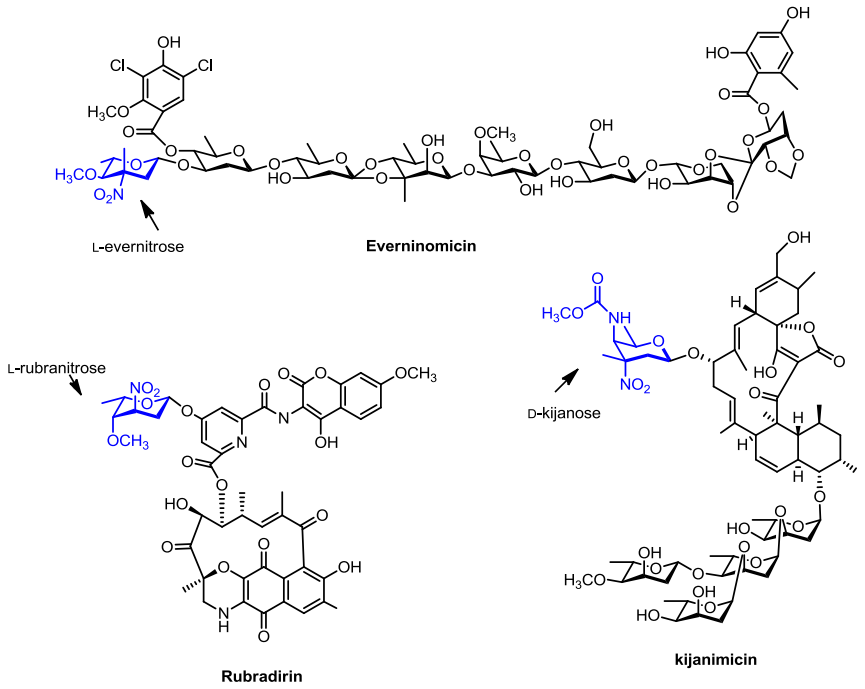

Figure II-1. Chemical structures of everninomicin, rubradirin, and kijanimicin.

Structurally related to everninomicins are the heptasaccharides avilamycins,[11] which lack the nitrosugar moiety and hence, were good candidates for performing comparative genomic analysis to identify the the nitrosugar biosynthetic gene in

everninomicins. These analyses identified a cassette of genes most of them having homologues in the biochemically characterized L-epivancosamine pathway in the biosynthesis of chloroeremomycin. The *orf36* gene from *M. carbonacea* var. *Africana* (*orf42* from *M.* Var. *aurantiaca*) was proposed to encode a flavin-dependent oxidase responsible for the N-oxidation of a TDP-aminosugar precursor to form the C-3 nitro group present in the nitrosugar moiety in everninomicin.[12]

Homologues of the putative ORF36 enzyme were also found in the recently sequenced gene clusters of the nitrosugar-containing compounds rubradirin and kijanimicin. ORF36 is 63% identical to RubN8 from the rubradirin biosynthetic pathway and 65% identical to KijD3 from the kijanimicin pathway. The high sequence similarities among these enzymes and their moderate homology to flavin-dependent enzymes, suggests that they play roles as N-oxidases in the biosynthesis of the nitrosugar moiety in their corresponding natural product pathways.

Despite this striking sequence-based analysis, biochemical characterization of these putative flavin-dependent enzymes in the N-oxidation of aminosugars has not been previously performed. In this study, we targeted the producers of everninomicin and rubradirin and amplified the two putative flavin dependent oxidase genes *orf36* from *M.carbonacea* var. *africana* and *rubn8* from *S. achromogenes* var*. rubradiris.* Genes were amplified from their corresponding genomic DNA by the polymerase chain reaction (PCR). The PCR products were subcloned into a pET28a expression plasmid and transfomed to *E.coli* BL21(*DE3*) via electroporation. The proteins were overexpressed

and purified to homogeneity by Ni^{+2}-affinity chromatography. A close analog to the authentic substrate evernosamine (TDP-L-epivancosamine), lacking the C4 O-methylation, was prepared *in situ* by a Staudinger reduction[13] of a synthetic azide congener with tris(2-carboxyethyl)phosphine. Next, we developed an LC-ESI-MS method to assay the activity of the putative oxidases with the synthetically prepared TDP-L-epivancosamine. Besides the putative oxidase and the substrate TDP-L-epivancosamine, the assay included FAD, NADPH and an external flavin reductase from *Photobacterium fischeri*[14] to generate reduced flavin required for catalysis.

Results and discussion

Comparative genomics

Avilamycins are heptasaccharides with structures very similar to everninomicins but lacking the nitrosugar moiety (Figure II-2). Another main structural difference is the lack of the terminal orsellinic acid moiety present in everninomicins which is replaced by an acetyl group in avilamycins. The availability of gene cluster data for these oligosaccharides from different bacterial producers facilitated a comparative genomic analysis to identify the genes responsible for the biosynthesis of the nitrosugar moiety in everninomicins. These analyses were performed on two everninomicin producers: *Micromonospora carbonacae var. aurantiaca* and *Micromonospora carbonacea var. africana,* and two avilamycin producers; *Streptomyces viridochromogenes* and

Streptomyces mobaraensis.[12] This comparative genomic approach identified a cassette of genes as candidates for the biosynthesis of the nitrosugar evernitrose, homologues of which are found in the biosynthetic pathway of the aminosugar L-epivancosamine from the chloroeremomycin biosynthesis. A list of these genes was shown in table I-1.

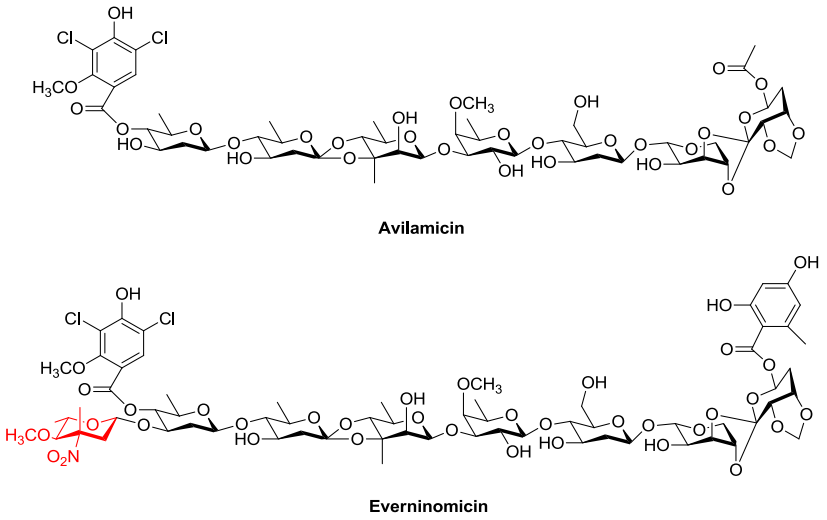

Figure II-2. Chemical structures of avilamycin and everninomicin.

The L-epivancosamine moiety in chloroeremomycin is an aminosugar structurally related to the nitrosugar evernitrose[15] lacking the C3 N-oxidation and the C4 O-methylation (Figure II-3); therefore, most enzymes responsible for its biosynthesis are shared with those in the L-evernitrose's biosynthetic pathway.[4] Additional genes were identified in the everninomicin clusters that likely account for the C4 O-methylation and the C3 N-oxidation. The *orf41* gene from the EVEA cluster encodes a SAM dependent C4

O-methyltransferase most likely responsible for the methylation of the C4 hydroxyl group to form the C4 methoxy group in L-evernitrose.

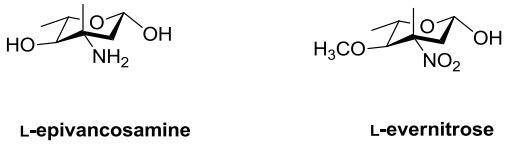

L-epivancosamine L-evernitrose

Figure II-3. Chemical structures of L-*epi*-vancosamine and L-evernitrose.

Three additional genes encoding putative oxidases in the everninomicin clusters were also identified in this comparative genomic analysis namely, *orf36, orf18, orf19* from the EVEA cluster. *Orf18* has a reasonable homology to RNA-methyltransferase genes, whereas *orf19* is homologous to copper-dependent oxidase genes involved in primary metabolism; therefore, neither is likely to be involved in the biosynthesis of the nitrosugar moiety in everninomicin. The only remaining and likely oxidase responsible for the N-oxidation an aminosugar precursor is *orf36* in the EVEA cluster. This gene has moderate sequence homology with the flavin-dependent monooxygenase dibenzothiophene oxidase DszC, which has been shown to oxidize a sulfide group to a sulfone via a sulfoxide intermediate.[16] The encoded ORF36, RubN8 and KijD3 proteins also shared moderate sequence similarity (~25%) with the acyl-CoA dehydrogenase family of enzymes. Acyl-CoA dehydrogenases are also flavin-dependent enzymes and are used as a structural model for class-D flavin-dependent monooxygenases.[17]

Preparation of the putative oxidases and their aminosugar substrate

We targeted the producers of everninomicin[18] and rubradirin[19] to prepare the putative enzymes responsible for the aminosugar oxidation to form the nitro group in their deoxynitrosugar moieties. The genes *orf36* from *Micromonospora* var. *africana* and *rubn8* from *Streptomyces achromogenes* var. *rubradiris* were proposed to encode a flavin-dependent monooxygenase responsible for the N-oxidation of a TDP-activated deoxyaminosugar precursor.[20-21] We amplified these genes using the genomic DNA of their producers via the polymerase chain reaction (PCR), and cloned the resulting gene products into the NdeI/HindIII site of the expression plasmid pET28.[22] The gene products were designed to encode an N-terminal hexahistidine tag to facilitate the protein purification using a Ni^{2+}-affinity column. The recombinant plasmids were transformed to the *E.coli* strain BL21 (DE3) for overexpression. Both proteins were found to require 0.1 mM β–D-1-thiogalactopyranoside (IPTG) and the best expression temperature was found to be 28 °C. Analysis of the purified proteins by SDS-PAGE showed protein bands consistent with their calculated molecular weight (~44 kD) as shown in figure II-4 for the Ni^{2+}-purified RubN8.

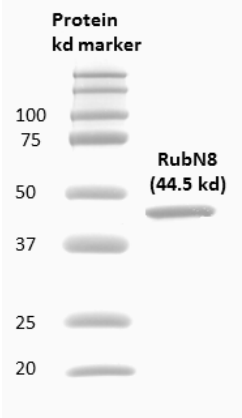

Figure II-4. SDS-PAGE gel of Ni2+-affinity purified RubN8.

A close substrate analogue, (5:1 β/α)-TDP-L-epivancosamine, in which the C-4 methoxy group is replaced by a hydroxyl group, was prepared by *in situ* Staudinger reaction of its synthetic azide congener with tris(2-carboxyethyl)phosphine (TCEP) (Figure II-5). The azide congener was kindly provided to us by Prof. Daniel Kahne's research group at Harvard University.[23] We expected TDP-L-epivancosomine to be a candidate substrate for the amine oxidation by the proposed oxidases although it lacked the C4 O-methylation because an everninomicin variant, in which the methoxy group at C-4 of the nitrosugar moiety is replaced by a hydroxyl group, was also isolated from the fermentation of *M. micromonospora* var. *africana*.[8] HPLC-MS analysis of the above mentioned Staudinger reaction showed that 95% of the (5:1)-β/α mixture of TDP-L-epivancosamine azide could be reduced to L-TDP-epi-vancosamine providing the aminosugar substrate for ORF36 and RubN8 biochemical characterization.

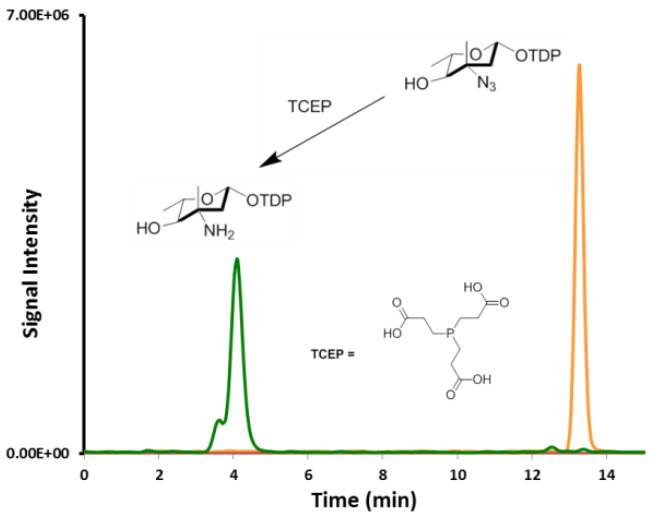

Figure II-5. LC-ESI-MS analysis of the Staudinger reduction of the synthetic (5:1 β/α)-azido congener of TDP-L-*epi*-vancosamine by TCEP.

Enzymatic activities of ORF36 and RubN8

As discussed in the introduction, ORF36 and RubN8 from the everninomycin and rubradirin biosynthetic pathways, respectively, are proposed to be flavin-dependent enzymes responsible for the N-oxidation of TDP-activated aminosugar, which ultimately produces its nitrosugar congener. These putative oxidases share moderate homology with the flavin-dependent enzyme DszC, which oxidizes dibenzothiophene (DBT) to DBT sulfone (DBTO2).[24] This two-step oxidation requires flavin mononucleotide (FMN), NADPH, and an external flavin reductase to provide reduced flavin which, in turn, provides reducing equivalents and mediates the monooxygenation. Reduced flavin reacts with molecular oxygen to form the C4a-hydroperoxyflavin, a reactive oxygen species that is responsible for the electrophilic oxidation of the substrate.[25] The oxygenation results in the incorporation of one oxygen, usually as a hydroxyl group, and

the formation of reduced C4a-hydroxy flavin. The hydroxyflavin readily loses a water molecule to generate the oxidized flavin required for a subsequent round of catalysis.

With flavin-dependent enzyme cofactor requirements taken into consideration,[26] we designed an enzymatic assay for both ORF36 and RubN8 to reconstitute their activities *in vitro*. In addition to the putative oxidase, the assay included FAD, *Photobacterium fischeri* flavin reductase, and NADPH. Considering the possibility that reactive oxygen species (ROS) may oxidize TDP-L-epi-vancosamine, all enzymatic reactions were also performed in the presence of a catalytic excess of catalase and superoxide dismutase. The catalase catalyzes the decomposition of hydrogen peroxide to oxygen and water while the superoxide dismutase catalyzes the dismutation of the superoxide anion into oxygen and hydrogen peroxide.[27]

Product formation was assayed by electrospray HPLC-MS using a graphitic Hypercarb column in the negative ion mode, which effectively separated all TDP products.[28] As shown in Figure II-6, time course assays revealed rapid disappearance of TDP-L-epivancosamine (m/z) 544), transient appearance of intermediary hydroxylamine (m/z) 560), and ultimately the formation of the nitroso compound TDP-epi-vancosonitrose (m/z) 558 and a species of +18 mass units at (m/z) 576. Of note, only the β anomer of TDP-L-epivancosamine was oxidized, consistent with the catalytic competence known for the TDP-sugar-modifying enzymes. The formation of the TDP-nitrosugar congener was only observed at slow rates ambiguous to be counted as an enzymatic conversion. Control reactions omitting ORF36/RubN8, FAD, or NADPH

produced no detectable oxidation products, which validated the authenticity of the RubN8's and ORF36's activities.

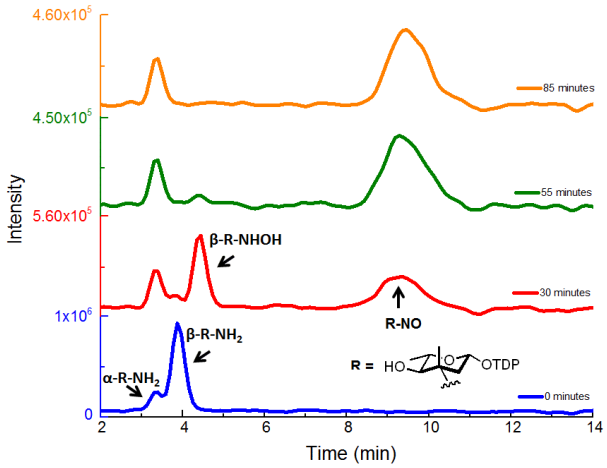

Figure II-6. HPLC-ESI-MS chromatograms of the time course of RubN8 oxidation reaction.

Tandem MS fragmentation of selected product ions (Figure II-7) showed diagnostic fragmentation patterns of the hydroxylamino intermediate and the nitroso product including the loss of TDP anion (m/z 401) and it's dehydrate (m/z 383). Another fragment ion with low intensity representing the loss of the hydroxylamino group from the TDP-3-hydroxyaminosugar intermediate was observed at m/z 527.

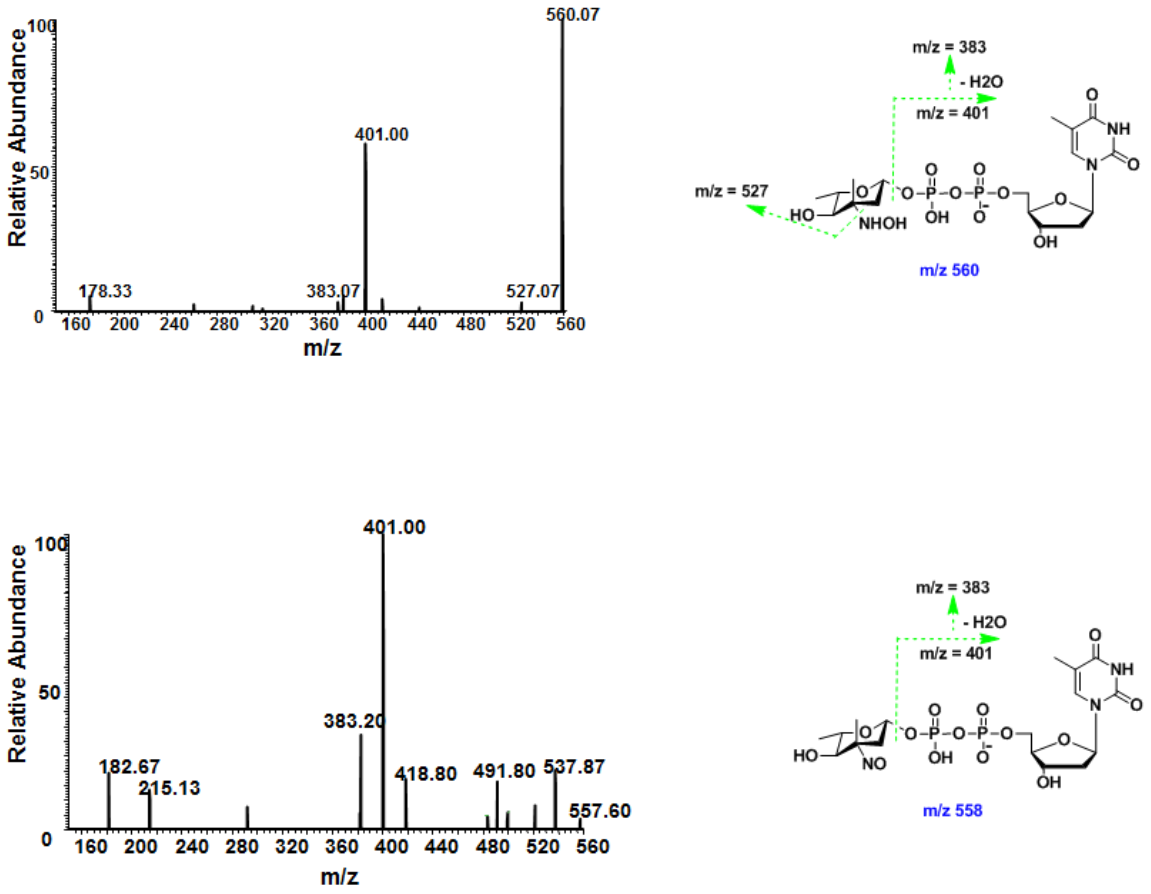

Figure II-7. Tandem MS spectra of the nucleotide-hydroxyaminosugar intermediate (above) and the nucleotide-nitrososugar product (below) from RubN8 oxidation reaction.

Proposed mechanism of nitrososynthase

Based on our biochemical data obtained in this work, a minimal mechanism can be proposed for the catalysis of this new nitrososynthase enzyme (Scheme II-1). The four-electron flavin-mediated oxidation of an amine to a nitroso functional group likely involves two monooxygenation steps. The first step involvs the oxidation of the aminosugar to the corresponding hydroxylamine via a flavin monooxygenase mechanism similar to that of L-ornithine N5-oxygenase[29] from pyoverdin biosynthesis and *p*-hydroxybenzoate hydroxylase from *Acinetobacter calcoaceticus* .[30] In this

mechanism, we propose that bound reduced FAD, generated by flavin reductase, reacts with molecular oxygen to form flavin C4a-hydroperoxide, which acts as the electrophilic oxidizing species in the formation of the hydroxylamino sugar. The resulting flavin-C4a-hydroxide loses a water molecule recycling the oxidized FAD cofactor. In the second step, the oxidation of the hydroxylamino sugar intermediate to the nitroso sugar may proceed via an iterative oxidative process in which the bound C4a-hydroperoxy flavin mediates another monooxygenation to ultimately form the nitroso sugar. This requires the regeneration of reduced flavin by the flavin reductase/NADPH for the second round of oxidation. To confirm FAD recycling, reactions were performed by stoichiometrically limiting NADPH. The formation of the hydroxylamine was observed, but no further oxidation products appeared until additional NADPH was added to the reaction, suggesting further reducing equivalents are required for the second monooxygenation step via the supplied NADPH/flavin reductase enzyme.

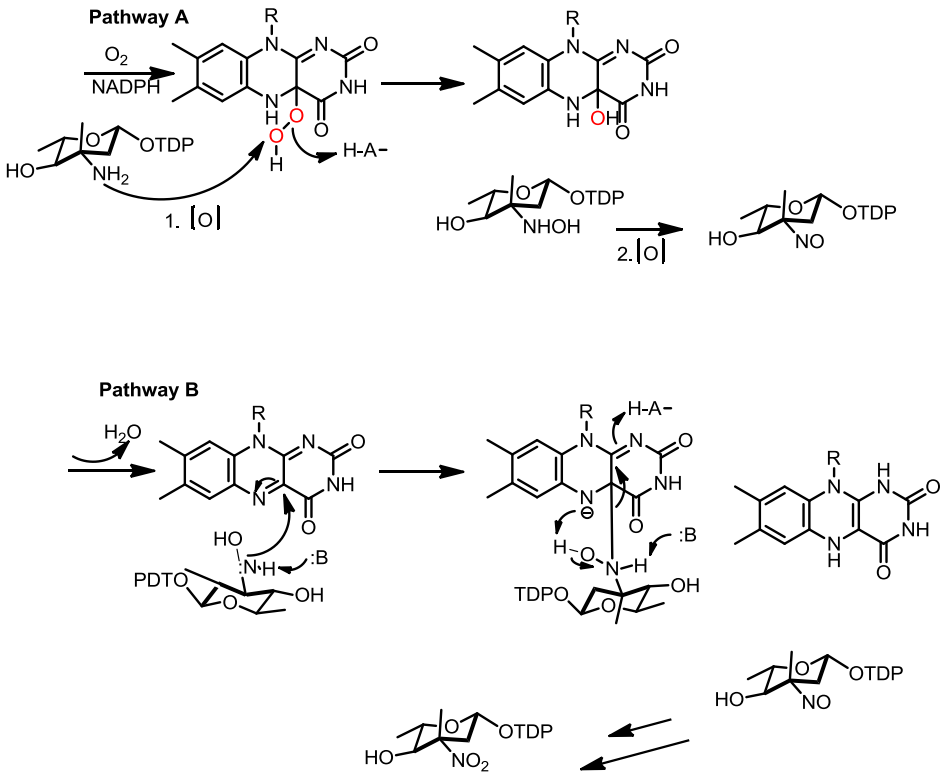

Scheme II-1. Proposed pathway for the nitrososynthase oxygenation reaction. Pathway B was proposed to be not likely to occur, because limiting the NADPH coenzyme resulted in the formation of only the hydroxylamino intermediate.

Conclusion

In this study, the proposed flavin-dependent enzymes RubN8 and ORF36 were shown to be capable of oxidizing a synthetic aminosugar substrate analogue (TDP-L-epivancosamine), lacking the C4 O-methylation, to its corresponding nitroso congener. The oxidation appears to proceed via a hydroxylamino intermediate and requires reduced FAD generated by an external flavin reductase with NADPH as reducing equivelent. Although the C4 O-methylation in the authentic aminosugar substrate may affect subsequent oxidation reactions, our data are consistent with previous studies showing that the nitroso variant of rubradirin is the direct oxidation product when

fermentations were performed in the absence of ambient light. Oxidation to the nitro group remains to be further investigated and possible pathways may include latent (photo)chemical process or endogenous reactive oxygen species (ROS).[31]

Taken together, the biochemical data presented in this work provide the first evidence for a new class of flavin-dependent monooxygenase we termed a nitrososynthase responsible for the N-oxidation of deoxyaminosugars in vast array of nitrosugar-containing natural product pathways. The observed monooxygenase activity of RubN8 and ORF36 is direct biochemical evidence for the deoxyaminosugar N-oxidation in the rubradirn and the everninomicin pathways, respectively, and can explain the roles of nitrososynthase homologues in related biosynthetic pathways. This study provided the basis for more detailed biochemical characterization of this important class of enzymes and their roles in several biosynthetic pathways.

Materials and methods

Bacterial strains, Plasmids and Material

All reagents were obtained from Sigma-Aldrich Corporation and used without further purification unless otherwise noted. *E. Coli* TOP10 and BL21(*DE3*) competent cells were obtained from Invitrogen Inc. (Carlsbad, CA) and Novagen (Madison, WI), respectively. Restriction endonucleases and T4 DNA ligase were obtained from New England Biolabs (Ipswich, MA). The pET28a expression vector was purchased from

Novagen Inc. Taqplus DNA polymerase was purchased from Stratagene Inc. (La Jolla, CA). DNA primers were obtained from Operon Biotechnologies (Huntsville, AL).

Preparation of the azido sugar substrate

The azido congener of TDP-L-epivancosamine shown in figure II-5, was prepared by Prof. Daniel Kahne's research group at the Department of Chemistry and Chemical Biology, Harvard University. The following procedure was provided: Solvents were reagent grade and were further dried when necessary. Analytical thin-layer chromatography was performed on glass plates precoated with silica gel (250 µm, Sorbent Technologies), with detection by UV and/or spraying with H_2SO_4 (50%). Flash chromatography was carried out on silica gel (60 Å, 32-63 µm), purchased from Sorbent Technologies. Analytical HPLC of synthetic reaction mixtures was performed on a Hewlett-Packard 1100 series instrument using a Phenomenex Luna 5 µm C18 column (250 mm x 4.6 mm). Compounds bearing a thymidine chromophore were monitored at an absorbance of 270 nm. Synthetic reactions were monitored by HPLC using gradient A (linear gradient from H_2O/0.1% NH_4HCO_3 to 100% MeOH/0.1% NH_4HCO_3 over the course of 25 min). Preparative HPLC was performed on a Varian ProStar instrument using a Phenomenex Luna 10 µm C18 column (250 mm x 50 mm). NMR spectra were recorded on Varian Inova 400 or 500 MHz spectrometers. Mass spectra (ESI) for synthetic compounds were obtained using an Agilent Technologies LC/MSD instrument (Model #G1956B).

Thymidine 5'-(3-amino-2,3,6-trideoxy-3-C-methyl-a,b-l-arabino hexopyranosyl diphosphate), TDP a,b-epi-L-vancosamine azide (5). The protected TDP epi-vancosamine (reference: Org. Lett., Vol 6, 2004) (38 mg, 60 µmol) was dissolved in MeOH/H_2O/Et3N (2:2:1, 4 mL) and stirred at room temperature for 16 h. Following evaporation, the residue was redissolved in MeOH/H_2O (2:1, 2 mL) and purified by reversed-phase HPLC. (18 mg, 92%) was obtained as its ammonium salt, tR = 9.0 min, method A. 1H NMR (400 MHz, D2O): 2.25b: δ = 7.62 (s, 1 H, 6-H), 6.24 – 6.21 (m, 1 H, 1'-H), 5.22 – 5.17 (dt, J1,2b = J1,P = 9.0, J1,2a = 2.1 Hz, 1 H, 1"-H), 4.47 (m, 1 H, 3'-H), 4.02 (m, 3 H, 4'-H, 5'-H2), 3.52–3.47 (m, 1 H, 5"-H), 3.16 (d, J4,5 = 10 Hz, 1 H, 4"-H), 2.22 - 2.08 (m, 2 H, 2'-H2) 2.07 (d, ,J2a,2b = 12.6 Hz, 1 H, 2"-Ha), 1.71 (s, 3 H, thymidine CH3), 1.56-1.51 (dd, J1,2b = 9.0, J2a,2b = 12.6 Hz, 1 H, 2"-Hb), 1.25 (s, 3 H, 3"-CH3), 1.13 (d, J5,6 = 6.4 Hz, 3 H, 6"-H3); 31P NMR (162 MHz, CD3OD): δ = –10.61, –12.82. LRMS (ESI) for C17H27N5O13P2 (570.12): 571 [M–1H]–.

Cloning and overexpression of ORF36

This protein was cloned, expressed and purified by Dr. Yunfeng Hu. The gene encoding ORF36 was amplified from genomic DNA of *Micromonospora carbonacea* var. *africana* (NRRL 15099) using the following primers: 5'-GCACATATGGCGGCGGATCTTCGCGC3' and 5'-TTGAAGCTTTTATTACGCCGA GGTCCGGGAGC-3' (NdeI and HindIII restriction enzyme sites underlined). PCR reactions were carried out using Taqplus DNA polymerase according to the manufacture protocol.

Subcloning of orf36 into the NdeI/HindIII sites of pET28a yielded the recombinant plasmid pET28-36N for expression as an N-terminal hexahistidine fusion protein. Plasmid pET28-36N was transformed into *E. Coli* BL21(DE3) for heterologous expression of ORF36. Cultures of *E. Coli* BL21(DE3)/pET28-36N was grown at 37°C to an OD600 of 0.6, at which point the culture was induced with 0.1mM isopropyl-beta-D-thiogalactopyranoside (IPTG) and grown an additional 6 hours at 28°C. Cells were harvested by centrifugation and stored at -80°C until needed. IPTG induced *E. Coli* BL21(DE3)/pET28-36N cells were resuspended in buffer A (20 mM Imidazole, 0.5M NaCl, 20mM Tris-Cl, pH 7.5) and lysed by sonication. The lyate was loaded onto a charged 5-ml Histrap crude column (Amersham Biosciences) and purified by FPLC at a flow rate of 5mL/min. The column was washed with buffer A (20 mM Imidazole, 0.5M NaCl, 20 mM Tris-Cl, pH 7.5) and buffer B (500 mM Imidazole, 0.5M NaCl, 20 mM Tris-Cl, pH 7.5) using a step gradient. Fractions containing ORF36 were analyzed by SDS-page. The protein was desalted via a desalting column (HisTrap) using buffer C (20 mM Tris-Cl, 1mM dithiothreitol and 5% glycerol, pH 7.5) and stored at -80 °C until assayed.

Cloning and overexpression of *rubN8*

The gene encoding RubN8 was amplified from *Streptomyces achromogenese* var. *rubradiris* (NRRL3061) genomic DNA. The following PCR primer pairs were used to clone the gene into the NdeI/HindIII site of pET28a (restriction sites underlined): 5'-TCCATATGA-TGGAGACGGAACAGGCCCC-3' and 5'-TCAAGCTTTCACCGGCTGTCCACCGGC-

3’. Restriction-digested PCR products were subcloned into the digested pET28a vector to yield pET28a-his6-RubN8. Cultures of *E.coli* BL21(DE3) transformants (1 L Luria broth (LB) media with 50 µg/mL kanamycin) were grown at 37 °C to an OD600 of 0.6 at which point the cultures were induced with 0.25 mM isopropyl-1-thio-β-D-galactoside (IPTG) and grown for additional 16 h. Cells were harvested by centrifugation and frozen at -80°C until needed. Frozen cells were resuspended in binding buffer [20 mM imidazole, 0.5 M NaCl, 20 mM sodium phosphate (pH 7.5)] and lysed by sonication. After clarification by centrifugation at 10000g, the lysates were loaded onto Ni2+-charged 5-mL HisTrap column and purified using FPLC (Amersham Biosciences) with a flow rate of 5 mL/min. The column was washed with 50 mL of binding buffer and proteins were eluted with a gradient of imidazole (20-500 mM imidazole). Fractions containing the proteins were analyzed by SDS-PAGE, pooled, concentrated to 5 mL and desalted by FPLC using a 5 mL size exclusion desalting column (HiTrap) from Amersham Biosciences. The column was equilibrated with 50 mL desalting buffer [20 mM Tris.HCl, 5%glycerol, 1 mM DTT, pH 7.5], the proteins were then loaded onto the column (maximum of 1.5 mL) and eluted at a flow rate of 5 mL/min. Fractions containing the protein were analyzed again by SDS-PAGE and stored at -80 °C until assayed.

Preparation of L-TDP-*epi*-vancosamine

L-TDP-epi-vancosamine (4-O-desmethyl L-TDP-evernosamine) was prepared by reduction of a synthetic azide congener (0.5mM) with 1mM tris(2-

carboxyethyl)phosphine (TCEP) in 20 mM Tris-Cl (pH 7.5) at 22°C for 24 hours. Amino sugar was stored in small aliquots at -80 °C for assays. HPLC/MS, performed for L-TDP-epi-vancosamine enzymatic reaction described below, indicated that the extent of reaction was > 96%.

ORF36/RubN8 enzymatic reactions

ORF36 activity was assayed in 20 mM Tris-HCl buffer (pH 7.5) in the presence of 0.4 – 2 mM NADPH, 30 µM FAD, 250 µM L-TDP-epi-vancosamine, 0.001 mg/ml of the NAD(P)H oxidoreductase of Photobacterium fischeri (Boehringer Mannheim, Mannheim, Germany) and 0.5mg/ml of ORF36 per 50 µl. Reactions were maintained at 30 °C.

Solutions of the substrate L-TDP-epi-vancosamine, flavin adenine dinucleotide (FAD) and nicotinamide adenine dinucleotide phosphate (NADPH), were made in 20 mM Tris-HCl pH 7.5. RubN8 was aliquoted in storage buffer [20 mM Tris.HCl, 5% glycerol, 1 mM DTT, pH 7.5]. Flavin reductase was stored in 40% glycerol, 1 mM EDTA, 0.1 mM DTT and 50 mM potassium phosphate, pH 7.0. The catalase and superoxide dismutase enzymes were made in [20 mM Tris.HCl 40% glycerol, pH 7.5]. In a total volume of 50 µL, 250 µM of the substrate, L-TDP-epi-vancosamine, was incubated with 30 µM FAD, 1 U/mL catalase, 1 U/mL superoxide dismutase, 0.001 mg/mL flavin reductase, and 2 mM NADPH. Control assays lacking RubN8, FAD or NADPH were performed. The reaction was initiated by the addition of 0.5 mg/mL RubN8 or 0.5 mg/mL ORF36. The time course of the reaction was followed by HPLC/MS at 30 °C.

HPLC/MS assay for L-TDP-*epi*-vancosamine reaction

The oxidation of L-TDP-epi-vancosamine to corresponding products was carried out using an Agilent 1100 HPLC system (Agilent, Palo Alto, CA), comprising a binary pump and refrigerated autosampler. Mass spectrometry was performed by using a ThermoFinnigan (San Jose, CA) LCQ Quantum Deca XP three-dimensional Ion Trap Mass Spectrometer equipped with an API electrospray ionization source outfitted with a 50 µm I.D. deactivated fused silica capillary. The injection volume was 5 µl. Products were detected using a Thermo Hypercarb column (3mm × 5cm). Mobile phases were: (A) H2O with 50 mM ammonium acetate and 0.1% (v/v) diethylamine and (B) H2O/acetonitrile (5:95) with 50 mM ammonium acetate and 0.1% (v/v) diethylamine. Gradient conditions were as follows: 0-5 min, B = 15%; 5-15 min, linear gradient to 35% B; 15 to 16 min, linear gradient to 100%B; 16 to 21 min, hold B = 100%; 21 to 22 min, linear gradient to 15% B; 22-30 min, B = 15%. The flow rate was maintained 0.3 ml/min. The mass spectrometer was operated in the negative ion mode, and the electrospray needle was maintained at 3,400 V. The ion transfer tube was operated at -47.50 V and 275 °C. The tube lens voltage was set to -46 V. The mass spectrometer was operated in full scan mode. Full scan spectra were acquired from m/z 50.0 to 1500.0 full and product ion scans as follows: 544→155-548 with collision energy of 30%; 558→155-560, with collision energy of 30%; 560→155-562 with collision energy of 30%; 544→155-548 with collision energy of 30%; 570→155-575 with collision energy of 30%. Data were acquired in profile mode. The following optimized parameters were used for the detection: N2 sheath gas 46 psi; N2 auxiliary gas 13 psi; spray voltage 3.4 kV.

References

1. Thibodeaux, C. J.; Melancon, C. E., 3rd; Liu, H. W., Natural-product sugar biosynthesis and enzymatic glycodiversification. *Angewandte Chemie* **2008,** *47* (51), 9814-59.

2. Allard, S. T.; Giraud, M. F.; Whitfield, C.; Messner, P.; Naismith, J. H., The purification, crystallization and structural elucidation of dTDP-D-glucose 4,6-dehydratase (RmlB), the second enzyme of the dTDP-L-rhamnose synthesis pathway from Salmonella enterica serovar typhimurium. *Acta Crystallographica. Section D, Biological Crystallography* **2000,** *56* (Pt 2), 222-5.

3. Nedal, A.; Zotchev, S., Biosynthesis of deoxyaminosugars in antibiotic-producing bacteria. *Applied Microbiology and Biotechnology* **2004,** *64* (1), 7-15.

4. Chen, H.; Thomas, M. G.; Hubbard, B. K.; Losey, H. C.; Walsh, C. T.; Burkart, M. D., Deoxysugars in glycopeptide antibiotics: enzymatic synthesis of TDP-L-epivancosamine in chloroeremomycin biosynthesis. *Proceedings of the National Academy of Sciences of the United States of America* **2000,** *97* (22), 11942-7.

5. Meyer, C. E., Rubradirin, a New Antibiotic. Ii. Isolation and Characterization. *Antimicrobial Agents and Chemotherapy* **1964,** *10*, 97-9.

6. Nakashio, S.; Iwasawa, H.; Dun, F. Y.; Kanemitsu, K.; Shimada, J., Everninomicin, a new oligosaccharide antibiotic: its antimicrobial activity, post-antibiotic effect and synergistic bactericidal activity. *Drugs under Experimental and Clinical Research* **1995,** *21* (1), 7-16.

7. Zhang, H.; White-Phillip, J. A.; Melancon, C. E., 3rd; Kwon, H. J.; Yu, W. L.; Liu, H. W., Elucidation of the kijanimicin gene cluster: insights into the biosynthesis of spirotetronate antibiotics and nitrosugars. *Journal of the American Chemical Society* **2007,** *129* (47), 14670-83.

8. Chu, M.; Mierzwa, R.; Jenkins, J.; Chan, T. M.; Das, P.; Pramanik, B.; Patel, M.; Gullo, V., Isolation and characterization of novel oligosaccharides related to Ziracin. *Journal of Natural Products* **2002,** *65* (11), 1588-93.

9. Marshall, S. A.; Jones, R. N.; Erwin, M. E., Antimicrobial activity of SCH27899 (Ziracin), a novel everninomicin derivative, tested against Streptococcus spp.: disk diffusion/etest method evaluations and quality control guidelines. The Quality Control Study Group. *Diagnostic microbiology and Infectious Disease* **1999,** *33* (1), 19-25.

10. Jones, R. N.; Marshall, S. A.; Erwin, M. E., Antimicrobial activity and spectrum of SCH27899 (Ziracin) tested against gram-positive species including recommendations for routine susceptibility testing methods and quality control. Quality Control Study Group. *Diagnostic Microbiology and Infectious Disease* **1999,** *34* (2), 103-10.

11. Mertz, J. L.; Peloso, J. S.; Barker, B. J.; Babbitt, G. E.; Occolowitz, J. L.; Simson, V. L.; Kline, R. M., Isolation and structural identification of nine avilamycins. *The Journal of Antibiotics* **1986,** *39* (7), 877-87.

12. Farnet, C. M.; Zazopoulos, E.; Staffa, A., Compositions and methods for identifying and distinguishing orthosomycin biosynthetic loci. *Google Patents:* **2002.**

13. Gololobov, Y. G.; Zhmurova, I.; Kasukhin, L., Sixty years of Staudinger reaction. *Tetrahedron* **1981,** *37* (3), 437-472.

14. Vetrova, E. V.; Kudryasheva, N. S.; Visser, A. J.; van Hoek, A., Characteristics of endogenous flavin fluorescence of Photobacterium leiognathi luciferase and Vibrio fischeri NAD(P)H:FMN-oxidoreductase. *Luminescence : the Journal of Biological and Chemical Luminescence* **2005,** *20* (3), 205-9.

15. Ganguly, A. K.; Sarre, O. Z.; Reimann, H., Evernitrose, a naturally occurring nitro sugar from everninomicins. *Journal of the American Chemical Society* **1968,** *90* (25), 7129-30.

16. Ohshiro, T.; Aoi, Y.; Torii, K.; Izumi, Y., Flavin reductase coupling with two monooxygenases involved in dibenzothiophene desulfurization: purification and characterization from a non-desulfurizing bacterium, Paenibacillus polymyxa A-1. *Applied Microbiololgy and Biotechnology* **2002,** *59* (6), 649-57.

17. Ghisla, S.; Thorpe, C., Acyl-CoA dehydrogenases. *European Journal of Biochemistry* **2004,** *271* (3), 494-508.

18. Wagman, G. H.; Luedemann, G. M.; Weinstein, M. J., Fermentation and Isolation of Everninomicin. *Antimicrobial Agents Chemotherapy (Bethesda)* **1964,** *10*, 33-7.

19. Bhuyan, B. K.; Owen, S. P.; Dietz, A., Rubradirin, a New Antibiotic. I. Fermentation and Biological Properties. *Antimicrobial Agents Chemotherapy (Bethesda)* **1964,** *10*, 91-6.

20. Kim, C. G.; Lamichhane, J.; Song, K. I.; Nguyen, V. D.; Kim, D. H.; Jeong, T. S.; Kang, S. H.; Kim, K. W.; Maharjan, J.; Hong, Y. S.; Kang, J. S.; Yoo, J. C.; Lee, J. J.; Oh, T. J.; Liou, K.; Sohng, J. K., Biosynthesis of rubradirin as an ansamycin antibiotic from Streptomyces achromogenes var. rubradiris NRRL3061. *Archives of Microbiology* **2008,** *189* (5), 463-73.

21. Hosted, T.; Horan, A.; Wang, T., Everninomicin biosynthetic genes. WO Patent WO/2001/051,639: 2001.

22. Hu, Y.; Al-Mestarihi, A.; Grimes, C. L.; Kahne, D.; Bachmann, B. O., A unifying nitrososynthase involved in nitrosugar biosynthesis. *Journal of the American Chemical Society* **2008,** *130* (47), 15756-7.

23. Oberthuer, M.; Leimkuhler, C.; Kahne, D., A Practical Method for the Stereoselective Generation of β-2-Deoxy Glycosyl Phosphates. *Organic Letters* **2004,** *6* (17), 2873-2876.

24. Ohshiro, T.; Kojima, T.; Torii, K.; Kawasoe, H.; Izumi, Y., Purification and characterization of dibenzothiophene (DBT) sulfone monooxygenase, an enzyme involved in DBT desulfurization, from Rhodococcus erythropolis D-1. *Journal of Bioscience and Bioengineering* **1999,** *88* (6), 610-6.

25. Massey, V., The chemical and biological versatility of riboflavin. *Biochemical Society Transactions* **2000,** *28* (4), 283-96.

26. Joosten, V.; van Berkel, W. J. H., Flavoenzymes. *Current Opinion in Chemical Biology* **2007,** *11* (2), 195-202.

27. Loprasert, S.; Vattanaviboon, P.; Praituan, W.; Chamnongpol, S.; Mongkolsuk, S., Regulation of the oxidative stress protective enzymes, catalase and superoxide dismutase in Xanthomonas--a review. *Gene* **1996,** *179* (1), 33-7.

28. Xing, J.; Apedo, A.; Tymiak, A.; Zhao, N., Liquid chromatographic analysis of nucleosides and their mono-, di-and triphosphates using porous graphitic carbon stationary phase coupled with electrospray mass spectrometry. *Rapid Communications in Mass Spectrometry* **2004,** *18* (14), 1599-1606.

29. Meneely, K. M.; Barr, E. W.; Bollinger, J. M., Jr.; Lamb, A. L., Kinetic mechanism of ornithine hydroxylase (PvdA) from Pseudomonas aeruginosa: substrate triggering of O2 addition but not flavin reduction. *Biochemistry* **2009,** *48* (20), 4371-6.

30. Clarkson, J.; Palfey, B. A.; Carey, P. R., Probing the chemistries of the substrate and flavin ring system of p-hydroxybenzoate hydroxylase by raman difference spectroscopy. *Biochemistry* **1997,** *36* (41), 12560-6.

31. Filip, M.; Paduraru, I.; Jerca, L.; Filip, F.; Saramet, A., [Oxygen biochemistry. I. Reactive species of reduced oxygen and endogenous sources]. *Revista Medico-Chirurgicala a Societatii de Medici si Naturalisti din Iasi* **1992,** *96* (3-4), 289-92.

Chapter III

STRUCTURAL AND MECHANISTIC STUDIES OF THE NITROSOSYNTHASE ORF36 FROM *MICROMONOSPORA CARBONACEA* VAR. *AFRICANA*

Introduction

The experiments outlined in Chapter II describing the activity of the nitrososynthases ORF36 from *Micromonospora carbonacea* var. *africana,* and RubN8 from *Streptomyces achromogenes* var. *rubradiris*, formed the basis for further biochemical characterization of this new class of flavin-dependent monooxygenases. ORF36 and RubN8 were shown to catalyze the 2-step N-oxidation of a close substrate analog, TDP-L-epivancosmine, resulting in the formation of its nitroso congener via a hydroxylamino intermediate.[1] Although no enzymatic oxidation to the nitro group was observed, the nitroso sugar product is consistent with previous studies with rubradirin, which suggested that the nitro oxidation state is a result of photo oxidation of the nitroso group.[2]

Several enzymes in nature catalize the N-oxidation of amines. For example, the Rieske, aminopyrrolnitrin N-oxygenase (PrnD) catalyzes the unusual flavin-dependent oxidation of an arylamine to an arylnitro group.[3] Another example is the non-heme di-iron monooxygenase (AurF) from *Streptomyces thioluteus* which catalyzes the formation of unusual polyketide synthase starter unit *p*-nitrobenzoic acid from *p*-aminobenzoic acid in the biosynthesis of the antibiotic aureothin.[4] N-Oxidation can also be catalyzed by P450 enzymes[5] and several single-component flavin monooxygenases.[6]

Our preliminary biochemical characterization of ORF36 and RubN8 showed that the nitrososynthase is a flavin-dependent monooxygenase.[1] Flavin-dependent monooxygenases are a diverse class of enzymes capable of efficient and specific insertion of one or more oxygen atoms into an organic substrate, a reaction that is difficult to achieve via standard chemical synthesis. Oxidation reactions catalyzed by flavin-dependent monooxygenases include hydroxylation, halogenation, sulfoxidation, and Baeyer-Villiger oxidation.[7] The double N-oxidation of aminosugars by the nitrososynthase represents a new addition to this set of reactivities. This new enzyme may be best classified as Class D flavin-containing monooxygenase based on its sequence homology with acyl-CoA dehydrogenases, which are sequence models for this class. Members of class D flavin-containing monooxygenases typically hydroxylate aromatic substrates.[8-11] Interestingly, nitrososynthases have more sequence similarities with acyl-CoA dehydrogenases (~25%) than with flavin-containing monooxygenases (~15%) contrary to their biochemical evidence suggesting a monooxygenase activity.

Class D flavoprotein monooxygenases are typically encoded by two genes; one encodes the monooxygenase while the other encodes the flavin reductase component. The reductase component uses FAD as a cofactor and NADH or NADPH as a coenzyme. These enzymes are structurally homologous to acyl-CoA dehydrogenases and are mostly α-helical proteins. In our previous biochemical characterization of the nitrososynthase ORF36, it was shown that its activity requires flavin and NADPH with significant enhancement reached upon the inclusion of an external flavin reductase.[1] Furthermore, ORF36 was shown to display weak, reversible binding for oxidized flavin. ORF36 was also

shown to utilize both FAD and FMN as its flavin cofactors with preference to FAD. This cofactor promiscuity was observed in the class D flavoprotein monooxygenase 4-hydroxyphenylacetate monooxygenase from *Acinetobacter baumannii*.[12]

Our recent biochemical characterization of the nitrososynthase ORF36 was impeded by several challenges including the lengthy synthesis of the TDP-sugar substrate, its storage instability, and the low affinity of the flavin cofactor which typically provides a convenient spectrophotometric monitoring of the flavin cofactor's redox states. To address these challenges, we developed a modified *in vitro* procedure utilizing six purified enzymes to generate the close substrate analog TDP-L-epivancosamine, lacking the C4 O-methylation, in sufficient quantities to study enzyme turnover of this substrate and its TDP-aminosugar precursors in its biosynthetic pathway.[13] Additionally, we studied the nitrososynthase oxidation reaction with the biogenic TDP-L-epivancosamine under $^{18}O_2$ and observed oxygen incorporation into the oxidation products and intermediates which provided more evidence for a monooxygenase mechanism. Finally, in collaboration with Prof. Tina Iverson's research group, Dr. Jessica Vey solved the 3-D structure of ORF36 by X-ray crystallography, which revealed important chemical and physical constraints of the protein scaffold that houses the flavin-dependent double N-oxidation of the TDP-aminosugar.[14] Taken together these studies provided important biochemical details of the nitrososynthase responsible for the N-oxidation of deoxyaminosugars in everninomicin and related nitro-sugar containing bioactive natural products.

Results

Substrate preference of ORF36

An ever-increasing number of nitrososynthase homologs have been deposited to the GenBank corresponding to their oxidative role as flavin-dependent enzymes in the biosynthesis of many nitrosugar-containing natural products.[15-17] The structural modifications of the nitrosugar moiety in these compounds are mostly conserved with notable functional variability at C-4 position which can be found as hydroxyl, O-methyl or N-carbamoyl group. Functional variability also includes the C-5 position leading to possibilities between the sugar's D and L configurations.[15-17] The diversity of structures of the aminosugar precursor substrates is in contrast with the high sequence identity between all the nitrososynthase homologues in several nitrosugar pathways[18], which prompted us to investigate whether the reported nitrososynthases act on a common intermediate biochemically upstream of the last biosynthesized aminosugar substrate in the corresponding pathways. [19]

To address this possibility and further investigate the timing of aminosugar oxidation to ultimately yield the nitroso functionality, we reconstituted the biosynthetic pathway for the aminosugar TDP-L-epi-vancosamine using enzymes obtained by the Walsh group from the chloroereomycin pathway[13], and studied the activity of ORF36 with two additional upstream TDP linked C4-keto-3-aminosugar intermediates in this pathway (Figure III-1). We were unable to isolate enough quantities from this multistep enzymatic synthesis of these TDP-sugar intermediates to perform Michaelis-Menten

kinetics due to their low storage stability; however, we were able to compare turnover of substrates at identical, titrated substrate concentrations (30 μM).

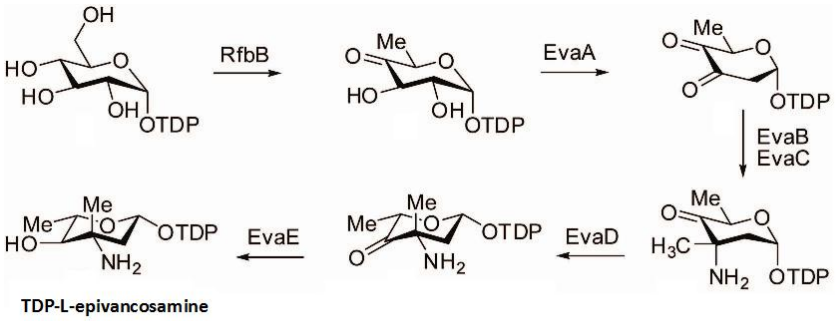

Figure III-1. Pathway utilized for biochemical synthesis of TDP-L-*epi*-vancosamine and the TDP-4-keto-3-amino sugar precursors. This figure is taken from reference 14 in which the author of this document is a coauthor.

Analysis of the enzyme assays by HPLC-MS showed that all potential aminosugar substrates displayed a degree of chemical competence for single oxidation to hydroxylamine, but only TDP-L-epivancosamine underwent double oxidation to form both the hydroxylamine and subsequently the nitrososugar product (Figure III-2).

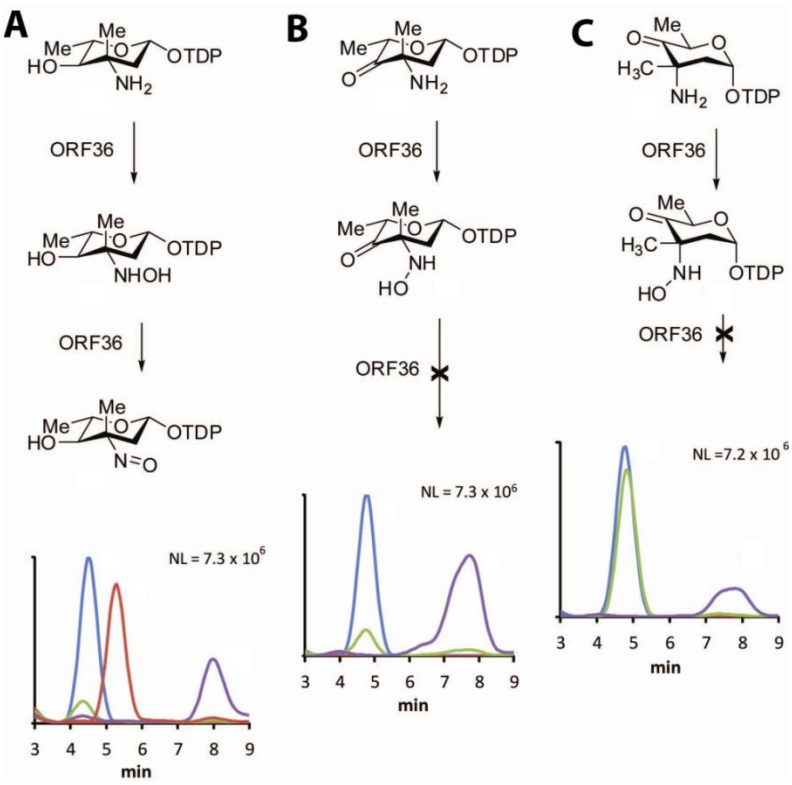

Figure Figure III-2. HPLC-ESI-MS traces of ORF36 oxidation reactions with three potential amino sugar substrates. (A) TDP-L-epivancosamine (m/z 544) at 0 min (blue) and 100 min (green), hydroxylamine intermediate (m/z 560) at 15 min (red), and nitroso product (m/z 558) at 100 min (purple). (B) TDP-L-3-amino-4-keto sugar substrate (m/z 542) at 0 min (blue) and 100 min (green) and hydroxylamine intermediate (m/z 558) at 100 min (purple). (C) TDP-D-3-amino-4-keto sugar substrate (m/z 542) at 0 min (blue) and 100 min (green) and hydroxylamine intermediate (m/z 558) at 100 min (purple). This figure is taken from reference 14 in which the author of this document is a coauthor.

The two 3-amino-4-keto sugar precursors of TDP-L-epivancosamine (Figure III-2B,C) differ in the configuration at C-5 with the first biosynthesized ketosugar having a D configuration and upon the activity of EvaD, its L congener is formed. The TDP-L-3-amino-4-keto sugar (Figure III-2B) was assayed by including a catalytic excess of the C-5 epimerase (EvaD) in the nitrososynthase oxidation reaction. This TDP-L-aminosugar substrate was rapidly oxidized to its hydroxylamino congener but did not further oxidize to other species under the ORF36 assay conditions (Figure III-2B). The TDP-D-3-amino-4-

keto sugar precursor was also oxidized to its hydroxylamino oxidation state, but at a substantially slower apparent rate than when the epimerase was added to reactions (Figure III-2C). This is in agreement with its recently reported partial oxidation by KijD3, which likewise only evidenced the formation of a hydroxylamine.[18] Unlike these studies, however, we did not observe additional peaks at m/z = 527 rationalized by the authors as a fragment of the hydroxylamine. This mass corresponds to a reduction product, the identity of which remains undetermined. In our ORF36 assays, the two 4-keto D- and L-aminosugar substrates were oxidized to their corresponding hydroxylamino compounds and no other detectable TDP-sugar decomposition products were apparent by MS or MS/MS analysis.

The oxidation of TDP-L-epivancosamine generated from the reconstitution of its natural biosynthetic pathway confirmed our previous results using the chemically synthesized compound[1] and importantly, validated the successful biosynthetic production of its two TDP-4-keto-3-amino sugar precursors. In summary, these data indicate that the double N-oxidation catalyzed by the nitrososynthase ORF36 improves with substrates more closely related to TDP-L-epivancosamine and only a single oxidation step to a hydroxylamine occurs for the TDP-3-amino-4-keto sugar precursors. The oxidation of the C-4 O-methylated congener of TDP-L-epivancosamine remains to be investigated to determine whether this additional methyl group has any effect on the oxidation activity of ORF36. However, the isolation of everninomicin variants from *M. carbonacea* var. *africana* with both O-methyl and hydroxyl functionality in their corresponding nitrosugar moieties[20], suggests that O-methyl substitution at this position

is not essential for nitrososynthase reactivity and may occur prior or subsequent to amine oxidation reactions.[20]

$^{18}O_2$ incorporation in the ORF36 oxidation reaction.

To determine whether the incorporation of the oxygen atom into the amino sugar substrate upon ORF36 activity with TDP-L-epivancosamine comes from molecular oxygen as opposed to oxygen from H_2O, we performed the ORF36 oxidation reaction under $^{18}O_2$. The incorporation of molecular oxygen into the substrate would also support the flavin-dependent monooxygenase catalysis. To provide a control reaction, the same previous ORF36 assay with TDP-L-epivancosamine under $^{16}O_2$ was repeated. Reactions contained the same concentrations of NADPH, FAD, flavin reductase, and ORF36 were incubated with catalytic excess of catalase[21] under atmosphere of either $^{18}O_2$ or $^{16}O_2$. As shown in figure III-3, HPLC-MS analysis showed single oxygen atom incorporation corresponding to the hydroxylamine intermediate (m/z = 560) and the nitroso product (m/z = 558), which demonstrated enrichment of the +2 m/z shift at 86% and 87% incorporation, respectively.

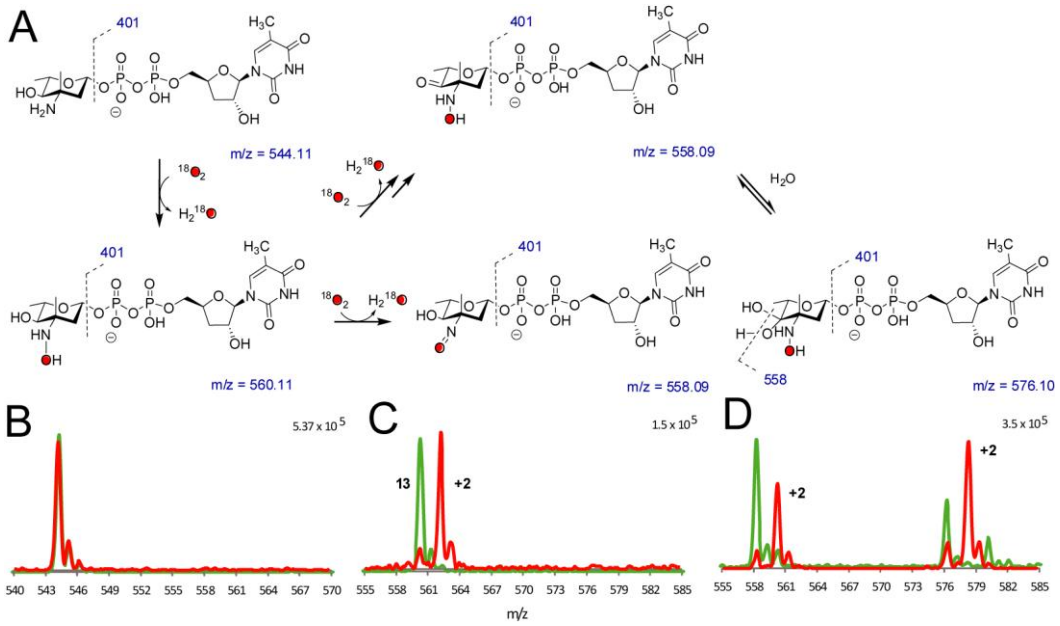

Figure III-3. The $^{18}O_2$ incorporation studies of ORF36 oxidation reaction. (A) Summary of proposed species observed in the $^{18}O_2$ incorporation experiments. (B-D) $^{18}O_2$ incorporation with ORF36 and TDP-L-epivancosamine incubated with $^{16}O_2$ (green) and $^{18}O_2$ (red). Masses shown under structures correspond to unlabeled species. HPLC-MS and MS/MS data were collected at a 15 min reaction time, when the hydroxylamine intermediate was most abundant. (B) TDP-L-epivancosamine (m/z 544 and t_R = 4.5 min). (C) Hydroxylamine (m/z 560, and t_R = 5.3 min). (D) Peaks at t_R values of 7-9 min are proposed to correspond to the nitroso compound (t_R = 8 min) and an additional oxidation product at m/z 576 (t_R = 7.8 min). This new mass has a retention time distinct from that of the nitroso sugar, and on the basis of MS/MS analysis, the additional mass of the m/z 576 ion is constrained to the pyranose ring. One possible structure is the 3-hydroxylamino-4-keto sugar, which is detected as a hydrate under ESI conditions. MS/MS analysis supports this hypothesis in that the labeled ion at m/z 578 readily fragments to an ion at m/z 560.09, and this fragmentation pattern is identical to the reaction product of the TDP-L-3-amino-4-keto sugar shifted by 2 mass units. This figure is taken from reference 14 in which the author of this document is a coauthor.

In addition to confirming the incorporation of molecular oxygen into the expected oxidation products, these experiments also showed oxygen incorporation for additional reaction products. We observed a +2 m/z shift in what we have previously assigned to be the electrospray induced hydrate of the TDP-nitroso sugar (M + H_2O, m/z = 576).[1] However, the single incorporation of oxygen into this species and the lack of demonstrable back-exchange of labeled nitroso with H_2O rule out the proposed

dihydroxylamino species. Closer examination of the HPLC/MS chromatograms indicated that within the broad peak encompassing this region, the nitrososugar (m/z 558), and the compound at m/z = 576 possess different retention times (8.8 and 7.8 min respectively). Both compounds contain fragmentation peaks diagnostic of a TDP-sugar including the loss of TDP (m/z = 401) and TMP (m/z = 321) but the unknown m/z 576 compound demonstrated an additional major fragment at 558, indicating loss of water. Further characterization of the compound at m/z 576 was impeded by the lack of the availability of enough quantities and the inherent storage stability. However, The MS/MS analysis demonstrated that the oxidation is constrained to the pyranose ring, and considering the likelihood that the oxidation is occurring on the C-3/4 heteroatoms, we proposed that the m/z 576 peak corresponds to a product oxidized at C-4, likely the C-4 ketone. Consistent with that, this putative structure shares similar retention time and fragmentation pattern with the hydroxylamino product generated from the oxidation of the substrate analog TDP-L-3-amino-4-keto sugar (Figure III-2). It should be noted however, that other structures are possible, including a possible electrocyclic rearrangement of the hydroxyketone (not shown).[22] Further structural elucidation of these oxidation products via chemical derivatization is discussed in chapter IV which revealed a surprising outcome.

X-ray crystal structure of ORF36

In collaboration with Prof. Tina Iverson's research group, Dr. Jessica Vey was able to crystallize and determine the structure of the ORF36 enzyme.[14] The polyalanine model of human short-branched chain acyl-CoA dehydrogenase (PDB 2JIF)[23] was used as the search model to determine the structure to a 3.15 Å resolution by molecular replacement (Figure III-4). ORF36 formed a tetramer with 3,500 $Å^2$ of surface area buried per monomer. Size exclusion chromatography on a Superdex S-200 column confirmed the tetrameric structure of ORF36 in solution. The monomers of ORF36 adopt a three-domain fold with the N- and C-terminal helical domains separated by a β-sheet domain (Figure III-4B). The oligomerization interface of ORF36 is predominated by interactions between the adjacent C-terminal helical domains.

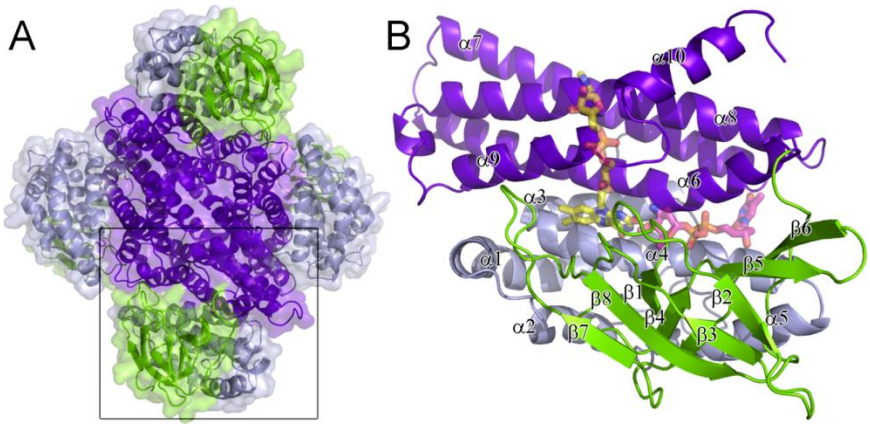

Figure III-4. Structure of ORF36. (A) The ORF36 tetramer is shown as a cartoon representation with a transparent surface, colored by domain.The N-terminal domains (residues 1-129) are colored gray, the central β-sheet domains (residues 130-235) green, and the C-terminal domains (residues 235-398) purple. (B) ORF36 monomer shown in cartoon representation with modeled FAD and TDP-L-evernosamine shown as transparent sticks. Colors are as follows: yellow for FAD carbons, magenta for TDP-L-evernosamine carbons, red for oxygen, blue for nitrogen, and orange for phosphate. The view in panel B is rotated 45° about a vertical axis from the bottom monomer shown boxed in panel A. This figure is taken from reference 14 in which the author of this document is a coauthor.

As this work was being prepared for publication early 2010, the structure of the nitrososynthase KijD3 was reported[18] and appeared in the EMBL Dali search[24] as the closest structural homolog. Both KijD3 and ORF36 share structural similarity with members of the acyl-CoA dehydrogenase superfamily[25] which includes oxidases, dehydrogenases and flavin-containing monooxygenases. The structural folds of ORF36 and KijD3 are surprisingly closer to those of the dehydrogenases than the monooxygenase functional homologs which is in contrast with their functions as monooxygenases. One explanation for this could be that the monooxygenase activity of the nitrososynthases evolved independently from acyl-CoA dehydrogenases, while other class D monooxygenases and the acyl-CoA dehydrogenases underwent a divergent evolutionary route.

Modeling of FAD and TDP-L-*epi*-vancosamine in the active site

Attempts to co-crystallize ORF36 with the flavin cofactors FAD and FMN each in their oxidized and reduced forms, as well as with the substrate TDP-L-epivancosamine were unsuccessful. None of these experiments resulted in the appearance of new electron density for the substrate or the flavin cofactor. Therefore, the FAD cofactor and the substrate TDP-L-epivancosamine were modeled into the active site of ORF36 using a combination of manual and automated methods. Ideal cofactor-substrate distances and geometry were predicted based on comparison with the co-structures of flaving-containing monooxygenases in complex with their substrates.[26-29]

The resulting predicted model suggests that the pre-formed pockets in the active site of ORF36 bind the isoalloxazine ring of the flavin cofactor and the TDP moiety of TDP-L-epivancosamine. Residues in the vicinity of the predicted isoalloxazine ring pocket, particularly at loops L3, L5 and L9, are conserved in nitrosynthases and are similar to those in acyl-CoA dehydrogenases and flavin-containing monooxygenases. In contrast, the adenine nucleotide moiety of the flavin cofactor in this predicted model is in a region in the active site where the loops are in an open conformation. Loop 7 in both dehydrogenases and flavin-containing monooxygenases, which forms specific contacts with flavin, is shorter in enzymes that preferentially bind FAD and longer in enzymes that preferentially bind FMN, and is known to undergo a conformational change upon flavin binding to facilitate contacts with the nucleotide moiety. This loop is similar to those found in acyl-CoA dehydrogenase superfamily that utilizes FAD as their flavin cofactor. This is supported by the observation that the activity of ORF36 is

significantly improved with the FAD cofactor as compared to that with FMN. In this ORF36 structure, loop L7 adopts a conformation that likely will undergo adjustment upon flavin binding.

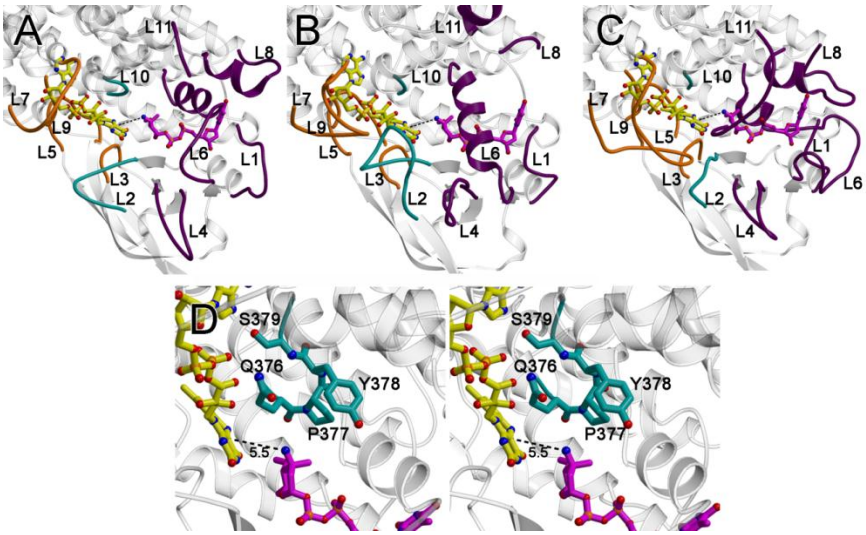

Figure III-5. Active site loops. The loops that form the active site are as follows: the loops between α3 and α4 (loop L1; residues 106 – 109), β1 and β2 (loop L2; residues 134-142), β3 and β4 (loop L3, residues 158-164), β4 and β5 (loop L4; residues 178-180), β6 and β7 (loop L5; residues 201-213), β9 and α6 (loop L6; residues 248-253), α6' and α7' (where the ' indicates this is from an adjacent monomer; loop L7; residues 272-280), α7 and α8 (loop L8; residues 310-317), α8' and α9' (loop L9, residues 351-353), α9 and α10, (loop L10; residues 375-379) and at the C-terminus (loop L11; residues 390-412). (A) A ribbon diagram of ORF36 shown with modeled flavin (yellow carbons) and TDP-L-evernosamine (magenta carbons) as sticks. Active site loops L3, L5, L7, and L9, are predicted to interact with flavin and are colored orange, active site loops L1, L4, L6, L8, and L11 are predicted to interact with substrate and are colored purple, and active site loops L2 and L10 are predicted to interact with both substrate and cofactor and are colored teal. (B) A ribbon diagram of human short branched-chain acyl Co-A dehydrogenase (PDB entry 2JIF) [30], highlighting loops L1 to L11 colored are colored as in (A). (C) A ribbon diagram of *A. baumannii* 4-hydroxyphenylacetate monooxygenase (PDB entry 2JBT) [31] highlighting loops L1 to L11 colored as in (A). (D) Stereoview of the ORF36 loop L10 containing a tandem cis-peptide. Loop L10 is shown in sticks with teal carbons. The Q376-P377 and P377-Y378 bonds both adopt a cis conformation. Modeled flavin and substrate are displayed as in (A). This figure is taken from reference 14 in which the author of this document is a coauthor.

Description of the active site

The predicted active site of ORF36 contains amino acid residues mainly from the central β-sheet domain and the N-terminal helical domain, but also includes residues from the C-terminal domain of an adjacent monomer.[25] The base of the active site cleft is formed along helix α4. Flavin binding is predicted to be mediated by interactions with residues in α4, β1, α6 and α8, whereas substrate binding presumably occurs via

interactions with residues in α4 and α6-α8 helices. Additionally, loops L1-L11 surrounding the active site likely play a role in substrate binding and catalysis. Loops L1, L2, L4, L5, L6, L7, L8 and L11 differ in structure compared to their counterparts in the aforementioned structural homologs of nitrososynthases, suggesting that they likely play an important role in conferring substrate and cofactor specificity.

The active sites of both ORF36 and KijD3 measure 30 Å wide by 20 Å deep and appear to be solvent exposed. This is in contrast to the active sites in flavin-containing monooxygenases and acyl-CoA dehydrogenases. This unusually large pocket results from the open conformations of loops L1, L2, L4, L6, L7, and L11 in ORF36 and KijD3, which is unlike the more compact conformations of their counterparts in the acyl-CoA dehydrogenases and flavin-containing monooxygenases. Most of these loops are known to have interactions with the substrate in the acyl-CoA dehydrogenase superfamily, suggesting that significant main chain conformational changes may occur upon substrate binding. Of note, loop L10 located on the floor of the active site cleft in ORF36 likely contains tandem cis-peptide bonds between Gln 376 and Pro 377 and between Pro377 and Tyr 378. Although the assignment of cis-peptide bond is speculative at this resolution, modeling the loop with trans-peptide bonds or with only a single cis-proline resulted in disallowed Ramachandran angles for Tyr 378 and poor agreement of the main chain with the electron density. This assignment is also supported with the observation that KijD3, with its L10 sequence identical to that of ORF36, contains tandem cis-peptide bonds in this location.[18]

The crystallographic temperature factors of residues in the loops surrounding the active site in both ORF36 and KijD3 are significantly higher when compared to residues in the remainder of the protein. Temperature factors, also known as atomic displacement parameters or B-factors, can reflect the thermal motion of atoms and hint at regions of increased relative mobility in a given structure.

Discussion

Substrate preference of ORF36

The nitrososynthase activity of ORF36 with TDP-L-epi-vancosamine confirms that this aminosugar is preferred over its 4-ketosugar upstream congeners. Moreover, the O-methylation of the C4 hydroxyl group of TDP-L-epivancosamine was shown not to be necessary for the nitrososynthase activity. This was an expected outcome, because a variant of everninomicin lacking the C4-O methylation in its nitrosugar moiety was also isolated from *M. carbonacea* var. *africana*.[20] The single oxidation of the TDP 4-keto sugar substrates suggests that nitrososynthases in the biosynthesis of other nitrosugar-containing natural products may act on closely related precursors not necessarily identical to TDP-L-eivancosamine. The retention times of the oxidation products from the 4-keto aminosugar substrates matches that of the nitroso sugar produced from the activity of ORF36 with TDP-L-epivancosamine. This led us to propose a shunt reaction product, the C4 ketone, in which the 4-hydroxy position of TDP-L-epivancosamine is oxidized perhaps via dehydrogenation or hydroperoxylation of the C4 hydroxyl to the

ketone oxidation state. Other oxidation possibilities may also exist. Preliminary experiments of the ORF36 activity with the authentic substrate TDP-evernosamine, which is protected by O-methylation at C4, showed the production of only the nitroso sugar with no additional oxidation products. The proposed oxidation of the C4 position of TDP-L-epivancosamine upon ORF36 activity is intriguing and further experimentation should be performed to validate the identity of the proposed structures. Chapter IV details some chemical derivatization experiments and HPLC/MS analysis of the derivatized oxidation products of the nitrososynthase activity with TDP-L-epivancosamine which reveals a surprising outcome.

Structural comparison of ORF36 and KijD3

The overall structure of ORF36[14] matches that of its KijD3[18] homolog from the kijanimicin biosynthetic pathway with a root-mean-square deviation of 0.76 Å between the Cα atoms of the tetramers of the two proteins. The main differences in both sequence and structure between these two homologs are found in the regions that map to the active site cleft, and may be related to differences in function and substrate binding. Of note, variations in the interface of the predicted isoalloxazine and the TDP binding sites may account for substrate preference. The TDP and the isoalloxazine binding pockets themselves are almost completely conserved in both enzymes. The major structural variations between ORF36 and KijD3 are apparent in the active site loops L2, L4 and L6 located within the central β-sheet domain, and L7 and L8 of the C-

terminal domain. The high crystallographic temperature factors of these regions in both enzymes may reflect flexibility that facilitates movements of the substrate or the cofactor upon catalysis.

The active site of both nitrosoynthases ORF36 and KijD3 are relatively large and highly solvent accessible with their loops adopting open conformations. In comparison with structures of the acyl-coA dehydrogenases and class D flavin-containing monooxygenases, exclusion of water from the active site is presumably facilitated by conformational changes of loops L2, L4, L6, L7, L8 and L11. The active site residues have elevated temperature factors compared to the remainder of the protein likely accounting for substrate and cofactor mobility. Additionally, both enzymes possess a tandem cis-peptide bond within the active site loop L10 which likely undergoes isomerization initiating a conformational change to facilitate catalysis. These observations suggest that the active site loops may undergo significant conformational changes following cofactor and substrate binding. Conformational adjustments upon substrate binding are known for many enzymes[30-31], which suggest that the open active site architecture of both ORF36[14] and KijD3[18] maybe be physiologically relevant. The open loops in these enzymes may facilitate entry of the relatively large TDP sugar substrates, and the FAD cofactor. While further experiments are required to examine this possibility, this conformational variability in the active site may be necessary to prevent unwanted side reactions or nonproductive FAD cycling in the absence of substrate.

Proposed minimal mechanism of ORF36

Our biochemical characterization experiments outlined in this work confirmed the previously proposed monooxygenase activity of the nitrososynthase ORF36. The HPLC-MS analysis of ORF36 activity suggests that the enzyme first oxidizes TDP-L-epivancosamine to the hydroxylamine intermediate which undergoes a second flavin-dependent N-oxidation step to yield the nitroso sugar. These two oxidation steps result in single incorporation of oxygen into in the nitrososugar product evidenced by the results from performing the ORF36 oxidation reaction under $^{18}O_2$. Based on these observations, and with typical falvin-dependent monooxygenase mechanisms taken into consideration, we propose that ORF36 oxidation activity is mediated by flavin-C4a-hydroperoxide acting as an electrophile in a nucleophilic substitution reaction.[32-33]

Under this monooxygenation scenario, ORF36 likely first binds reduced flavin, generated by an external flavin reductase which readily reacts with molecular oxygen to form the oxidative electrophile flavin-C4a-hydroperoxide. This series of transformations are typical for flavin-dependent monooxygenases.[34] Subsequently, the aminosugar substrate binds and undergoes oxidation to form the hydroxylamino intermediate while the flavin cofactor is transformed to the C4a-hydroxyflavin which upon dehydration regenerates the diffusible oxidized flavin to be released along with the hydroxylamine. A similar second N-oxidation step followed by dehydration generates the nitroso sugar product. Alternatively, the nitroso sugar could be generated via a dehydrogenase mechanism similar to that catalyzed by the homologous acyl-CoA dehydrogenase. We performed the ORF36 oxidation reaction with TDP-L-epivancosamine under limited

concentration of NADPH (0.4 mM) and observed the formation of only the hydroxylamine intermediate suggesting that the second oxidation step requires reduced flavin. Therefore, we favor a monooxygenase activity that involves iterative electrophilic oxygenation followed by dehydration over the dehydrogenase mechanism. In support of molecular oxygen participation in catalysis, incorporation of single ^{18}O atom into the final product could be only observed when the oxidation reaction was performed under $^{18}O_2$, but not $H_2{}^{18}O$.

Conclusions

This work provided important biochemical characterization of the new flavin-dependent nitrososynthase ORF36 which catalyzes the N-oxidation of the aminosugar TDP-L-epivancosamine to its corresponding nitrososugar. We propose that the tetrameric enzyme undergoes conformational changes upon binding of the flavin cofactor and the substrate to facilitate the monooxygenation catalysis. The nitrososynthase enzyme represents a new class of flavin-dependent monooxygenases with an acyl-CoA dehydrogenase fold. The surprising contrast in the function of the nitrososynthase compared to its structural closest homologs suggests that nitrososynthases have functionally evolved divergently from acyl-CoA dehydrogenases. This could have implications on the growing number of enzymes annotated as acyl-CoA dehydrogenase-like enzymes, while they possibly perform different oxidation reactions. Future investigations of the activity of ORF36 with other aminosugar substrates such as

the authentic C4 O-methylated TDP-L-evernosamine will lead to a better understanding of the molecular determinants controlling selectivity and catalysis by this new class of enzymes. The biochemical characterization experiments provided in this work allowed the proposal of reasonable minimal mechanism which sets the stage for future mechanistic and structural studies.

Materials and methods

Overexpression and purification of enzymes. ORF36 from *M. carbonacea* var. *africana*[14], EvaA–E from *Amycolatopsis orientalis*[13], and RfbB from *Salmonella enterica* (strain LT2)[35-36] were purified from freshly transformed *E. coli* BL21(DE3) by nickel affinity chromatography as previously described with the exception of EvaE, which was isolated as an insoluble preparation. EvaE preparations were generated from 3 L induced cultures, which were disrupted via a French pressure cell. The insoluble fraction was isolated by centrifugation and washed with 20 mM Tris-HCl, pH 7.5, resuspended in 10 mL, 20 mM Tris-HCl, pH 7.5, 5% glycerol, and stored at -80 °C prior to use.

Preparation of TDP-6-deoxy-4-keto-D-glucose. Reactions (1 mL) containing 8 mM thymidine 5'-diphosphate-glucose disodium salt (4.5 mg), 50 mM Tris-HCl (pH 8.0), 4 mM $NADP^+$, and 160 µM RfbB were incubated at 24 °C for two hours. Proteins were removed by 10K molecular weight cutoff filtration (Centricon, Millipore Corp.) and the product was purified via SAX-HPLC (see below) followed by lyophilization. The final yield

was 4.0 mg of TDP-6-deoxy-4-keto-D-glucose (88% yield). TDP-6-deoxy-4-keto-D-glucose was analyzed by ESI-LC/MS, which determined the m/z to be 563.20 ($[M-H + H2O]^-$, calculated for $C_{16}H_{25}N_2O_{16}P_2$ is 563.07).

Preparation of other TDP-sugars substrates and intermediates. Other TDP-sugars were biochemically synthesized from TDP-6-deoxy-4-keto-D-glucose using purified enzyme preparations and the general procedures outlined by Chen *et. al*.[13] with the following modifications. Briefly, thimidine-5'-diphosphate-3-amino-2,3,6-trideoxy-3-C-methyl-D-erythrohexopyranos-4-ulose (the TDP-4-keto-3-amino D-sugar), was synthesized via tandem reaction with EvaA, EvaB and EvaC and purified as described below in a 36% overall yield for three steps. ESI-LC mass spectra yielded the m/z of 560.27 ($[M-H + H_2O]^-$, calculated for $C_{17}H_{28}N_3O_{14}P_2$ is 560.10). The substrate thymidine-5-diphospho-3-amino-2,3,6-trideoxy-3-C-methyl-L-arabinohexose (TDP-epivancosamine) was generated from the TDP-4-keto-3-amino D-sugar (1 mM) in a 1-mL reaction containing 100 mM Tris-HCl (pH 7.5), 5 mM NADPH, 20 µM EvaD and 50 µL of the resuspended EvaE pellet. The reaction was incubated at 24 °C for 2 h, proteins and cell debris were removed using a 10K centrifugal filter (Centricon), and the product was purified by SAX-HPLC (described below) followed by lyophilization which resulted in 300 µg (55% yield) of TDP-L-epivancosamine. ESI-LC MS confirmed the mass of TDP-L-epivancosamine ($[M-H]^-$ calculated for $C_{17}H_{28}N_3O_{13}P_2$ is 544.11, found 544.27).

Purification of TDP-sugars. Preparative enzymatic reaction progress was followed via HPLC using a series 600 Waters HPLC system with a Waters 2996 diode

array detector. Analytical separations were performed on an Adsorbosphere strong anion exchange (SAX) column (5 mm, 4.6 x 20 mm, Alltech Associates) and a linear gradient of 50 to 500 mM NH_4HCO_2, pH 3.5, at 1 mL/min for 45 min. Preparative HPLC separations were performed using a semi-preparative Adsorbosphere SAX column (5 µm, 22 x 250 mm) using a similar protocol, but at 10 mL/min. The pH of the fractions containing TDP-chromophores (267 nm) were immediately adjusted to ~7 with 1 M NH_4OH and fractions containing reaction product were pooled, lyophilized and stored at -80 °C until assayed. Resuspended compound concentrations were determined by measuring the absorbance at 267 nm using a Nanodrop spectrophotometer (Thermo, Inc.) and comparison to a standard curve of dTDP.

ORF36 enzymatic reactions with the aminosugar substrates. Reactions of ORF36 with the TDP-4-keto-3-amino D-sugar and TDP-L-epivancosamine were performed in a total volume of 50 µL containing 30 µM of the corresponding substrates with 30 µM FAD, 1 U/mL catalase, 0.05 U flavin reductase, and 2.0 mM NADPH. The TDP-4-keto-3-amino L-sugar was generated in situ by including 20 µM EvaD in the reaction with its D-sugar precursor. All reactions were initiated by addition of 12 µM ORF36 and 10 µL samples were withdrawn at increasing time points (0 - 120 min) and were quenched with 10 µL of acetone and stored at -80 °C until analyzed by LC-ESI/MS. Control assays were performed omitting ORF36, FAD, or NADPH.

$^{18}O_2$-incorporation assays. Reactions with $^{18}O_2$ gas were performed in a 5 mL round bottom flask fitted with a rubber septum and a balloon (~5 mL, connected via a

syringe needle). The reaction vessel at 4 °C was connected via stainless steel cannula to a closed gas cylinder (Cambridge Isotope Laboratories) containing 1 L, 22 psi of $^{18}O_2$ that was also fitted with a rubber septum. A freshly prepared solution (200 µL) containing 20 mM Tris-HCl, pH 7.5, 30 µM FAD, 1 U/mL catalase, 0.05 U/mL flavin reductase, 2.0 mM NADPH, and 0.5 mg/mL ORF36 was introduced into the flask and the entire reaction system was degassed in vacuo (25 - 50 mm Hg) for 20 minutes. The $^{18}O_2$ cylinder was opened to release sufficient $^{18}O_2$ to fill the flask and the small balloon with ~5-10 mL of gas. Reactions were initiated by the addition of 30 µM of vacuum degassed TDP-L-epi-vancosamine via a gas-tight syringe. Reactions were followed for 2 h at 30 °C by withdrawing 25 µL aliquots via syringe at increasing time points, quenching via addition of 25 µL acetone and storing samples at -80 °C until analyzed by LC-ESI/MS as described below.

LC-ESI/MS method for ORF36 Substrates. The oxidation of ORF36 substrates was analyzed using Agilent 1100 HPLC system (Agilent, Palo Alto, CA) with a LCQ Quantum Decca XP ion trap mass analyzer (ThermoFinnigan, San Jose, CA) equipped with an API electrospray ionization source fitted with a 50 µm I.D. deactivated fused silica capillary. Injections of 10 µl were separated using a Hypercarb column (3 × 50 mm, Thermo Inc). Mobile phases were: (A) H_2O with 50 mM $NH_4CH_3COO^-$ and 0.1% (v/v) diethylamine and (B) H_2O/acetonitrile (5:95) with 50 mM $NH_4CH_3COO^-$ and 0.1% (v/v) diethylamine. Gradient conditions were as follows: 0-5 min, B = 15%; 5-15 min, linear gradient to 35%

B; 15 to 16 min, linear gradient to 100% B; 16 to 21 min, B = 100%; 21 to 22 min, linear gradient to 15% B; 22-30 min, B = 15%. The flow rate was maintained at 0.3 ml/min. The mass spectrometer was operated in both the negative ion and full scan profile modes and the electrospray needle was maintained at 3,400 V. The ion transfer tube was operated at -47.50 V and 275°C. The tube lens voltage was set to -46 V. The collision energy for all product ion scans was set at 30%. For TDP-L-epi-vancosamine 10, full product and ion scans were set as follows: 544→155-548; 558→155-560; 560→155-562. For the assays with the 3-amin-4-keto sugars, the scans were set as follows: 542→155-548; 560→155-562; 558→155-560. Data were acquired in profile mode. The following optimized parameters were used for the detection: N_2 sheath gas 46 psi; N_2 auxiliary gas 13 psi; spray voltage 3.4 kV.

Crystallization of ORF36. Initial crystallization conditions for ORF36 were identified by sparse matrix screening and were improved using diffraction-based feedback on the Life Sciences Collaborative Access Team (LS-CAT) beamlines 21-ID-D, 21-ID-F, and 21-ID-G at the Advanced Photon Source (APS), and beamline 9-1 at Stanford Synchrotron Radiation Lightsource (SSRL). Optimized crystals of ORF36 were grown using the hanging drop vapor diffusion technique at 277 K from drops containing 1 μL protein solution (7 mg/mL ORF36 in 20 mM Tris.HCl, 5% glycerol, 1 mM DTT, pH 7.5) and 1 μL crystallization solution (0.1 M Tris-HCl pH 8.5, 0.2 M $MgCl_2$, 10% polyethylene glycol 4000), equilibrated against 1 mL crystallization solution. Crystals belonging to the hexagonal space group P65 reached a maximal size of 0.1 mm x 0.1 mm x 0.4 mm in 5-6 days. The volume of the unit cell was consistent with a tetramer in the

asymmetric unit and 53% solvent content. Crystals were cryoprotected by equilibration in crystallization solution supplemented with 20% glycerol or 20% ethylene glycol and cryo-cooled in liquid nitrogen prior to data collection.

Native data set 1 was collected at 100 K at the beamline 21-ID-D of the Advanced Photon Source using a Rayonix MX 225 detector. Native data set 2 was collected at 100 K on beamline 9-2 at SSRL using a MarUSA MarMosaic-325 CCD detector. Data integration and scaling were performed with the HKL2000 suite of programs.

Structure determination and refinement. The structure of ORF36 was determined by molecular replacement in Phaser[37] using a polyalanine version of the human short-branched chain acyl-CoA dehydrogenase tetramer as the search model (PDB entry 2JIF[23] (35), 25% sequence identity). Molecular replacement was only successful with the Native data set 1. The molecular replacement solution was transferred into the higher-resolution Native data set 2 and refined using alternating rounds of manual model building in XtalView[38] and refinement in CNS[39] with strict non-crystallographic symmetry (NCS) constraints. Once the R¬cryst reached 26%, each chain was examined for main chain differences, which were observed within the central β-domain between the ORF36 monomers. As a result, during the final four cycles of refinement, each monomer was refined with NCS restraints applied to the N- and C-terminal domains, but deviations from NCS were allowed in the central β-domain.

The final model of ORF36 comprises residues 1 to 395 (of 412 total residues), with several breaks observed in chains B, C, and D. In chain B, electron density for

residues 143-151, 177-184, and 229-235 is not observed; in chain C, electron density for residues 144-156, 176-182, 218-221 and 235 is not observed; in chain D electron density for residues 226-227 and 316 is not observed. The test set of reflections for the R_{free} consisted of 9.1% of the data, totaling 2816 reflections. The final model has an R_{cryst} of 24.2%, an R_{free} of 28.1%, 88.5% of residues in the most favored regions of the Ramachandran diagram, 10.9% in the additionally allowed regions, 0.6% in the generously allowed regions, and 0.0% in the disallowed regions. Figures III-4 was prepared with PyMOL.[40] Figure III-5 was prepared using MOLSCRIPT[41] and Raster3D.[42]

Modeling of substrate and cofactor. FAD was modeled into the active site by superpositioning the ORF36 structure with that of human short-branched chain acyl-CoA dehydrogenase (PDB entry 2JIF[23]) and using the position of bound FAD from 2JIF as a starting point. Attempts to improve the position of FAD using the molecular docking program Molecular Operating Environment (MOE, Chemical Computing Group, Montreal, Canada) did not result in a solution that both alleviated steric clashes between the FAD and protein and retained a reasonable position for the isoalloxazine ring.

A model for TDP-L-evernosamine was constructed by manual combination of deoxythymidine diphosphate (ligand name TYD) and the epi-vancosaminyl derivative of vancomycin (ligand name VAX), both available via the HIC-Up server.[43] The TDP-L-evernosamine was manually positioned within the active site such that the amino sugar was within 5.5 Å of the expected position of the C4a of the isoalloxazine ring, but the

location of the TDP varied. The docking algorithm in MOE was used to improve each manual starting point. Docking was performed using a radius of 10 Å around the initial position of the ligand, the triangle matcher algorithm for placement, London dG rescoring, and force field refinement. Between 30 and 100 positions were retained from each trial and validated manually by evaluating the orientation of the sugar moiety in the active site, and the distance of the amino group from the expected position of C4a of the isoalloxazine ring. The optimized position for TDP-L-evernosamine had a location of the TDP similar to that experimentally observed for the ordered dTDP moiety of dTDP-phenol in complex with the nitrososynthase KijD3.[18]

References

1. Hu, Y.; Al-Mestarihi, A.; Grimes, C. L.; Kahne, D.; Bachmann, B. O., A unifying nitrososynthase involved in nitrosugar biosynthesis. *Journal of the American Chemical Society* **2008,** *130* (47), 15756-7.

2. Bannister, B.; Zapotocky, B. A., Protorubradirin, an antibiotic containing a C-nitroso-sugar fragment, is the true secondary metabolite produced by Streptomyces achromogenes var. rubradiris. Rubradirin, described earlier, is its photo-oxidation product. *The Journal of Antibiotics* **1992,** *45* (8), 1313-24.

3. Lee, J.; Zhao, H., Mechanistic studies on the conversion of arylamines into arylnitro compounds by aminopyrrolnitrin oxygenase: Identification of intermediates and kinetic studies. *Angewandte Chemie* **2006,** *118* (4), 638-641.

4. Simurdiak, M.; Lee, J.; Zhao, H., A New Class of Arylamine Oxygenases: Evidence that p-Aminobenzoate N-Oxygenase (AurF) is a Di-iron Enzyme and Further Mechanistic Studies. *ChemBioChem* **2006,** *7* (8), 1169-1172.

5. Seto, Y.; Guengerich, F., Partitioning between N-dealkylation and N-oxygenation in the oxidation of N, N-dialkylarylamines catalyzed by cytochrome P450 2B1. *Journal of Biological Chemistry* **1993,** *268* (14), 9986-9997.

6. Joosten, V.; van Berkel, W. J. H., Flavoenzymes. *Current Opinion in Chemical Biology* **2007,** *11* (2), 195-202.

7. Van Berkel, W.; Kamerbeek, N.; Fraaije, M., Flavoprotein monooxygenases, a diverse class of oxidative biocatalysts. *Journal of Biotechnology* **2006,** *124* (4), 670-689.

8. Duffner, F. M.; Kirchner, U.; Bauer, M. P.; Müller, R., Phenol/cresol degradation by the thermophilic Bacillus thermoglucosidasius A7: cloning and sequence analysis of five genes involved in the pathway. *Gene* **2000,** *256* (1), 215-221.

9. Kadiyala, V.; Spain, J. C., A Two-Component Monooxygenase Catalyzes Both the Hydroxylation of p-Nitrophenol and the Oxidative Release of Nitrite from 4-Nitrocatechol in Bacillus sphaericusJS905. *Applied and Environmental Microbiology* **1998,** *64* (7), 2479-2484.

10. Kirchner, U.; Westphal, A. H.; Müller, R.; van Berkel, W. J. H., Phenol hydroxylase from Bacillus thermoglucosidasius A7, a two-protein component monooxygenase with a dual role for FAD. *Journal of Biological Chemistry* **2003,** *278* (48), 47545.

11. van den Heuvel, R. H. H.; Fraaije, M. W.; van Berkel, W. J. H., Direction of the reactivity of vanillyl-alcohol oxidase with 4-alkylphenols. *FEBS Letters* **2000,** *481* (2), 109-112.

12. Xun, L.; Sandvik, E. R., Characterization of 4-hydroxyphenylacetate 3-hydroxylase (HpaB) of Escherichia coli as a reduced flavin adenine dinucleotide-utilizing monooxygenase. *Applied and Environmental Microbiology* **2000,** *66* (2), 481-486.

13. Chen, H.; Thomas, M. G.; Hubbard, B. K.; Losey, H. C.; Walsh, C. T.; Burkart, M. D., Deoxysugars in glycopeptide antibiotics: enzymatic synthesis of TDP-L-epivancosamine in chloroeremomycin biosynthesis. *Proceedings of the National Academy of Sciences* **2000,** *97* (22), 11942.

14. Vey, J. L.; Al-Mestarihi, A.; Hu, Y.; Funk, M. A.; Bachmann, B. O.; Iverson, T. M., Structure and mechanism of ORF36, an amino sugar oxidizing enzyme in everninomicin biosynthesis. *Biochemistry* **2010,** *49* (43), 9306-17.

15. Hosted, T.; Horan, A.; Wang, T., Everninomicin biosynthetic genes. WO Patent WO/2001/051,639: 2001.

16. Kim, C. G.; Lamichhane, J.; Song, K. I.; Nguyen, V. D.; Kim, D. H.; Jeong, T. S.; Kang, S. H.; Kim, K. W.; Maharjan, J.; Hong, Y. S.; Kang, J. S.; Yoo, J. C.; Lee, J. J.; Oh, T. J.; Liou, K.; Sohng, J. K., Biosynthesis of rubradirin as an ansamycin antibiotic from Streptomyces achromogenes var. rubradiris NRRL3061. *Archives of Microbiology* **2008,** *189* (5), 463-73.

17. Zhang, H.; White-Phillip, J. A.; Melancon, C. E., 3rd; Kwon, H. J.; Yu, W. L.; Liu, H. W., Elucidation of the kijanimicin gene cluster: insights into the biosynthesis of spirotetronate antibiotics and nitrosugars. *Journal of the American Chemical Society* **2007,** *129* (47), 14670-83.

18. Bruender, N. A.; Thoden, J. B.; Holden, H. M., X-ray structure of kijd3, a key enzyme involved in the biosynthesis of D-kijanose. *Biochemistry* **2010,** *49* (17), 3517-24.

19. Timmons, S. C.; Thorson, J. S., Increasing carbohydrate diversity via amine oxidation: aminosugar, hydroxyaminosugar, nitrososugar, and nitrosugar biosynthesis in bacteria. *Current Opinion in Chemical Biology* **2008,** *12* (3), 297-305.

20. Chu, M.; Mierzwa, R.; Jenkins, J.; Chan, T. M.; Das, P.; Pramanik, B.; Patel, M.; Gullo, V., Isolation and characterization of novel oligosaccharides related to Ziracin. *Journal of Natural Products* **2002,** *65* (11), 1588-93.

21. Greenwald, R. A., Superoxide dismutase and catalase as therapeutic agents for human diseases. A critical review. *Free Radical Biology & Medicine* **1990,** *8* (2), 201-9.

22. Chow, Y. L.; Chen, S. C.; Mojelsky, T., Nitrosamine photoaddition to norbornene and the mechanism of nitrosoalkane cleavage. *J. Chem. Soc., Chem. Commun.* **1973,** (21), 827-828.

23. Pike, A. C. W., Hozjan, V., Smee, C., Niesen, F. H., Kavanagh,K. L.,; Umeano, C., Turnbull, A. P., Von Delft, F., Weigelt, J., Edwards, A.,; Arrowsmith, C. H., Sundstrom, M., and Oppermann, U., Crystal Structure of Human Short-Branched Chain Acyl-Coa Dehydrogenase. **2010,** *Manuscript being prepared for publication.*

24. Holm, L.; Kaariainen, S.; Rosenstrom, P.; Schenkel, A., Searching protein structure databases with DaliLite v.3. *Bioinformatics* **2008,** *24* (23), 2780-1.

25. Thorpe, C.; Kim, J. J., Structure and mechanism of action of the acyl-CoA dehydrogenases. *FASEB journal: official publication of the Federation of American Societies for Experimental Biology* **1995,** *9* (9), 718-25.

26. McCulloch, K. M.; Mukherjee, T.; Begley, T. P.; Ealick, S. E., Structure of the PLP degradative enzyme 2-methyl-3-hydroxypyridine-5-carboxylic acid oxygenase from Mesorhizobium loti MAFF303099 and its mechanistic implications. *Biochemistry* **2009,** *48* (19), 4139-49.

27. Alfieri, A.; Fersini, F.; Ruangchan, N.; Prongjit, M.; Chaiyen, P.; Mattevi, A., Structure of the monooxygenase component of a two-component flavoprotein monooxygenase. *Proceedings of the National Academy of Sciences of the United States of America* **2007,** *104* (4), 1177-82.

28. Lindqvist, Y.; Koskiniemi, H.; Jansson, A.; Sandalova, T.; Schnell, R.; Liu, Z.; Mantsala, P.; Niemi, J.; Schneider, G., Structural basis for substrate recognition and specificity in aklavinone-11-hydroxylase from rhodomycin biosynthesis. *Journal of Molecular Biology* **2009,** *393* (4), 966-77.

29. Gatti, D. L.; Entsch, B.; Ballou, D. P.; Ludwig, M. L., pH-dependent structural changes in the active site of p-hydroxybenzoate hydroxylase point to the importance of proton and water movements during catalysis. *Biochemistry* **1996,** *35* (2), 567-78.

30. Weikl, T. R.; von Deuster, C., Selected-fit versus induced-fit protein binding: kinetic differences and mutational analysis. *Proteins* **2009,** *75* (1), 104-10.

31. Johnson, K. A., Role of induced fit in enzyme specificity: a molecular forward/reverse switch. *The Journal of Biological Chemistry* **2008,** *283* (39), 26297-301.

32. Massey, V., Activation of molecular oxygen by flavins and flavoproteins. *The Journal of Biological Chemistry* **1994,** *269* (36), 22459-62.

33. Palfey, B. A.; McDonald, C. A., Control of catalysis in flavin-dependent monooxygenases. *Archives of Biochemistry and Biophysics* **2010,** *493* (1), 26-36.

34. Massey, V., The chemical and biological versatility of riboflavin. *Biochemical Society Transactions* **2000,** *28* (4), 283-96.

35. Romana, L. K.; Santiago, F. S.; Reeves, P. R., High level expression and purification of dthymidine diphospho-D-glucose 4,6-dehydratase (rfbB) from Salmonella serovar typhimurium LT2. *Biochemical and Biophysical Research Communications* **1991,** *174* (2), 846-52.

36. Takahashi, H.; Liu, Y. N.; Liu, H. W., A two-stage one-pot enzymatic synthesis of TDP-L-mycarose from thymidine and glucose-1-phosphate. *Journal of the American Chemical Society* **2006,** *128* (5), 1432-3.

37. McCoy, A. J.; Grosse-Kunstleve, R. W.; Adams, P. D.; Winn, M. D.; Storoni, L. C.; Read, R. J., Phaser crystallographic software. *Journal of Applied Crystallography* **2007,** *40* (Pt 4), 658-674.

38. McRee, D. E., XtalView/Xfit--A versatile program for manipulating atomic coordinates and electron density. *Journal of Structural Biology* **1999,** *125* (2-3), 156-165.

39. Brunger, A. T.; Adams, P. D.; Clore, G. M.; DeLano, W. L.; Gros, P.; Grosse-Kunstleve, R. W.; Jiang, J. S.; Kuszewski, J.; Nilges, M.; Pannu, N. S., Crystallography & NMR system: A new software suite for macromolecular structure determination. *Acta Crystallographica Section D: Biological Crystallography* **1998,** *54* (5), 905-921.

40. DeLano, W., *The PyMOL Molecular Graphics System*, DeLano Scientific, San Carlos, CA, USA, 2002. Number of salt bridge-forming Arg Residues Higher in A. Tropicalis Higher in A. pasteurianus No difference **2002**.

41. Kraulis, P. J., MOLSCRIPT: a program to produce both detailed and schematic plots of protein structures. *Journal of Applied Crystallography* **1991,** *24* (5), 946-950.

42. Merritt, E.; Murphy, M. E. P., Raster3D Version 2.0. A program for photorealistic molecular graphics. *Acta Crystallographica Section D: Biological Crystallography* **1994,** *50* (6), 869-873.

43. Kleywegt, G. J., Crystallographic refinement of ligand complexes. *Acta Crystallographica Section D: Biological Crystallography* **2006,** *63* (1), 94-100.

Chapter IV

RETRO-ALDOL ACTIVITY OF THE NITROSOSYNTHASE DNMZ

Introduction

The anthracycline antibiotics and anticancer agents are very important class of aromatic microbial polyketides.[1-3] These red compounds are produced by some strains of *Streptomyces*, and about one quarter of them was found in so-called rare actinomycetes.[4] Anthracyclines are diversified structurally through modifications in their tetracyclic polyketide core and a wide array of attached deoxysugar appendages. The high interest in studying anthracyclines arose from their remarkable pharmaceutical properties especially their potent antitumor activities. Consequently, they have been some of the most intensively studied natural products over the past 50 years.[5]

Daunorubicin and doxorubicin produced by *Streptomyces peucetius* are among the first isolated anthracyclines (Figure IV-1).[6-7] Clinically, they are useful against several types of cancer especially solid tumors that are normally resistant to most types of chemotherapy. However, the use of anthracyclines for cancer treatment is usually accompanied by undesired side effects such as dose-related cardiotoxicity.[8] Therefore, researchers have been interested in developing synthetic and other biogenic anthracycline derivatives to achieve improved pharmacological properties. To that end,

many efforts have been made to diversify the structures of anthracyclines with the aim of creating a wider spectrum of activities and reduced toxicity.[9-14]

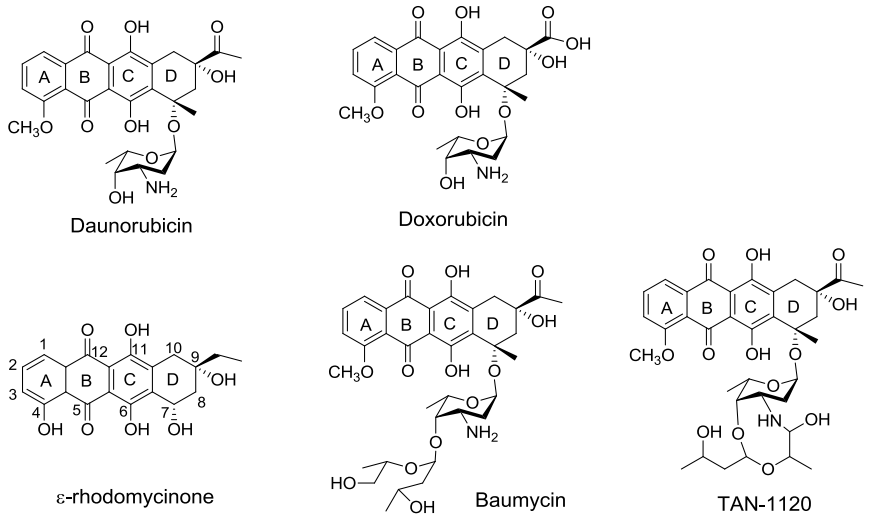

Figure IV-1. Chemical structure of known anthracyclines

The tetracyclic polyketide core in anthracyclines is typically assembled from acetyl units in the form of malonyl- CoA by an iterative, type II polyketide synthase followed by aromatase, cyclase and tailoring enzymes.[15-17] This yields the basic tetracyclic structure which undergoes subsequent enzymatic modification steps. The biosynthesis of most anthracyclines starts with the incorporation of a propinyl starter unit from propinyl-CoA, catalyzed by a ketoreductase and a thioesterase. In daunorubicin, a precursor for baumycin, the minimal PKS proteins that catalyze the formation of the long chain polyketide, are an acyl carrier protein (ACP), ketosynthase (KS) and a malonyl-CoA:ACP acyltransferase (MAT).[18] The polyketide chain is converted to 12-deoxyalkalonic acid catalyzed by the dps gene cluster which includes DpsE, an

NADPH dependent 9-ketoreductase, and cyclases DpsF and DpsY that catalyze the formation of ring D and C, respectively.[19] The subsequent polyketide modifications are catalyzed by the dnr gene cluster which includes C-12 oxygenase, a SAM dependent alkalonic acid methyltransferase, ring A cyclase, C-7 ketoreductase, and a C-11 hydroxylase.[20] This series of polyketide modifications yields ε-rhodomycinone (Figure IV-1), the precursor for doxorubicin and daunorubicin.

Perhaps the most important chemical modification of the anthracycline aglycone core is glycosylation at one or several positions. It has been shown that the deoxysugar moieties are required for the antimicrobial and antitumor activities.[21] The deoxysugar moieties are usually attached at position C-7 and/or C-10 of the aglycone core by a variety of glycosyltransferases.[22-24] In daunorubicin, the deoxysugar L-daunosamine is attached at C-7 of the tetracyclic polyketide. The biosynthesis of the L-daunosamine sugar has been studied via molecular genetics, which identified six biosynthetic genes responsible for the formation of its TDP-activated derivative starting from glucose-1-phosphate.[25] The presence of additional deoxysugar genes in the daunorubicin gene cluster such as *dnrh* which encodes a glycosyltransferase, indicated that daunorubicin is a precursor for further glycoslated downstream derivatives. Daunorubicin was shown to be a precursor of baumycin, which includes a non-sugar acetal moity attached at C-4 hydroxyl of the daunosamine sugar.[26] Other baumycin-like compounds such as the angiostatic agent TAN-1120 (Figure IV-1) have also been isolated from *Streptomyces peucetius.*[27] Besides *dnrh*, two more deoxysugar genes were found in the daunorubicin gene cluster: *dnrx* which encodes a SAM dependent C-3-methyltransferase, and *dnmz*

which encodes a flavin-dependent nitrososynthase homologous to ORF36 described in chapters II and III.[28]

The DnmZ protein shares high sequence homology with the nitrososynthases ORF36, RubN8 and KijD3.[29-30] For example, DnmZ[25] shares 70% sequence similarity with ORF36 (59% Identity). This strongly suggests that DnmZ catalyzes a flavin-dependent deoxyaminosugar oxidation. Given the fact that there are no N-oxidized deoxysugar moieties in any of the anthracycline derivatives produced by *Streptomyces peucetius* isolated to date, the role of DnmZ in the biosynthesis of these compounds is seemingly puzzling. However, one scenario can be envisioned in which DnmZ catalyzes a deoxyaminosugar oxidation similar to that carried out by its nitrososynthase homologues, whereby the resulting sugar undergoes further enzymatic and/or chemical transformations either before or after glycoslation.

Our investigations to elucidate the role of DnmZ in the biosynthesis of baumycin-like anthracyclines from *Streptomyces peucetius*, aimed at providing biochemical evidence of its activity as a flavin-dependent nitrososynthase. Additionally, we were interested in investigating the fate of the N-oxidation product of DnmZ and the possible pathways for its further enzymatic or chemical modifications.

Results and discussion

Proposed activity of DnmZ

The biosynthesis of the non-sugar acetal moiety attached at the C4 hydroxyl of L-daunosamine in baumycin (Figure IV-1) is not yet studied. Synthesis of its carbon skeleton and functionalities are hard to assign to known enzymatic transformations. One possibility is that this 7-carbon moiety originates from a deoxysugar precursor which undergoes enzymatic and/or chemical modifications involving a carbon-carbon bond cleavage. The presence of additional genes that encode for deoxysugar modifying enzymes in the anthracycline gene cluster of *Streptomyces peucetius*, is in support of this hypothesis.[31] We proposed that the DnmZ enzyme could catalyze a flavin-dependent N-oxidation of a TDP-aminosugar precursor to yield its nitroso congener given its high similarity with the nitrososynthases ORF36 and RubN8. The C-3 methyltransferase DnrX[28] is likely involved in the production of the TDP activated deoxyaminosugar substrate of the DnmZ enzyme. One biosynthetic pathway of this substrate could be proposed in which the SAM dependent methyltransferase DnrX activity follows the transamination by DnmJ forming the C-3 methylated TDP-sugar. This methylation step is not required for the biosynthesis of L-daunosamine[25] and maybe a key requirement for subsequent deoxyaminosugar oxidation activity. This is consistent with the methylation at C-3 in the deoxynitrosugars L-evrnitrose, D-rubranose, and L-kijanose biosynthesized via a nitrososynthase activity.[32-34] The subsequent step to produce the DnmZ substrate could be carried out by a C-4 ketoreductase (possibly

DnmV) to yield TDP-L-epivancosamine, which was shown to be a substrate for the nitrososynthase homologue ORF36. Amine oxidation of this TDP-sugar by DnmZ could set the stage for further enzymatic and/or chemical transformations ultimately resulting in the formation of the 7-carbon acetal moiety in baumycin.

Pillay and co-workers[35] reported a chemical precedent in which a carbon-carbon bond cleavage of the norbornane 2-*exo*-nitroso-3-*exo*-hydroxybicyclo[2.2.1]heptane was observed upon reflux of this compound in methanol (Figure IV-2). It was shown that the cleavage results in the formation of an aldehyde at C3 and an oxime at C2 of the molecule. The authors clarified that the cis-C-2-nitroso-3-hydroxy configuration is required for the cleavage reaction because it facilitates the easy proton transfer from the hydroxyl group to the nitroso group.

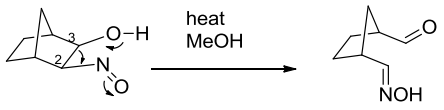

Figure IV-2. Carbon-carbon bond cleavage reaction of 2-exo-nitroso-3-exo-hydroxy norbornane.

A similar scenario could be envisioned for the TDP linked C3-nitroso-C-4-hydroxy sugar product of DnmZ in which an enzyme mediated C3-C4 bond cleavage results in the formation of an aldehyde at C4 and an oxime at C3 (figure IV-3). The nitroso congener of TDP-L-epivancosamine[36] possesses the trans-configuration for the nitroso-hydroxy groups and a cleavage reaction in this case would likely be enzymatically catalyzed. If this proposed transformation is proven true, it would represent a retro-aldol activity of

the nitrososynthase DnmZ, a function not known for any falvin dependent monooxygenase characterized to date.

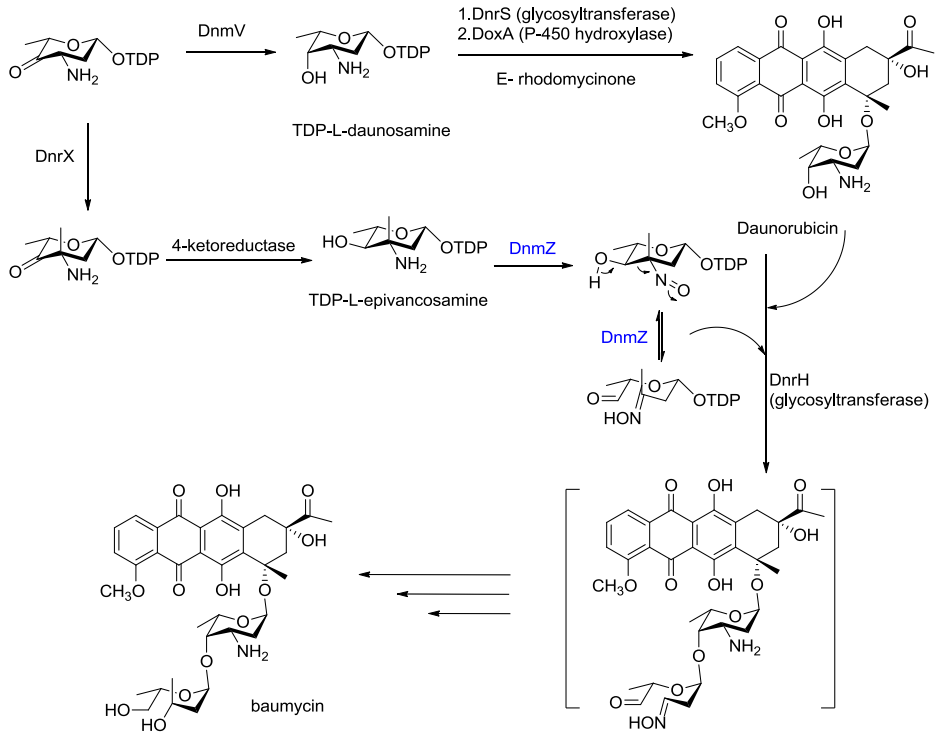

Figure IV-3. Proposed pathway for the DnmZ monooxygenation activity and the subsequent cleavge and glycoslation activities.

Activity of DnmZ as a nitrososynthase

Given the high sequence homology of DnmZ with the characterized flavin-dependent nitrososynthase ORF36, it is expected that both enzymes catalyze similar deoxysugar N-oxidation reaction. To confirm this, we amplified the *dnmz* gene from *Streptomyces peucetius* via the polymerase-chain reaction (PCR), cloned it into the NdeI/HindIII sites of pET28a expression vector, and transformed the resulting plasmid

into the BL21 DE3 *E.coli* bacterial strain via electroporation. Expression conditions for the protein were found to be similar to those previously described for its ORF36 and RubN8 homologues. The protein was purified by Ni-affinity chromatography and analyzed by SDS-PAGE (Figure IV-4).

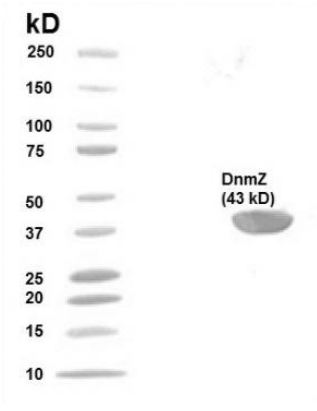

Figure IV-4. SDS-PAGE gel of Ni-affinity purified DnmZ

We used the biogenic aminosugar TDP-L-epivancosamine as a substrate to assay the nitrososynthase activity of DnmZ and followed the same assay conditions performed for ORF36 oxidation reaction. The HPLC-MS analysis of the DnmZ assay showed similar reaction profile as that of ORF36 ultimately yielding products with m/z 558 and 576 previously identified as the nitrososugar congener and a shunt oxidation product respectively.

According to our proposed retro-aldol activity of Dnmz, the C3-C4 bond cleavage would result in an aldehyde at C4 and an oxime at C3 of the TDP-3-nitro-4-hydroxy sugar (Figure IV-3). This TDP linked compound with terminal oxime and aldehyde groups has an m/z of 558 in the negative mode. Aldehydes are known to exist in their hydrated

form which is consistent with the compound appearing at m/z 576 previously proposed to be an oxidation shunt product. These two compounds elute at a very similar retention time suggesting that they exist in equilibrium.

Hydrazone derivatization of the DnmZ oxidation product

The proposed oxime-aldehyde product formed upon TDP-L-epivancosamine oxidation by DnmZ could be confirmed by a hydrazone derivatization at the aldehyde group (Scheme IV-2). Aldehydes are known to react with hydrazines to form their corresponding hydrazone derivatives.[37]

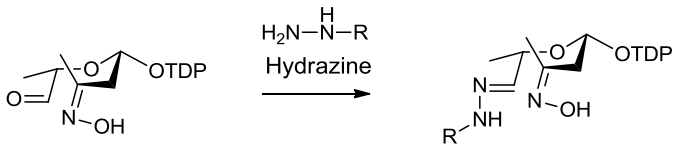

Scheme IV-2. Hydrozone derivatization of the proposed oxime-aldehyde product.

We performed this derivatization by incubating the completed DnmZ assay separately with three hydrazine compounds; phenyl hydrazine; 2-bromophenylhydrazine; and 2-hydrazino-N,N,N-trimethyl-2-*oxo*-ethanaminium chloride, known as Girard's T reagent (GirT).[38] The incubation time for these reactions was 2h at room temperature and the mixtures were immediately analyzed by HPLC-MS. The GirT hydrazone derivative advantageously possesses the positively charged trimethylammonium group facilitating analysis in the positive mode unlike the phenyl- and the 2-bromophenyl hydrazone derivatives which were best analyzed in the negative

mode aided by deprotonation of their attached nucleotide phosphates. As shown in figure IV-5, HPLC-MS peaks at m/z's corresponding to all of the expected three hydrazone derivatives were observed at different retention times. The phenylhydrazone derivative was observed at 31.1 minutes matching the expected m/z of 648. The 2-bromophynlhydrazone derivative appeared at 34.4 minutes with m/z's of 726 and 728 at similar abundance corresponding to the bromine isotopic distribution.[39] Finally, the GirT hydrazone derivative was observed at 26.4 minutes with m/z of 673 in the positive mode. The observation of m/z's matching these hydrozone conjugates is consistent with the proposed TDP-linked oxime-aldehyde product; however, further structure characterization is required to validate the identity of these conjugates.

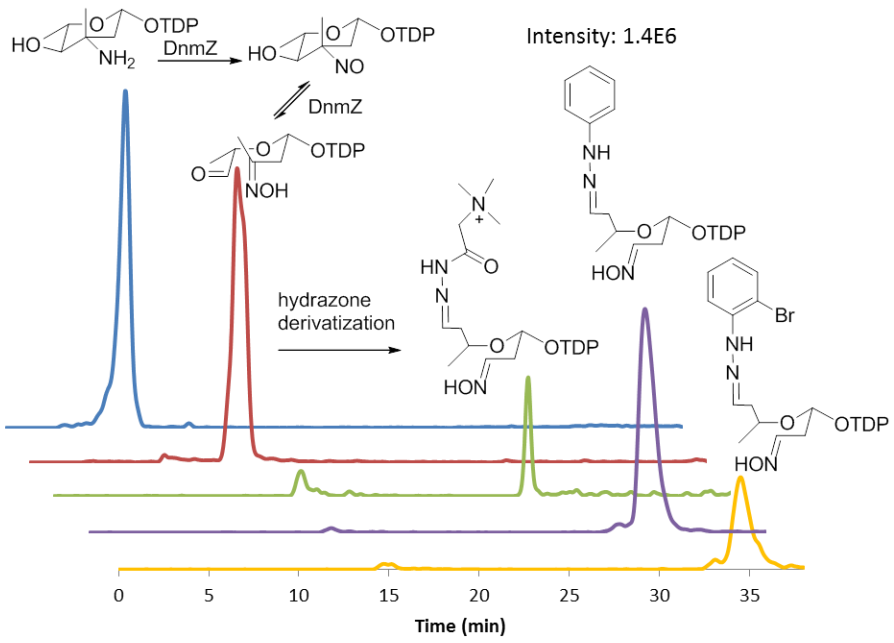

Figure IV-5. HPLC-MS analysis of the DnmZ reaction and the hydrozone conjugates of the oxidation product.

Tandem MS analysis of the hydrazone derivatives.

To further confirm the identity of the three TDP-linked hydrazone derivatives, we performed a tandem MS fragmentation of their corresponding product ions. Fragmentation of the phenyl- and the 2-bromophenylhydrazone product ions at m/z's 648 and 728 respectively, resulted in the diagnostic fragment ion at m/z 401, corresponding to the TDP anion, and its dehydrated form at m/z 383 (Figure IV-6). The presence of these fragment ions, confirms the thymidine diphosphate linkage present in their deoxyaminosugar precursors. Another species with lower intensity at m/z 529 was observed from the fragmentation of the 2-bromophenylhydrazone product ion of m/z 728 (Figure IV-6). This fragment corresponds to the loss of the 2-bromophenyl hydrazone moiety which supports the presence of the proposed TDP linked oxime.

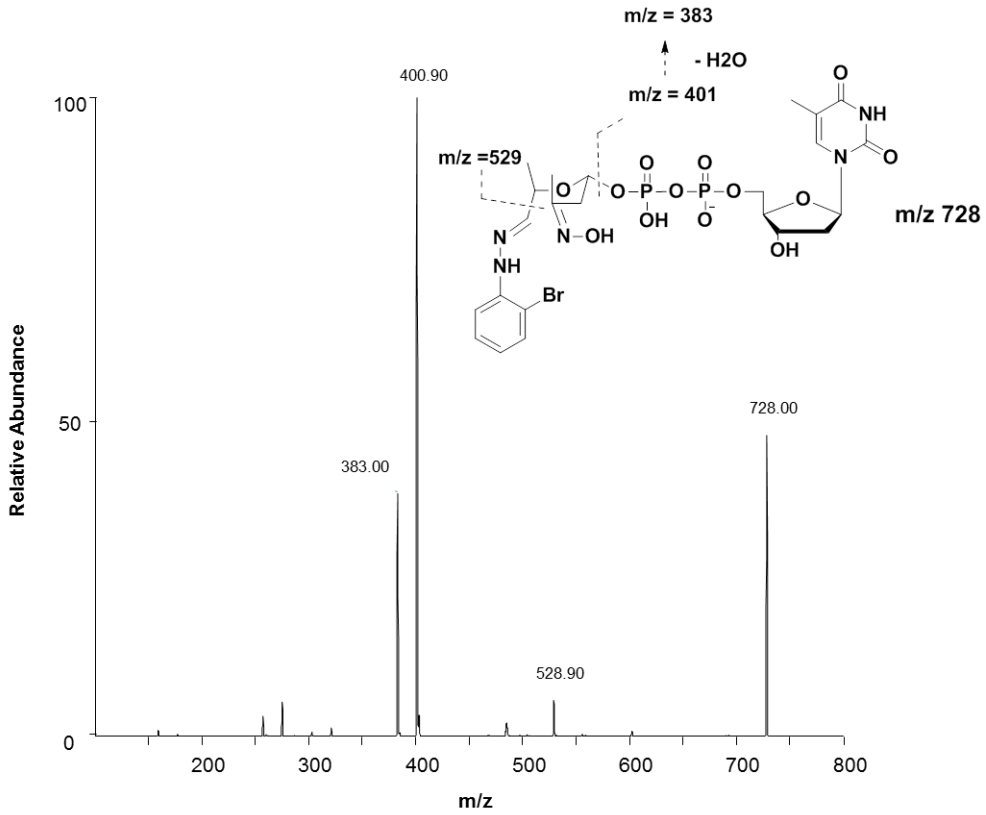

Figure IV-6. Tandem LC-ESI-MS of the 2-bromophenyl hydrozone derivative

Changing the fragmentation conditions for these two hydrazones in both the negative and the positive modes did not result in any additional observable fragment ions diagnostic of the hydrazone side of these derivatives. Therefore, we performed tandem MS fragmentation of the GirT hydrazone product ion of m/z 673 in the positive mode. The hydrazone side of this molecular ion is positively charged, and as expected its fragmentation produced several fragment ions that could be easily assigned to relevant structures. Of note were the fragments that represented to the loss of thymidine monophosphate (TMP) at m/z 351, and the loss of TDP at m/z 271 (Figure IV-7).

Another fragment was observed at m/z 170 which is a result of the cleavage of the acetal's C-O bond as shown in Figure IV-7.

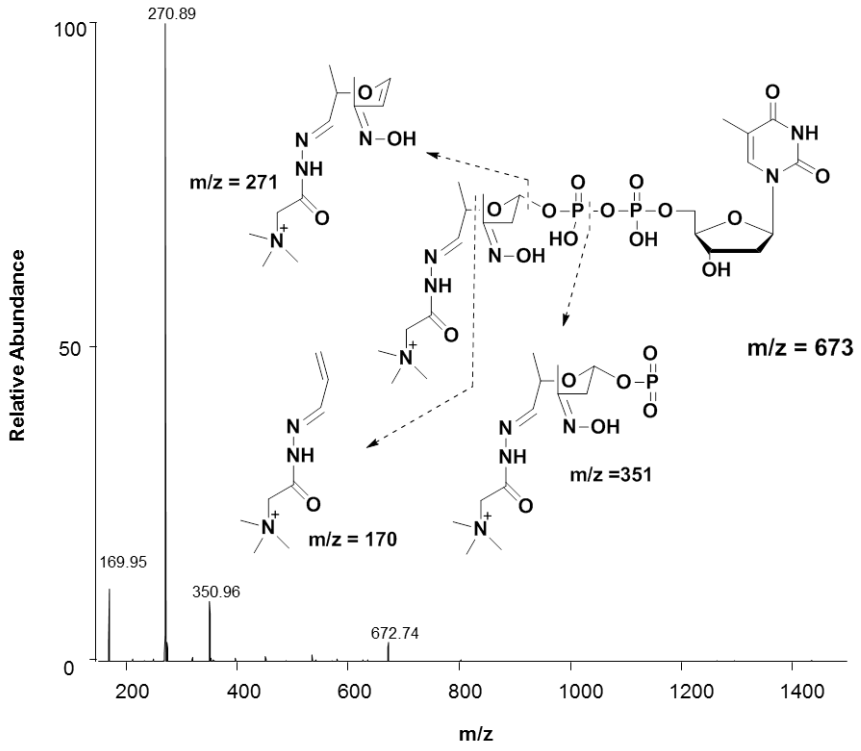

Figure IV-7. Tandem LC-ESI-MS of the GirT hydrozone derivative

Acid hydrolysis and HPLC-MS analysis of the Girard's hydrazone derivative

We aimed to obtain more structural evidence of the hydrazone conjugates by hydrolyzing these derivatives with 1 M HCl and analyzing the resulting mixture by HPLC-MS. The acid hydrolysis of these acetal molecules would result in the formation of an alcohol on the hydrazone side and an aldehyde on the oxime side of the molecule (Figure IV-8). The TDP moiety is readily hydrolyzed upon acid treatment. Since the

hydrazine is present in excess, the newly formed aldehyde species is expected to form a second hydrazone conjugate at the anomeric C1 of the original sugar. HPLC-MS analysis both in the negative and positive modes identified no molecular ions corresponding to the expected hydrolyzed fragments of the acid-treated phenyl- and 2-bromophenyl hydrazone derivatives. This is perhaps due to the lack of ionization of the small molecular weight hydrolysis products possessing neutral charge. However, the acid treatment of the positively charged GirT hydrazone derivative produced two species at m/z 188 and 215 corresponding to both the oxime and the alcohol hydrazone conjugates while the original GirT hydrozone disappeared (Figure IV-8).

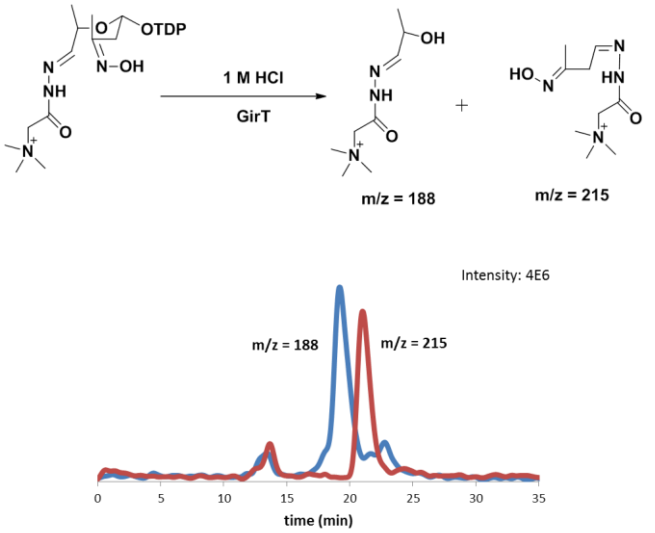

Figure IV-8. Acid hydrolysis of the (carboxymethyl)trimethylammonium hydrazone derivative (above), and LC-ESI-MS chromatograms of the hydrolyzed species (below).

Further MS/MS analysis of these species showed fragment ions consistent with their structures (Figure IV-9). Of note, fragmentation of the hydrazone derivative at m/z

188 resulted in species corresponding to the loss of the trimethylammonium group at m/z 129; dehydration of the secondary alcohol at m/z 170, and the cleavage of the amide bond to yield a fragment ion with m/z 87. The oxime hydrazone derivative at m/z 215 also showed a fragment corresponding to the loss of the trimethylammonium group at m/z 156 as well as a fragment corresponding to the formation of the protonated trimethylammonium species at m/z 60. These tandem MS data strongly support the structure assignment of the original GirT hydrazone derivative and provide more evidence for the carbon-carbon bond cleavage of the TDP-attached nitrososugar product of DnmZ oxidation.

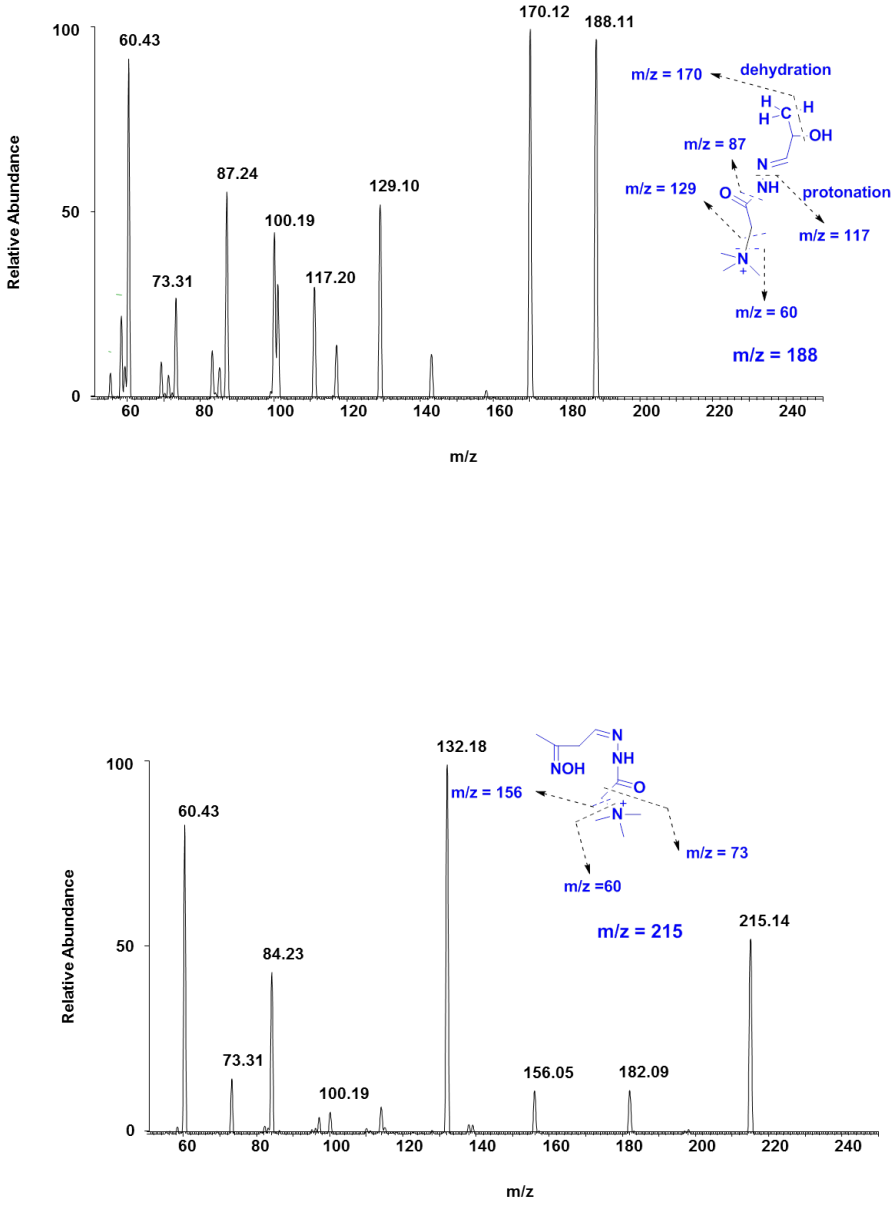

Figure IV-9. Tandem LC-ESI-MS spectra of the hydrolysis products of the acid treated GirT hydrazone derivative. Fragmentation of the hydrazone at m/z 188 (above), and the hydrazone at m/z 215 (below).

High resolution MS measurements of the hydrazone derivatives

To further verify the identity of the hydrazone derivatives, we performed high resolution LC-ESI-MS measurements. Reaction mixtures of all three original hydrazone conjugates and the two formed upon acid treatment of the GirT hydrazone were

measured. As shown in Figure IV-10, mass accuracies of less than 2.70 ppm were confirmed for all of the hydrazone conjugates measured. Taken together, these high resolution mass measurements are consistent with the assigned structures of the TDP linked hydraznes and are in support of the proposed deoxysugar C-C bond cleavge mediated by DnmZ activity.

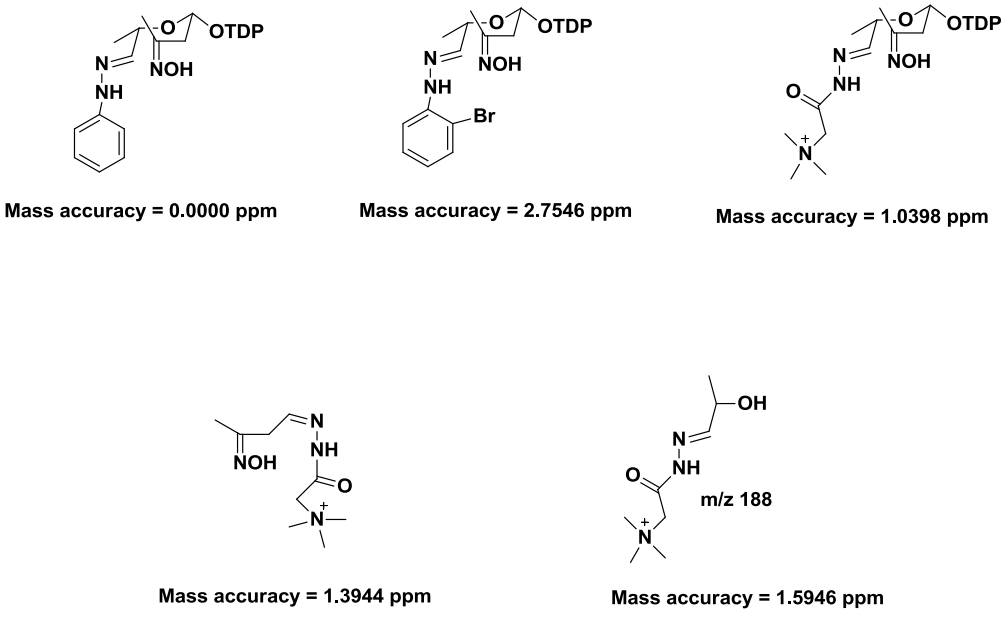

Figure IV-10. High resolution mass measurements of the hydrazone derivatives.

Conclusion

In this work, we used the nitrososynthase Dnmz from *Streptomyces peucetius* to show that the formation of the previously uncharecterized acetal moiety in baumycin is derived from the cleavage of a carbon-carbon bond mediated by DnmZ N-oxidation of a TDP-deoxyaminosugar. This retro-aldol activity of DmnZ represents a new flavin-

dependent monooxygenase function which is of great significance for elucidating the biosynthetic pathways of various natural products such as baumycin-like anthracyclines. This additional monooxygenase reactivity is also helpful in chemical synthesis and provides green biocatalysis for some difficult to perform retro-aldol reactions. Future investigations of this pathway should focus on elucidating the glycosylation requirements as well as the reduction steps of the oxime and aldehyde groups to ultimately form the alcohol functionalities.

Materials and methods

Bacterial strains, Plasmids and Materials.

All reagents were obtained from Sigma-Aldrich Corporation and used without further purification unless otherwise noted. *E. coli* TOP10 and BL21 (DE3) competent cells were obtained from Invitrogen Inc. (Carlsbad, CA) and Novagen (Madison, WI), respectively. Restriction endonucleases and T4 DNA ligase were obtained from New England Biolabs (Ipswich, MA). The pET28a expression vector was purchased from Novagen Inc. Taqplus DNA polymerase was purchased from Stratagene Inc. (La Jolla, CA).

Cloning and overexpression of dnmZ.

The gene encoding DnmZ was amplified from the genomic DNA of *Streptomyces peucetius*[17] using the following primers 5'- CATATGACAAAGCCATCTGTGCACG-3' and 5'-

AAGCTTTCATCGGCCCAACGCC- ACTT-3' (NdeI and HindIII restriction enzyme sites underlined). PCR reactions were carried out using Taqplus DNA polymerase according to the manufacture's protocol. Subcloning of *dnmZ* into the NdeI/HindIII sites of pET28a yielded recombinant plasmid pET28-ZN for expression as an N-terminal hexahistidine fusion protein. Plasmid pET28-ZN was transformed by electroporation into *E. coli* BL21(DE3) for heterologous expression of DnmZ. Cultures of *E. coli* BL21(DE3)/pET28-ZN were grown at 37°C to an OD600 of 0.6, at which point the culture was induced with 0.1 mM isopropyl-beta-D-thiogalactopyranoside (IPTG) and grown an additional 6 hours at 28°C. Cells were harvested by centrifugation and stored at -80°C until needed. IPTG induced E. coli BL21(DE3)/pET28-ZN cells were resuspended in buffer A (20 mM Imidazole, 0.5M NaCl, 20mM Tris-Cl, pH 7.5) and lysed by sonication. The lysate was loaded onto a charged 5-mL Histrap crude column (Amersham Biosciences) and purified by FPLC at a flow rate of 5mL/min. The column was washed with buffer A (20 mM Imidazole, 0.5 M NaCl, 20 mM Tris-Cl, pH 7.5) and buffer B (500 mM Imidazole, 0.5 M NaCl, 20 mM Tris-Cl, pH 7.5) using a step gradient. Fractions containing DnmZ were analyzed by SDS-page and buffer was exchanged via a desalting column (HisTrap) using buffer C (20 mM Tris-Cl, 1 mM dithiothreitol and 5% glycerol, pH 7.5) and stored at -80 °C until assayed.

Preparation of TDP-L-*epi*-vancosamine.

TDP-L-epivancosamine was biochemically synthesized from Thymidine-5'-diphospho-α-D-glucose using the general procedures outlined by Chen et al. The

following enzymes were used to biochemically transform Thymidine-5'-diphospho-α-D-glucose to TDP-L-epivancosamine: RfbB from the rhamnose biosynthetic pathway[40]and, EvaA-E from chloroeremomycin biosynthetic pathway. Preparative enzymatic reaction progress was followed via HPLC using a series 600 Waters HPLC system with a Waters 2996 diode array detector. Analytical separations were performed on an Adsorbosphere strong anion exchange (SAX) column (5 µm, 4.6 mm 20 mm, Alltech Associates) and a linear gradient from 50 to 500 mM NH_4HCO_2 (pH 3.5) at 1 mL/min for 45 min. Preparative HPLC separations were performed using a semipreparative Adsorbosphere SAX column (5 µm, 22 mm 250 mm) using a similar protocol, but at 10 mL/min. The pH values of the fractions containing TDP chromophores (267 nm) were immediately adjusted to ~7 with 1 M NH_4OH, and fractions containing reaction product were pooled, lyophilized, and stored at -80 °C until they were assayed. Resuspended compound concentrations were determined by measurement of the absorbance at 267 nm using a Nanodrop spectrophotometer (Thermo, Inc.) and comparison to a standard curve of dTDP.

DnmZ assay with TDP-L-*epi*-vancosamine.

Reactions of DnmZ with TDP-L-epivancosamine were performed in a total volume of 50 µL containing 30 µM substrate, 30 µM FAD, 1 unit/mL catalase, 1 U/mL superoxidedismutase, 0.4 U/mL flavin reductase, and 2.0 mM NADPH. All reactions were initiated by addition of 15 µM DnmZ, reactions were quenched with equal volume of

acetone, and mixtures stored at -80 °C until they were analyzed by LC-ESI-MS. Control assays were performed without DnmZ, FAD, or NADPH.

Derivatization of DnmZ products with hydrazines.

Upon completion of the DnmZ reaction with TDP-L-epivancosamine, the reaction mixture (50 uL) was incubated with the corresponding hydrazine (1 mM) for 2 h at room temperature. The mixture was kept at - 80 °C until analyzed by HPLC-MS. The following hydrazines were used for the derivatization experiments: phenylhydrazine, 2-bromophenylhydrazine, and Girard's reagent (Carboxymethyl)trimethylammonium chloride hydrazide; 2-Hydrazino-N,N,N-trimethyl-2-oxo-ethanaminium chloride).

LC-ESI-MS Method for DnmZ assays.

DnmZ assays were analyzed using Thermo Finnigan (San Jose, CA) TSQ® Quantum triple quadrupole mass spectrometer equipped with a standard electrospray ionization source outfitted with a 50 µm inside diameter deactivated fused silica capillary. Injections of 10 µL were separated using a Hypercarb column (3mm x 50mm, Thermo Inc.). Mobile phases were (A) H_2O with 50 mM NH_4CH_3COO and 0.1% (v/v) diethylamine and (B) a H_2O/acetonitrile mixture (5:95) with 50 mM NH_4CH_3COO and 0.1% (v/v) diethylamine. Gradient conditions were as follows: linear gradient from 0 to 100% B from for 30 min, 100% B from 30 to 40 min, 100% A from 40 to 50 min. The flow rate was maintained at 0.2 mL/min. The mass spectrometer was operated in both the negative ion and full scan profile modes, and the electrospray needle was maintained at

3100 V. The ion transfer tube was operated at -47.50 V and 275 °C. The tube lens voltage was set to -46 V. The collision energy for all product ion scans was set at 25%.

References

1. du Bois, A.; Luck, H. J.; Pfisterer, J.; Meier, W.; Bauknecht, T., [Anthracyclines in therapy of ovarian carcinoma: a systematic review of primary and 2nd-line therapy after platinum]. *Zentralblatt fur Gynakologie* **2000,** *122* (5), 255-67.

2. Garcia, A.; Muggia, F. M., Activity of anthracyclines in refractory ovarian cancer: recent experience and review. *Cancer Investigation* **1997,** *15* (4), 329-34.

3. Mazue, G.; Iatropoulos, M.; Imondi, A.; Castellino, S.; Brughera, M.; Podesta, A.; Dellatorre, P.; Moneta, D., Anthracyclines - a review of general and special toxicity studies. *International Journal of Oncology* **1995,** *7* (4), 713-26.

4. Laatsch, H.; Fotso, S., Naturally occurring anthracyclines. *Anthracycline Chemistry and Biology I* **2008**, 3-74.

5. Krohn, K., *Anthracycline Chemistry and Biology II: Mode of Action, Clinical Aspects and New Drugs*. Springer Verlag: 2008; Vol. 2.

6. Aubel-Sadron, G.; Londos-Gagliardi, D., Daunorubicin and doxorubicin, anthracycline antibiotics, a physicochemical and biological review. *Biochimie* **1984,** *66* (5), 333-52.

7. Trouet, A.; Deprez-De Campeneere, D., Daunorubicin-DNA and doxorubicin-DNA. A review of experimental and clinical data. *Cancer Chemotherapy and Pharmacology* **1979,** *2* (1), 77-9.

8. Hortobagyi, G., Anthracyclines in the treatment of cancer. An overview. *Drugs* **1997,** *54*, 1.

9. Chhikara, B. S.; St Jean, N.; Mandal, D.; Kumar, A.; Parang, K., Fatty acyl amide derivatives of doxorubicin: synthesis and in vitro anticancer activities. *European Journal of Medicinal Chemistry* **2011,** *46* (6), 2037-42.

10. Altreuter, D. H.; Dordick, J. S.; Clark, D. S., Nonaqueous biocatalytic synthesis of new cytotoxic doxorubicin derivatives: exploiting unexpected differences in the regioselectivity of salt-activated and solubilized subtilisin. *Journal of the American Chemical Society* **2002,** *124* (9), 1871-6.

11. Vey, J. L.; Al-Mestarihi, A.; Hu, Y.; Funk, M. A.; Bachmann, B. O.; Iverson, T. M., Structure and mechanism of ORF36, an amino sugar oxidizing enzyme in everninomicin biosynthesis. *Biochemistry* **2010,** *49* (43), 9306-17.

12. Stefanska, B.; Dzieduszycka, M.; Bontemps-Gracz, M.; Borowski, E.; Martelli, S., Synthesis and antileukemic activity of N-enamine derivatives of daunorubicin, 5-iminodaunorubicin, and doxorubicin. *Journal of Antibiotics (Tokyo)* **1988,** *41* (2), 193-8.

13. Ghirmai, S.; Mume, E.; Tolmachev, V.; Sjoberg, S., Synthesis and radioiodination of some daunorubicin and doxorubicin derivatives. *Carbohydrate Research* **2005,** *340* (1), 15-24.

14. Chhikara, B. S.; Mandal, D.; Parang, K., Synthesis, anticancer activities, and cellular uptake studies of lipophilic derivatives of doxorubicin succinate. *Journal of Medicinal Chemistry* **2012,** *55* (4), 1500-10.

15. Madduri, K.; Hutchinson, C. R., Functional characterization and transcriptional analysis of the dnrR1 locus, which controls daunorubicin biosynthesis in Streptomyces peucetius. *Journal of Bacteriology* **1995,** *177* (5), 1208-15.

16. McGuire, J. C.; Thomas, M. C.; Stroshane, R. M.; Hamilton, B. K.; White, R. J., Biosynthesis of daunorubicin glycosides: role of epsilon-rhodomycinone. *Antimicrobial Agents and Chemotherapy* **1980,** *18* (3), 454-64.

17. Otten, S. L.; Stutzman-Engwall, K. J.; Hutchinson, C. R., Cloning and expression of daunorubicin biosynthesis genes from *Streptomyces peucetius* and *S. peucetius* subsp. caesius. *Journal of Bacteriology* **1990,** *172* (6), 3427-34.

18. Hutchinson, C. R., Biosynthetic Studies of Daunorubicin and Tetracenomycin C. *Chemical Reviews* **1997,** *97* (7), 2525-2536.

19. Krohn, K., *Anthracycline Chemistry and Biology I: Biological Occurence and Biosynthesis, Synthesis and Chemistry*. Springer Verlag: 2008; Vol. 1.

20. Liu, E. H.; Qi, L. W.; Wu, Q.; Peng, Y. B.; Li, P., Anticancer agents derived from natural products. *Mini Reviews in Medicinal Chemistry* **2009,** *9* (13), 1547-55.

21. Fujii, I.; Ebizuka, Y., Anthracycline Biosynthesis in Streptomyces galilaeus. *Chemical Reviews* **1997,** *97* (7), 2511-2524.

22. Miyamoto, Y.; Johdo, O.; Nagamatsu, Y.; Yoshimoto, A., Cloning and characterization of a glycosyltransferase gene involved in the biosynthesis of anthracycline antibiotic beta-rhodomycin from *Streptomyces violaceus. FEMS Microbiology Letters* **2002,** *206* (2), 163-8.

23. Sianidis, G.; Wohlert, S. E.; Pozidis, C.; Karamanou, S.; Luzhetskyy, A.; Vente, A.; Economou, A., Cloning, purification and characterization of a functional anthracycline glycosyltransferase. *Journal of Biotechnology* **2006,** *125* (3), 425-33.

24. Garrido, L. M.; Lombo, F.; Baig, I.; Nur, E. A. M.; Furlan, R. L.; Borda, C. C.; Brana, A.; Mendez, C.; Salas, J. A.; Rohr, J.; Padilla, G., Insights in the glycosylation steps during biosynthesis of the antitumor anthracycline cosmomycin: characterization of two glycosyltransferase genes. *Applied Microbiology and Biotechnology* **2006,** *73* (1), 122-31.

25. Otten, S. L.; Gallo, M. A.; Madduri, K.; Liu, X.; Hutchinson, C. R., Cloning and characterization of the Streptomyces peucetius dnmZUV genes encoding three enzymes required for biosynthesis of the daunorubicin precursor thymidine diphospho-L-daunosamine. *Journal of Bacteriology* **1997,** *179* (13), 4446-50.

26. Yoshimoto, A.; Fujii, S.; Johdo, O.; Kubo, K.; Nishida, H.; Okamoto, R.; Takeuchi, T., Anthracycline metabolites from baumycin-producing Streptomyces sp. D788. II. New anthracycline metabolites produced by a blocked mutant strain RPM-5. *The Journal of Antibiotics* **1993,** *46* (1), 56.

27. Nozaki, Y.; Hida, T.; Iinuma, S.; Ishii, T.; Sudo, K.; Muroi, M.; Kanamaru, T., TAN-1120, a new anthracycline with potent angiostatic activity. *The Journal of Antibiotics* **1993,** *46* (4), 569.

28. Lomovskaya, N.; Doi-Katayama, Y.; Filippini, S.; Nastro, C.; Fonstein, L.; Gallo, M.; Colombo, A. L.; Hutchinson, C. R., The Streptomyces peucetius dpsY and dnrX genes govern early and late steps of daunorubicin and doxorubicin biosynthesis. *Journal of Bacteriology* **1998,** *180* (9), 2379-86.

29. Hu, Y.; Al-Mestarihi, A.; Grimes, C. L.; Kahne, D.; Bachmann, B. O., A unifying nitrososynthase involved in nitrosugar biosynthesis. *Journal of the American Chemical Society* **2008,** *130* (47), 15756-7.

30. Bruender, N. A.; Thoden, J. B.; Holden, H. M., X-ray structure of kijd3, a key enzyme involved in the biosynthesis of D-kijanose. *Biochemistry* **2010,** *49* (17), 3517-24.

31. Hutchinson, C.; Colombo, A., Genetic engineering of doxorubicin production in Streptomyces peucetius: a review. *Journal of Industrial Microbiology & Biotechnology* **1999,** *23* (1), 647-652.

32. Ganguly, A. K.; Sarre, O. Z.; Reimann, H., Evernitrose, a naturally occurring nitro sugar from everninomicins. *Journal of the American Chemical Society* **1968,** *90* (25), 7129-30.

33. Zhang, H.; White-Phillip, J. A.; Melancon, C. E., 3rd; Kwon, H. J.; Yu, W. L.; Liu, H. W., Elucidation of the kijanimicin gene cluster: insights into the biosynthesis of spirotetronate antibiotics and nitrosugars. *Journal of the American Chemical Society* **2007,** *129* (47), 14670-83.

34. Mizsak, S. A.; Hoeksema, H.; Pschigoda, L. M., The chemistry of rubradirin. II. Rubranitrose. *J Antibiot (Tokyo)* **1979,** *32* (7), 771-2.

35. K. Somosekharen Pillay, S. C. C., Thomas Mojelsky, Yuan L. Chow Photoreaction of Nitroso Compounds in Solution. Part XXXI. Mechanisms of Intramolecular Acid Catalyzed Cleavage Reactions and a Hydride Initiated Rearrangement of C-Nitroso Alkanes. *Canadian Journal of Chemistry* **1975,** *53* (20), 3014-3021.

36. Chen, H.; Thomas, M. G.; Hubbard, B. K.; Losey, H. C.; Walsh, C. T.; Burkart, M. D., Deoxysugars in glycopeptide antibiotics: enzymatic synthesis of TDP-L-epivancosamine in chloroeremomycin biosynthesis. *Proceedings of the National Academy of Sciences of the United States of America* **2000,** *97* (22), 11942-7.

37. Shriner, R. L.; HERMANN, C. K., *The Systematic Identification or Organic compounds, WIE*. John Wiley & Sons (New York, 1980): 2003.

38. Johnson, D. W., A modified Girard derivatizing reagent for universal profiling and trace analysis of aldehydes and ketones by electrospray ionization tandem mass spectrometry. *Rapid Communications in Mass Spectrometry : RCM* **2007,** *21* (18), 2926-32.

39. Cameron, A. E.; Lippert, E. L., Jr., Isotopic Composition of Bromine in Nature. *Science* **1955,** *121* (3135), 136-7.

40. Marolda, C. L.; Valvano, M. A., Genetic analysis of the dTDP-rhamnose biosynthesis region of the *Escherichia coli* VW187 (O7:K1) rfb gene cluster: identification of functional homologs of rfbB and rfbA in the rff cluster and correct location of the rffE gene. *Journal of Bacteriology* **1995,** *177* (19), 5539-46.

CHAPTER V

SUMMARY AND FUTURE DIRECTIONS

Synopsis

Flavin-dependent monooxygenases are a diverse class of oxidative biocatalysts many of which have been extensively studied over the past few decades.[1-3] They have been shown to catalyze a remarkable wide variety of reactions such as regioselective hydroxylations, epioxidations, Bayer-Villiger oxidations and enantioselective sulfoxidations. The exquisite specificity and efficiency of these enzymes are often unparalleled compared to chemical catalysts. Recent advances in genome sequence data suggested that many more flavin-dependent monooxygenases exist and await discovery and characterization. The work presented in this dissertation describes the biochemical characterization of a new flavin-dependent monooxygnase, which catalyzes the N-oxidation of deoxyaminosugars in vast array of glycosylated natural products.

The nitrososynthase homologues ORF36 and RubN8 from the everninomicn and the rubradirin biosynthetic pathways, respectively, were shown to catalyze the amine to nitroso oxidation of the deoxyaminosugar TDP-L-epivancosamine.[4-5] Biochemical evidence provided in this work, indicates that the nitrososynthase catalysis involves two FAD-dependent monooxygenation steps in which the aminosugar is first oxidized to the corresponding hydroxylamine, followed by a second iterative N-oxygenation to ultimately form the nitrososugar. The nitrososynthase activity is significantly enhanced

by the inclusion of an external flavin reductase which generates the reduced flavin cofactor required for mediating the oxygenation catalysis. The co-enzyme used for reducing equivalents in this interesting flavin-dependen monooxygenation catalysis is NADPH.

Several TDP-aminosugar intermediates in the biosynthetic pathway of TDP-L-epivancosamine[6] were examined as candidate substrates for the N-oxidation by the nitrososynthases ORF36 and RubN8. The aminosugar substrates upstream of TDP-L-epivancosamine underwent only single-oxidation reactions terminating in the hydroxylamine oxidation state pointing to the substrate catalytic competence of the nitrososynthase enzyme. Performing the nitrososynthase catalysis under $^{18}O_2$ demonstrated that the source of oxygen in the oxidation intermediates and products stems from molecular oxygen rather than from water, which is consistent with flavin-dependent monooxygenase catalysis. The X-ray crystal structure of the nitrososynthase ORF36[4] revealed a tetrameric enzyme that shares a fold with acyl-CoA dehydrogenases but has an unusually large open active site.

Surprisingly, the nitrososynthase DnmZ from *Streptomyces peucetius* was shown to mediate a carbon-carbon bond cleavage of the β-hydroxy-nitrososugar produced from the N-oxidation of TDP-L-epivancosamine, catalyzed by the same enzyme. This retro-aldol activity represents a new and important addition to the functions known for flavin-dependent monooxygenases. Furthermore, it explains the biosynthetic origin of the once not understood non-sugar acetal moiety in baumycin-like natural products.

Future directions

Mechanism of the nitro group formation

The pathway for the conversion of nitrososugars to their nitrosugar congeners remains to be elucidated. To that end, fermentations of *S. achromogenes* in complete darkness produced predominantly protorubradirin, the nitroso congener of rubradirin, which reportedly converted to rubradirin (i.e the nitrososugar moiety was oxidized to its nitrosugar congener) upon exposure to ambient light.[7] This suggested that the oxidation to the nitro group is induced photochemically and that the nitrososugar natural product congeners are the original biosynthetic metabolites. Seemingly at odds with this, the nitrososugar analog of everninomicin was also produced from the fermentation of *M. carbonacae* var. *africana* along with other derivatives including the nitrosugar analog under ambient light.[8] Other possibilities for the nitro group formation include oxidation via endogenous reactive oxygen species[9] or by flavin-dependent monooxygenation catalyzed by the nitrososynthase. In our HPLC-MS analysis of the nitrososynthase assay, we observed a mass peak corresponding to the TDP-nitrosugar, but it was forming at low rates, ambiguous to be counted as an enzymatic conversion.[5] Since the TDP-L-epivancosmine substrate lacks C4 O-methylation and was shown to undergo enzymatic carbon-carbon bond cleavage upon the nitrososynthase catalysis, the authentic C4 O-methylated TDP-aminosugar substrtae (TDP-L-evernosamine) is perhaps more suitable for studying the nitro group formation mechanism. We performed preliminary nitrososynthase assays with this substrate, which was prepared enzymatically from TDP-

L-epivancosaime via the C4-methyltransferase RubN7 from the rubradirin pathway (Figure V-1), and found that both ORF36 and RubN8 were able to catalyze conversions to the nitrososugar (Figure V-II). Additionally, and as expected, there was no hydrate observed for this nitrososugar product, consistent with the protection of the C-4 position. Surprisingly, DnmZ did not oxidize TDP-L-evernosamine suggesting diversity in catalytic competence among nitrososynthases.

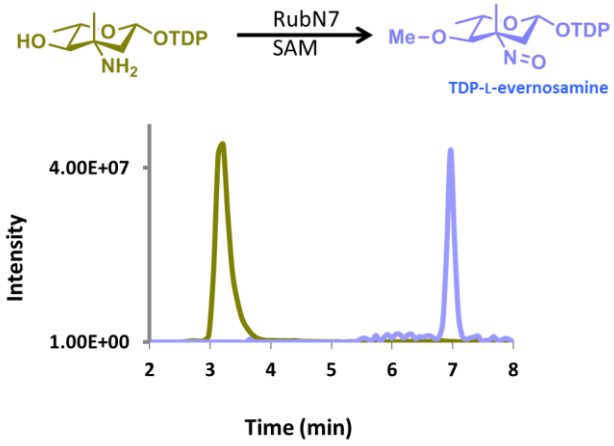

Figure V-1. LC-ESI/MS chromatograms of the preparation of TDP-L-evernosamine via the methyltransferase Rubn7 from the rubradirin pathway.

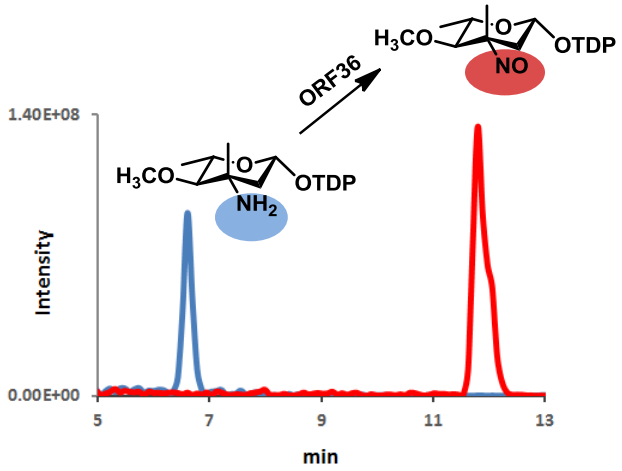

Figure V-2. LC-ESI-MS chromatograms of the monooxygenation of TDP-L-evernosamine by ORF36.

A good way to study whether the nitro group formation is catalyzed by a nitrososynthase activity is to isolate the C4 O-methylated TDP-nitrososugar and perform enzymatic assays of this substrate with the nitrososynthase ORF36. Analysis by HPLC-MS using our established methods would show whether this transformation is carried out enzymatically. The major challenge that faces this approach is that these TDP-sugars are produced in low quantities and are susceptible to hydrolysis of their attached TDP moiety. Chemical synthesis of these deoxysugar nucleotides is an alternative route to obtain sufficient quantities for enzymatic assays.[10]

Structural studies

Cocrystallization of the nitrososynthases with FAD or FMN cofactors and/or an aminosugar substrate remains an important experiment to perform. Preliminary cocrystallization attempts have been so far unsuccessful perhaps due to the complexity of substrate and cofactor binding requirements. The nitrososynthase KijD3 from *Kijaniata actinomadura* was successfully cocrystallized with the nucleotide thymidine diphosphate phenol (dTDP-phenol).[11] While the resulting structure provided only little details about the molecular determinates of catalysis, it gave hope for finding appropriate cocrystallization conditions for the enzyme-substrate or enzyme-substrate-cofactor complexes.

The nitrososynthase co-structures would reveal important amino acid residues required for catalysis, while site directed mutagenesis of these residues would validate their roles in the monooxygenation mechanism. We performed site directed mutagenesis experiments on selected residues chosen based on modeling TDP-L-epivancosamine and FAD into the active site of ORF36; however, none of the mutations abolished the nitrososynthase activity. As discussed in chapter III, the nitrososynthase likely undergoes significant conformational adjustment upon substrate binding and catalysis thus, identifying the active site residues would require obtaining enzyme-substrate-FAD co-structures.

As mentioned above, preliminary experiments suggested that the catalytic competence vary among nitrososynthases. For example, unlike ORF36, DnmZ showed

no monooxygenase activity with the C4 O-methylated substrate (TDP-L-evernosamine). It is intriguing to investigate the structural differences among nitrososynthases that allows this interesting selectivity. The recent success in crystallizing the DnmZ enzyme by Dr. Jessica Vey's research group at California State University, Northridge, is a step towards the completion of these structural investigations.

Catalytic competence and kinetic studies

Biochemical characterization of the nitrososynthase enzymes included in this work revealed important substrate preference data and set the stage for further catalytic competence studies. Our successful enzymatic production of the aminosugar substrate TDP-L-evernosamine and the preliminary data of its oxidation by the nitrososynthases studied in this work is an effort towards the completion of this goal. Michaelis-Menten kinetic measurements[12] of the available aminosugar substrates will aid in the elucidation of the nirososynthase's monooxygenation mechanism. Challenges that may render kinetic studies problematic via our HPLC-MS methods include the availability of the substrates in sufficient quantities, and the susceptibility to hydrolysis of their attached TDP moieties. Chemical synthesis of the TDP-sugar substrates[10] and the use of internal standards are possible solutions for these issues.

The interplay between the nitrososynthases and glycosyltransferases

The remarkable nitrososynthase catalysis described in this work, results in the formation of TDP-linked sugar donor substrates of unusual modifications. The subsequent sugar cleavage upon the DnmZ activity raises the question as to how this cleaved sugar gets attached to its corresponding anthracycline aglycone to ultimately form baumycin-like glycosides. One possible scenario for the glycoslation is that the resulting cleaved sugar exists in equilibrium with its non-cleaved form which can facilitate its glycoslation by the glycosyltransferase DnrH.[13] This equilibrium could further exist after glycoslation and combined with subsequent chemical or enzymatic reduction steps may result in the formation of several baumycin-like compounds.[14-15] Performing glycoslation experiments using the glycosyltransferase DnrH identified in the anthracycline biosynthetic pathway in *Streptomyces peucetius* would test this proposed pathway. Some natural product glycosyltransferases require a partner for activity and it has been shown that co-expression of the GT with its partner greatly improves the solubility of GTs. Gene disruption studies showed that the DnrS glycosyltransferese in the daunorubicin biosynthesis requires a protein partner, DnrQ, for its activity.[13] These considerations should be taken into account when designing the glycoslation experiments. The commercial availability of the aglycone substrate daunorubicin is advantageously suited for conducting these studies.

It is also intriguing to determine the preferred substrate for the GT responsible for glycoslating of the N-oxidized sugar in everninomicin biosynthesis. The identity of the TDP-sugar donor substrate of glycoslation would reveal important clues into the

interplay between the nitrososynthase ORF36 and the subsequent activity of the GT. The aglycone substrate can be obtained via a mild hydrolysis of everninomicin described by Ganguly, Sarre, and Szmulewicz in U.S. Patent 3,920,629. Our successful production of two biogenic sugar donor substrate candidates will aid in the completion of these studies.

References

1. Massey, V., The chemical and biological versatility of riboflavin. *Biochemical Society Transactions* **2000,** *28* (4), 283-96.

2. Joosten, V.; van Berkel, W. J. H., Flavoenzymes. *Current Opinion in Chemical biology* **2007,** *11* (2), 195-202.

3. van Berkel, W. J.; Kamerbeek, N. M.; Fraaije, M. W., Flavoprotein monooxygenases, a diverse class of oxidative biocatalysts. *Journal of Biotechnology* **2006,** *124* (4), 670-89.

4. Vey, J. L.; Al-Mestarihi, A.; Hu, Y.; Funk, M. A.; Bachmann, B. O.; Iverson, T. M., Structure and mechanism of ORF36, an amino sugar oxidizing enzyme in everninomicin biosynthesis. *Biochemistry* **2010,** *49* (43), 9306-17.

5. Hu, Y.; Al-Mestarihi, A.; Grimes, C. L.; Kahne, D.; Bachmann, B. O., A unifying nitrososynthase involved in nitrosugar biosynthesis. *Journal of the American Chemical Society* **2008,** *130* (47), 15756-7.

6. Chen, H.; Thomas, M. G.; Hubbard, B. K.; Losey, H. C.; Walsh, C. T.; Burkart, M. D., Deoxysugars in glycopeptide antibiotics: enzymatic synthesis of TDP-L-epivancosamine in chloroeremomycin biosynthesis. *Proceedings of the National Academy of Sciences of the United States of America* **2000,** *97* (22), 11942-7.

7. Bannister, B.; Zapotocky, B. A., Protorubradirin, an antibiotic containing a C-nitroso-sugar fragment, is the true secondary metabolite produced by Streptomyces achromogenes var. rubradiris. Rubradirin, described earlier, is its photo-oxidation product. *The Journal of Antibiotics* **1992,** *45* (8), 1313-24.

8. Chu, M.; Mierzwa, R.; Jenkins, J.; Chan, T. M.; Das, P.; Pramanik, B.; Patel, M.; Gullo, V., Isolation and characterization of novel oligosaccharides related to Ziracin. *Journal of Natural Products* **2002,** *65* (11), 1588-93.

9. Filip, M.; Paduraru, I.; Jerca, L.; Filip, F.; Saramet, A., [Oxygen biochemistry. I. Reactive species of reduced oxygen and endogenous sources]. *Revista medico-chirurgicala a Societatii de Medici si Naturalisti din Iasi* **1992,** *96* (3-4), 289-92.

10. Oberthuer, M.; Leimkuhler, C.; Kahne, D., A Practical Method for the Stereoselective Generation of β-2-Deoxy Glycosyl Phosphates. *Organic Letters* **2004,** *6* (17), 2873-2876.

11. Bruender, N. A.; Thoden, J. B.; Holden, H. M., X-ray structure of kijd3, a key enzyme involved in the biosynthesis of D-kijanose. *Biochemistry* **2010,** *49* (17), 3517-24.

12. Matthews, J. N.; Allcock, G. C., Optimal designs for Michaelis-Menten kinetic studies. *Statistics in Medicine* **2004,** *23* (3), 477-91.

13. Scotti, C.; Hutchinson, C. R., Enhanced antibiotic production by manipulation of the Streptomyces peucetius dnrH and dnmT genes involved in doxorubicin (adriamycin) biosynthesis. *Journal of Bacteriology* **1996,** *178* (24), 7316-21.

14. Matsuzawa, Y.; Yoshimoto, A.; Kouno, K.; Oki, T., Baumycin analogs isolated from Actinomadura sp. *The Journal of Antibiotics* **1981,** *34* (6), 774-6.

15. Nozaki, Y.; Hida, T.; Iinuma, S.; Ishii, T.; Sudo, K.; Muroi, M.; Kanamaru, T., TAN-1120, a new anthracycline with potent angiostatic activity. *The Journal of Antibiotics* **1993,** *46* (4), 569-79.

APPENDIX A

SUPPLEMENTARY FIGURES FROM CHAPTER II

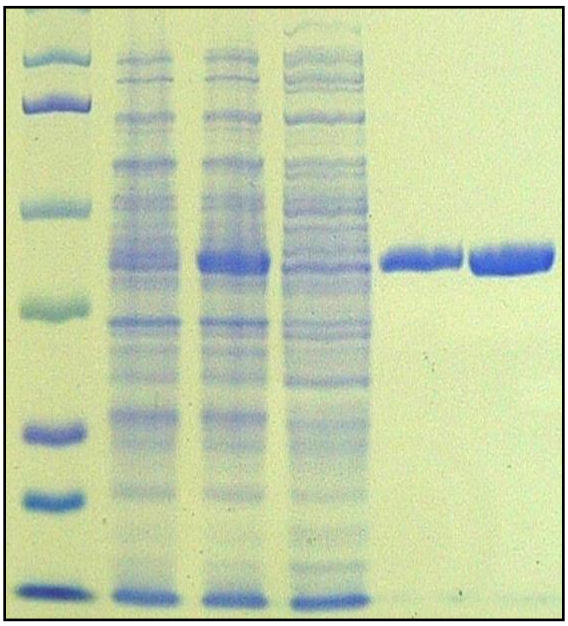

Figure A1. SDS-PAGE analysis of the overproduction of RubN8. From left to right, Lane 1: Molecular weight markers; Lane 2: Uninduced total protein extract; Lane 3 Induced total protein; Lane 4: Flow-through of Ni^{2+} column; Lane 5: Pooled fractions from Ni^{2+} column; Lane 6: Desalted fraction.

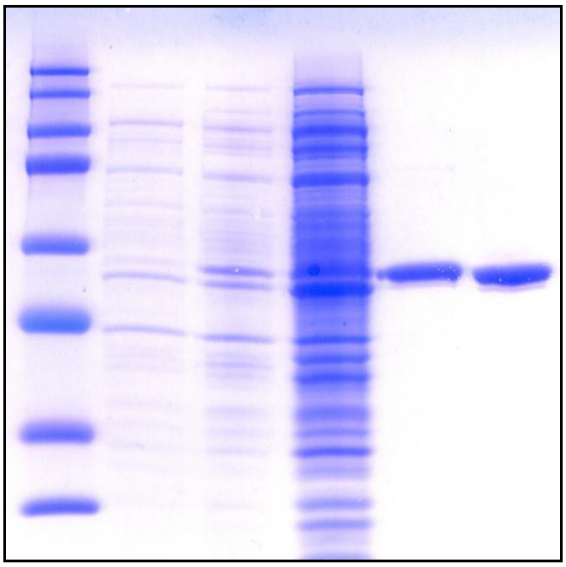

Figure A2. DSD-PAGE analysis of the overproduction of RubN8. From left to right, Lane 1: Molecular weight markers; Lane 2: Uninduced cell-free extract; Lane 3 Induced cell-free extract; Lane 4: Flow-through of Ni^{2+} column; Lane 5: Pooled fractions from Ni^{2+} column; Lane 6: Desalted fraction.

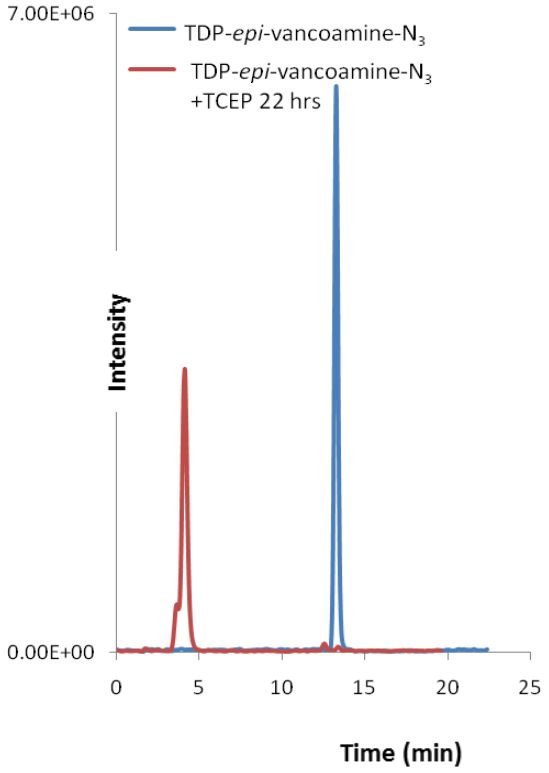

Figure A3. HPLC/MS analysis of the reduction of TDP-L-*epi*-vancosamine with TCEP.

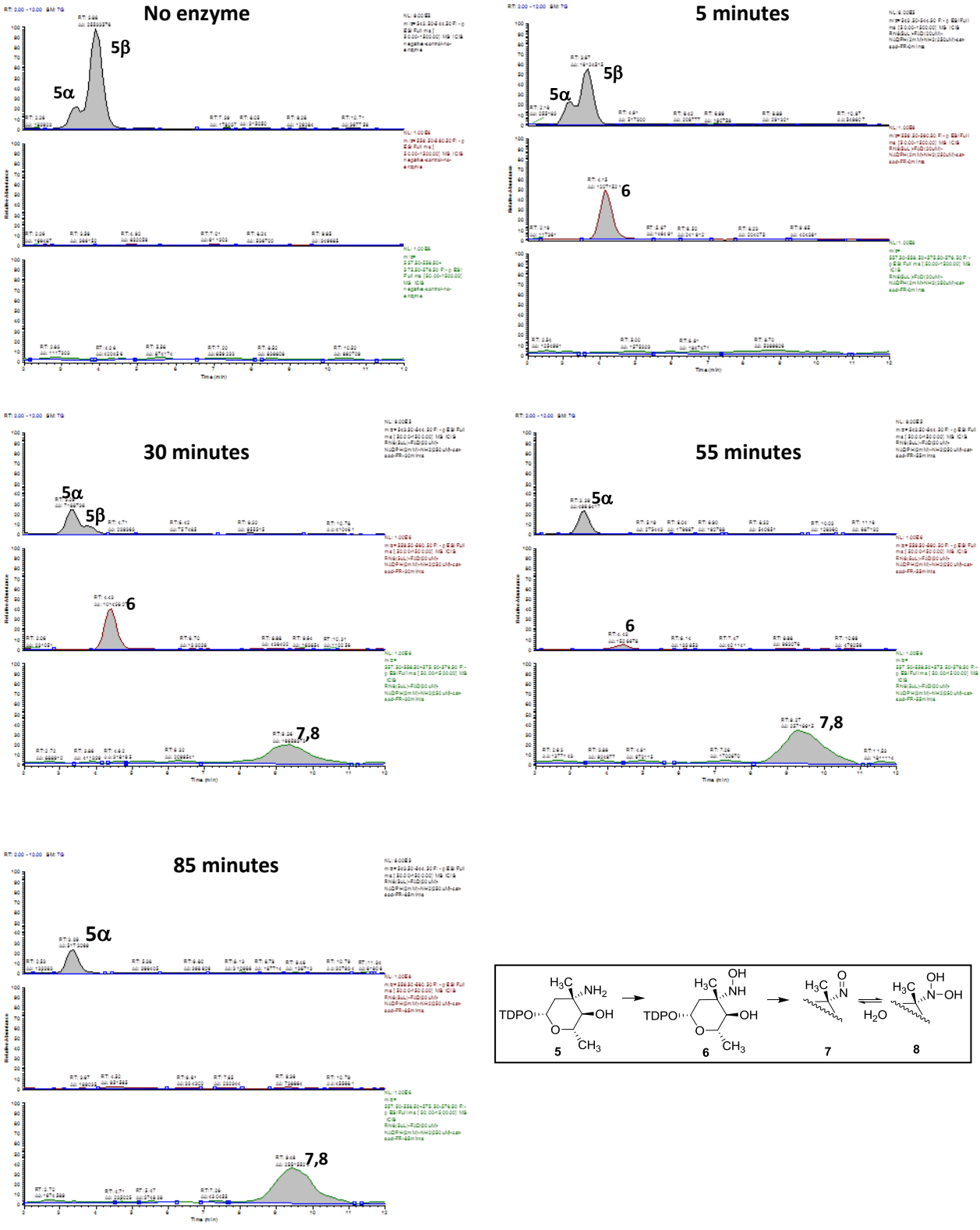

Figure A4. HPLC/MS analysis of RubN8 catalyzed oxidation reactions with 250 µM TDP-L-*epi*-vancosamine and 2 mM NAD(P)H.

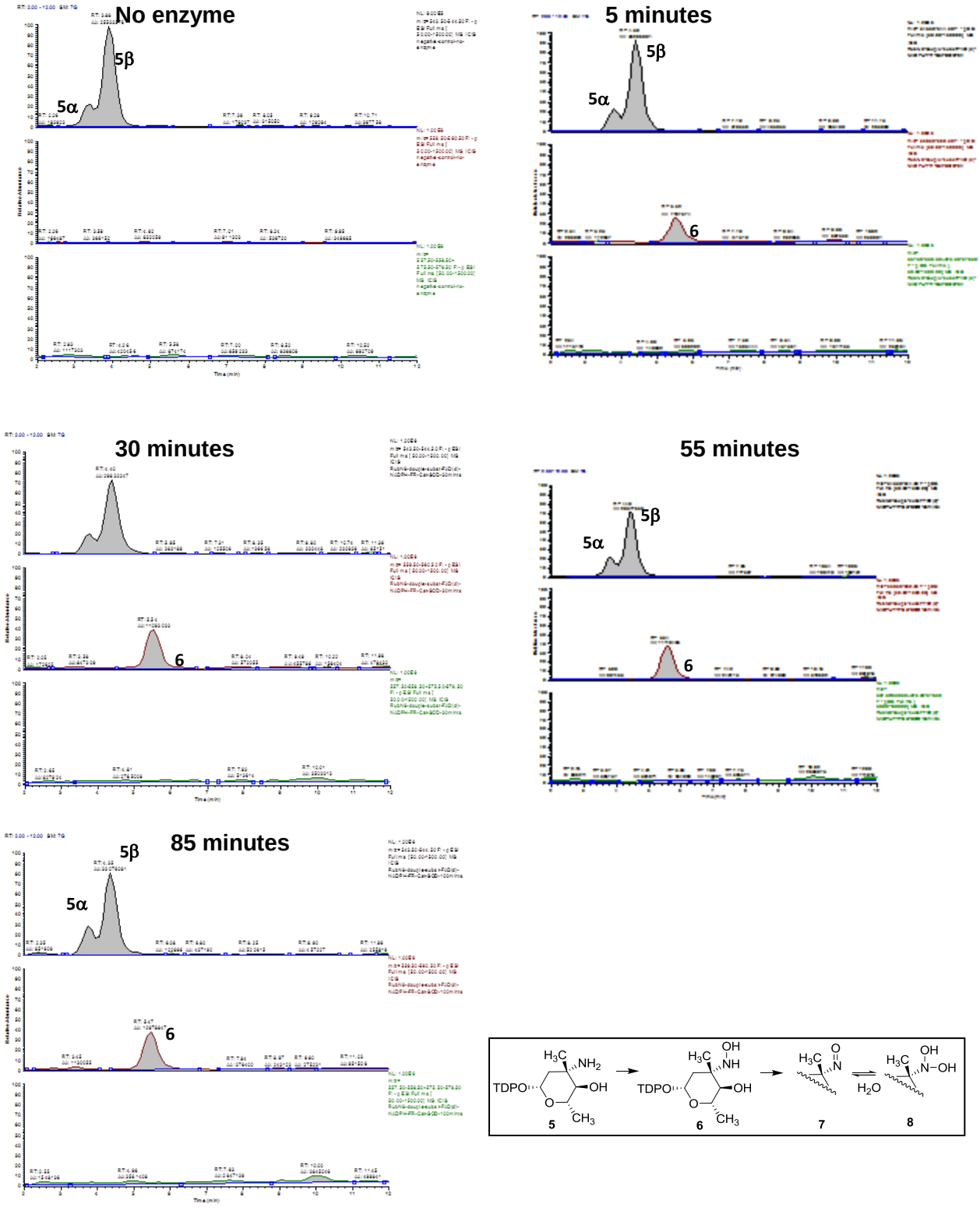

Figure A5. HPLC/MS analysis of RubN8 catalyzed oxidation reactions with TDP-L-*epi*-vancosamine and 400 µM NAD(P)H.

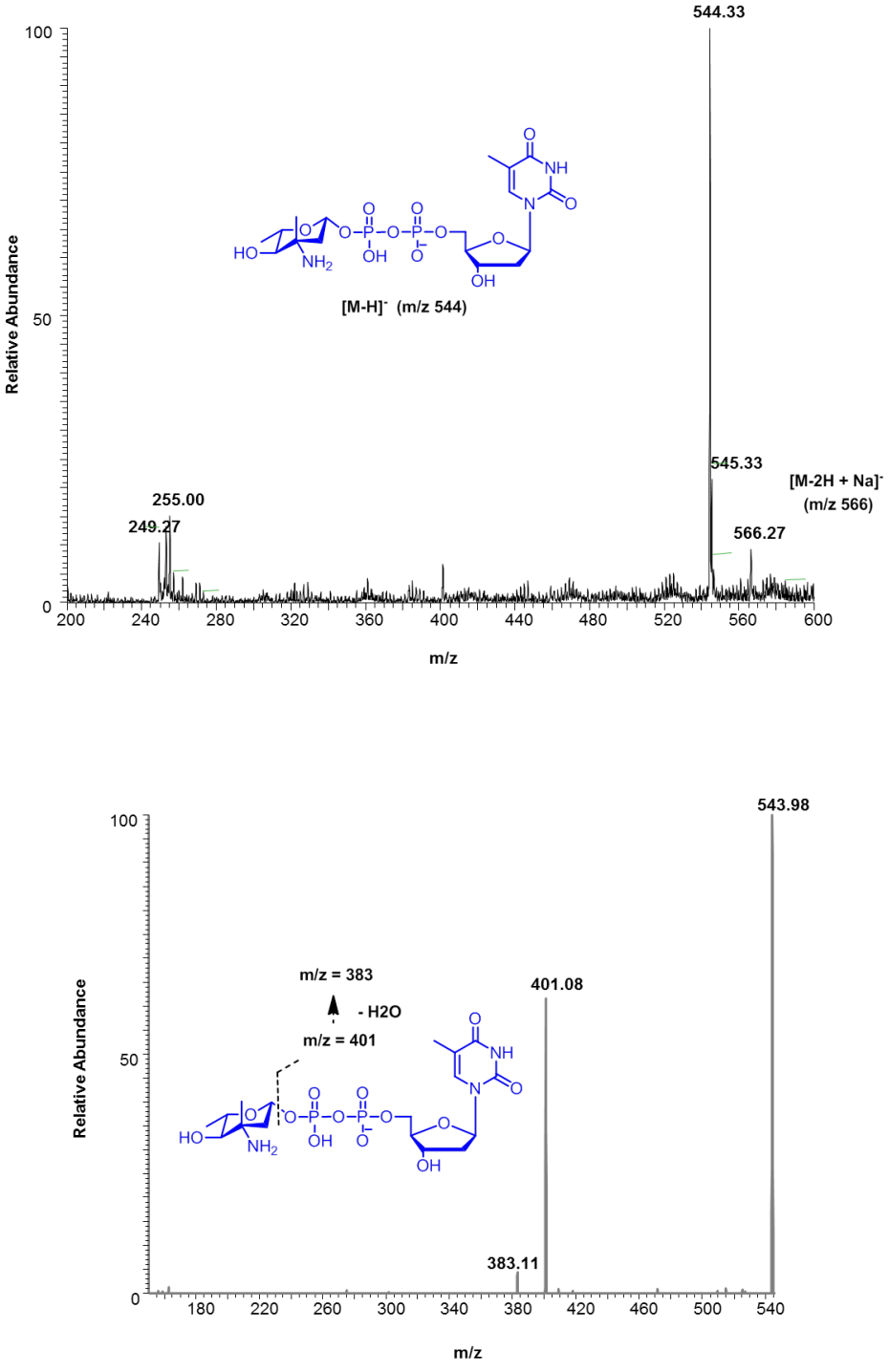

Figure A6. MS and Tandem MS of product ions for RubN8 catalyzed reactions. Shown spectra are MS (above) and MS/MS (below) of the substrate (starting material) TDP-L-*epi*- vancosamine.

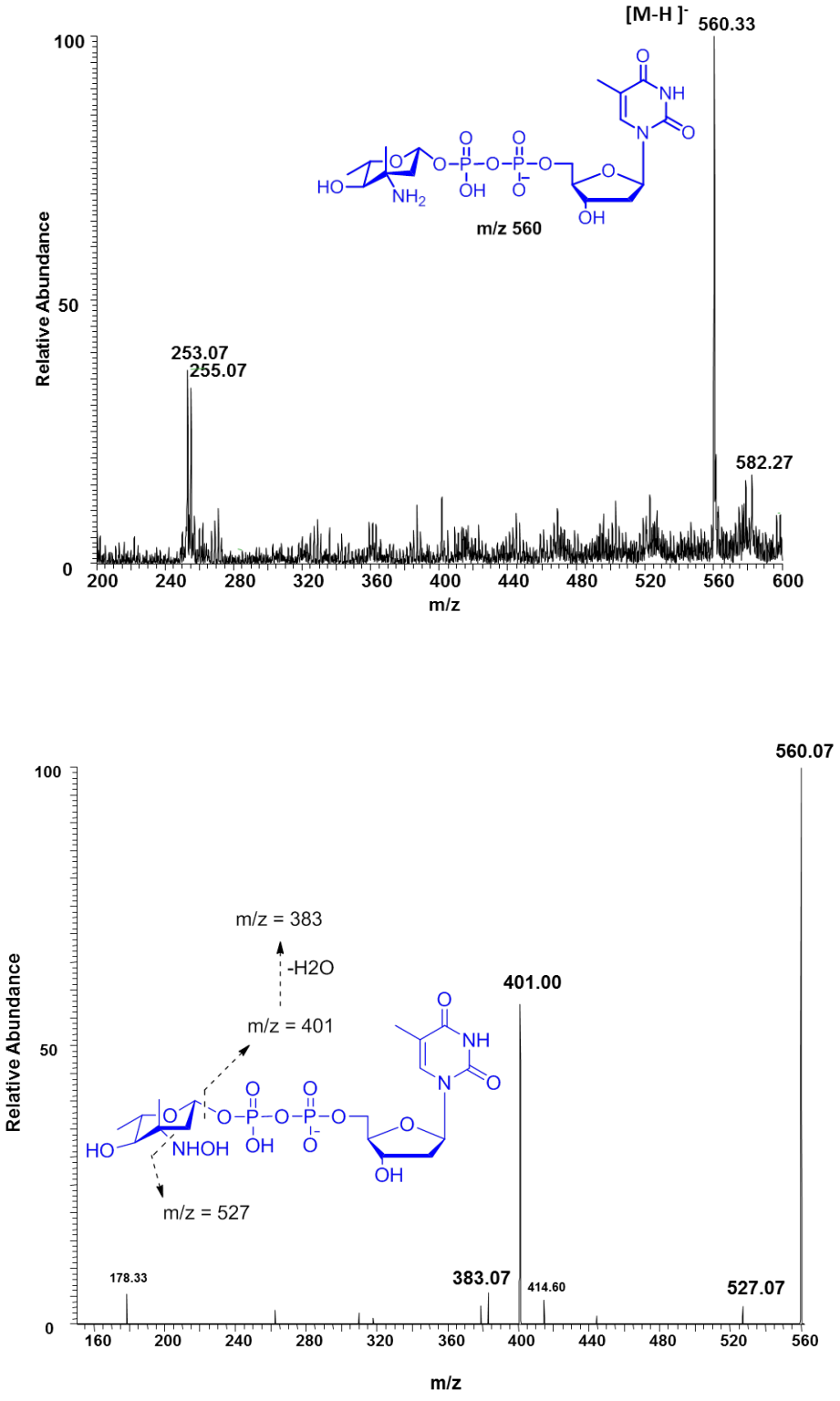

Figure A7. MS and Tandem MS of product ions for RubN8 catalyzed reactions. Shown spectra are MS (above) and MS/MS (below) of the hydroxylamine intermediate TDP-L-*epi*- vancoshydroxylamine.

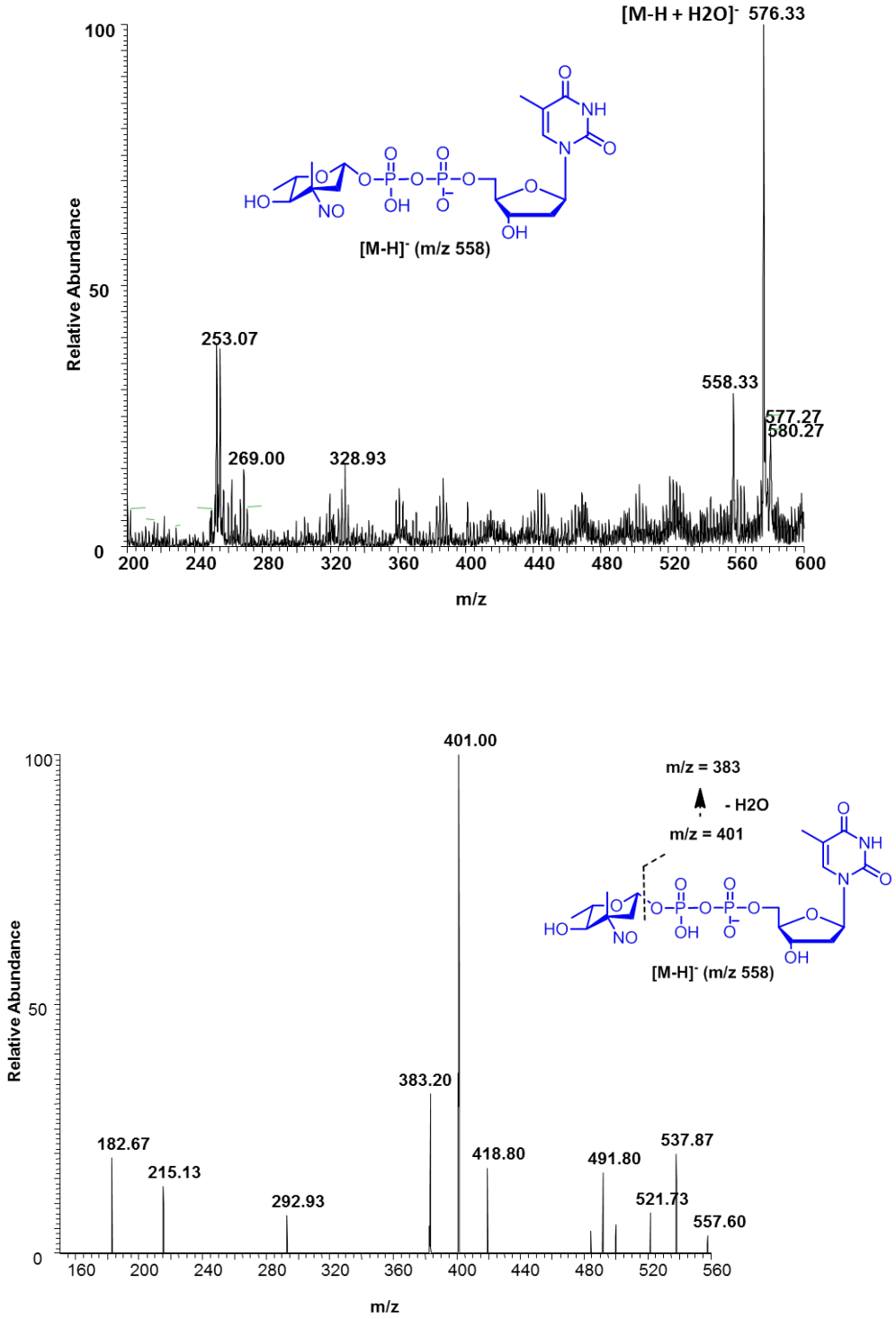

Figure A8. MS and Tandem MS of product ions for RubN8 catalyzed reactions. Shown spectra are MS (above) and MS/MS (below) of TDP-L-*epi*-vanconitrose oxidation product (m/z 558).

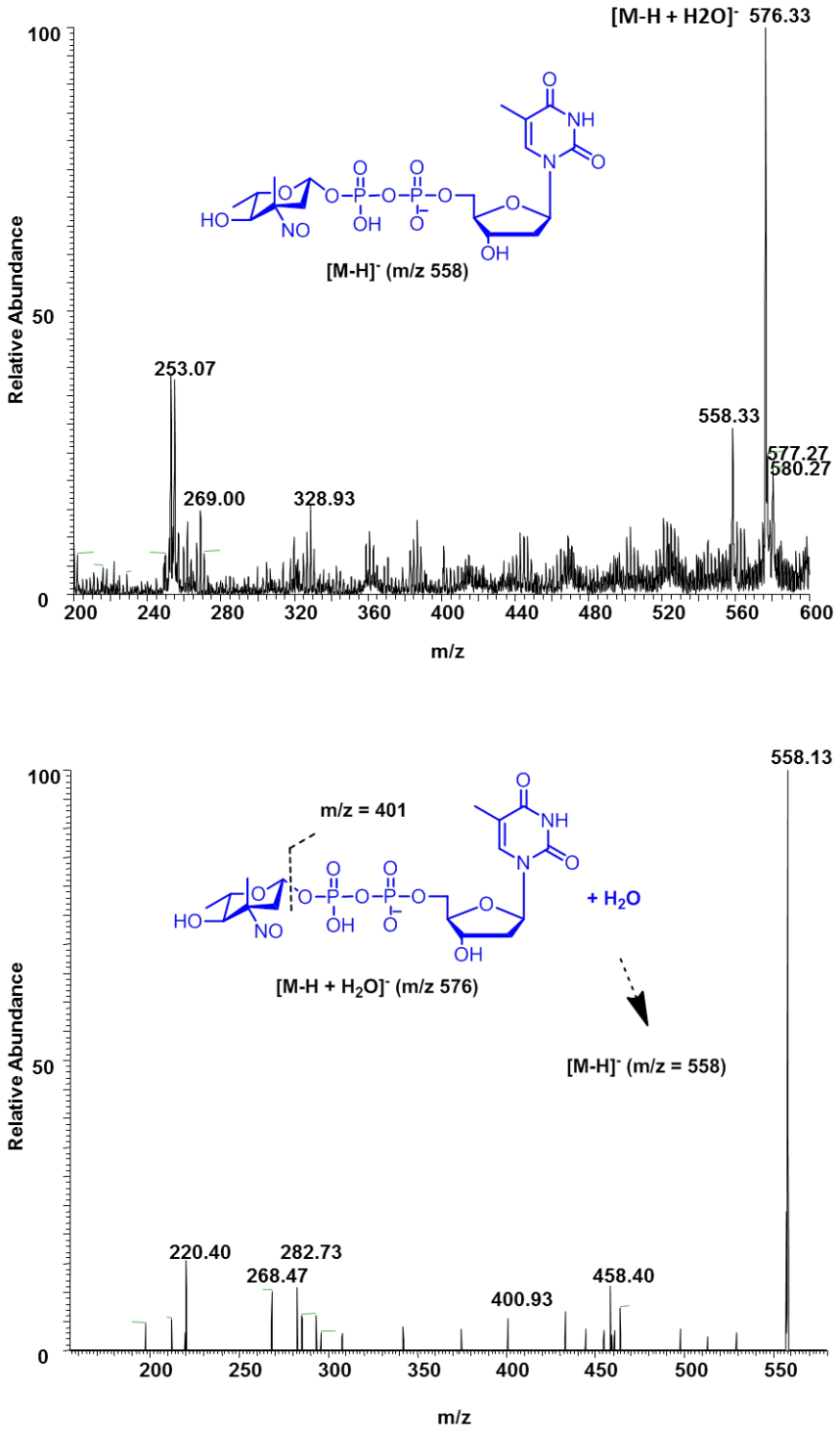

Figure A9. MS and Tandem MS of product ions for RubN8 catalyzed reactions. Shown spectra are MS (above) and MS/MS (below) of the hydrated TDP-L-*epi*-vanconitrose oxidation product (m/z 576).

5 minutes **65 minutes**

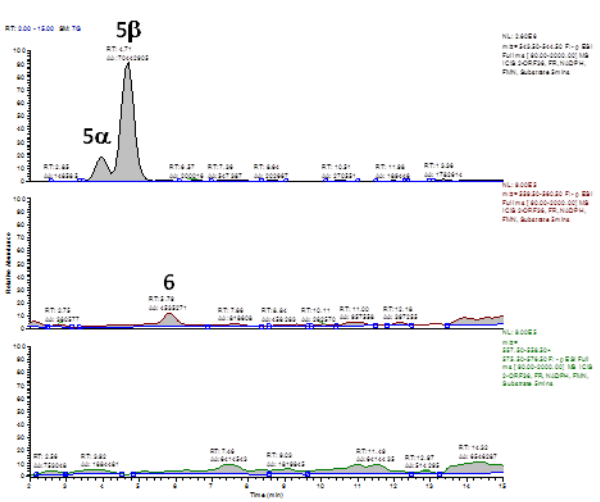

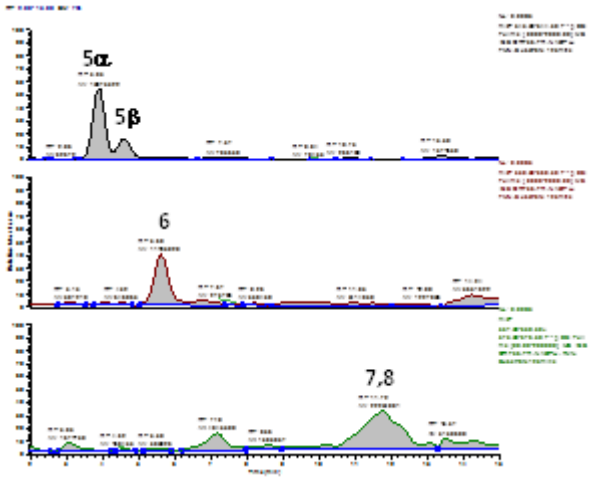

125 minutes

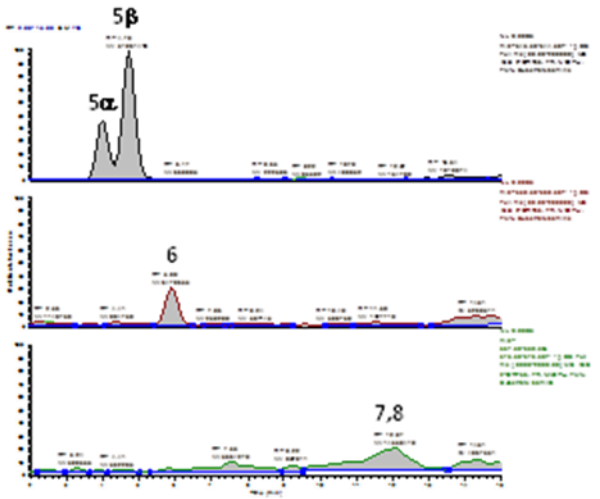

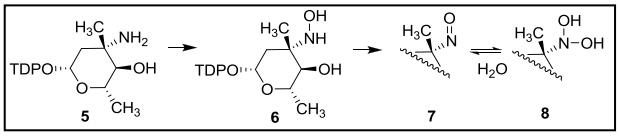

Figure A10. HPLC/MS analysis of ORF36 catalyzed oxidation reactions 250 µM and and 400 µM NAD(P)H.

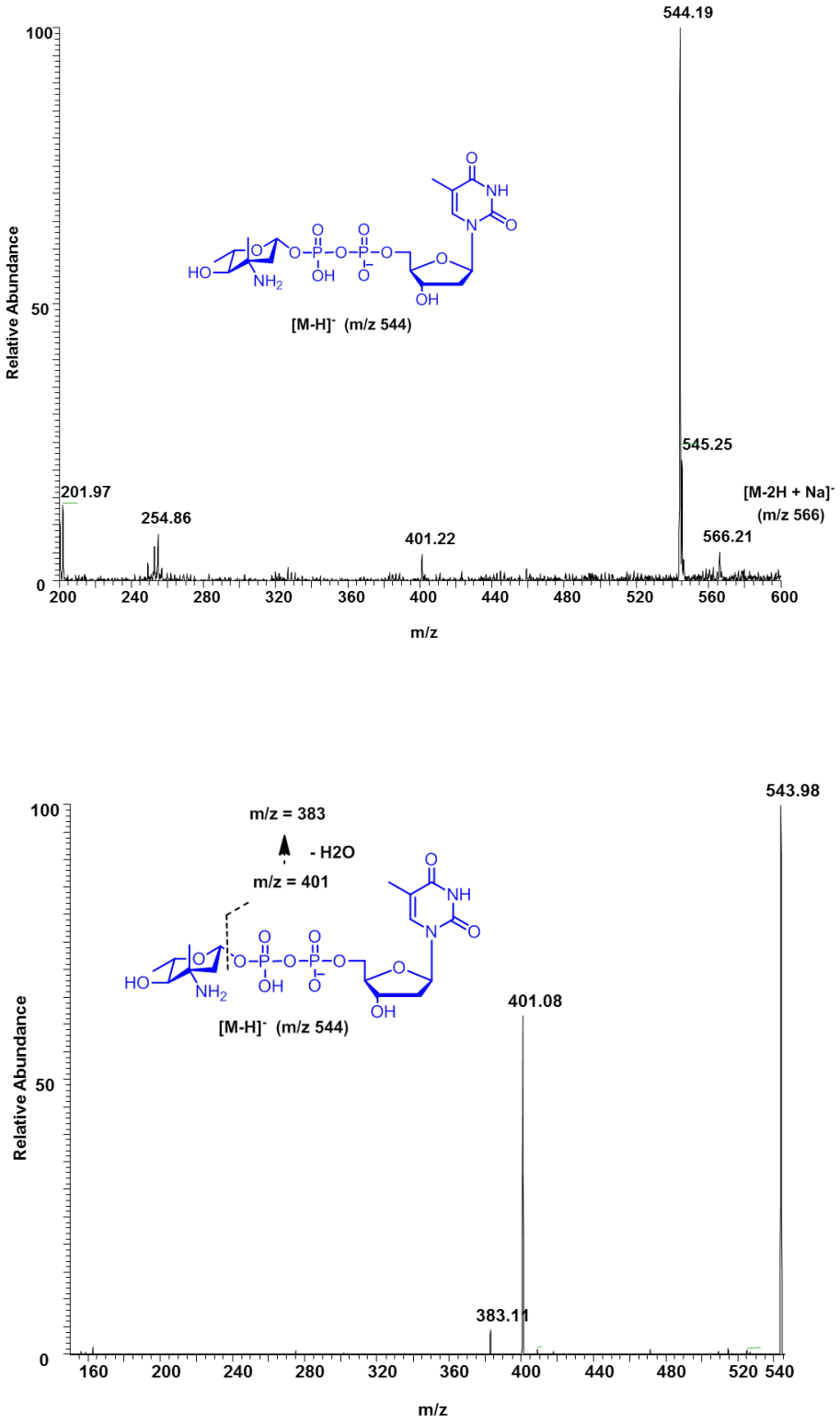

Figure A11. MS and Tandem MS of product ions for ORF36 catalyzed reactions. Shown spectra are MS (above) and MS/MS (below) of the substrate (starting material) TDP-L-*epi*- vancosamine.

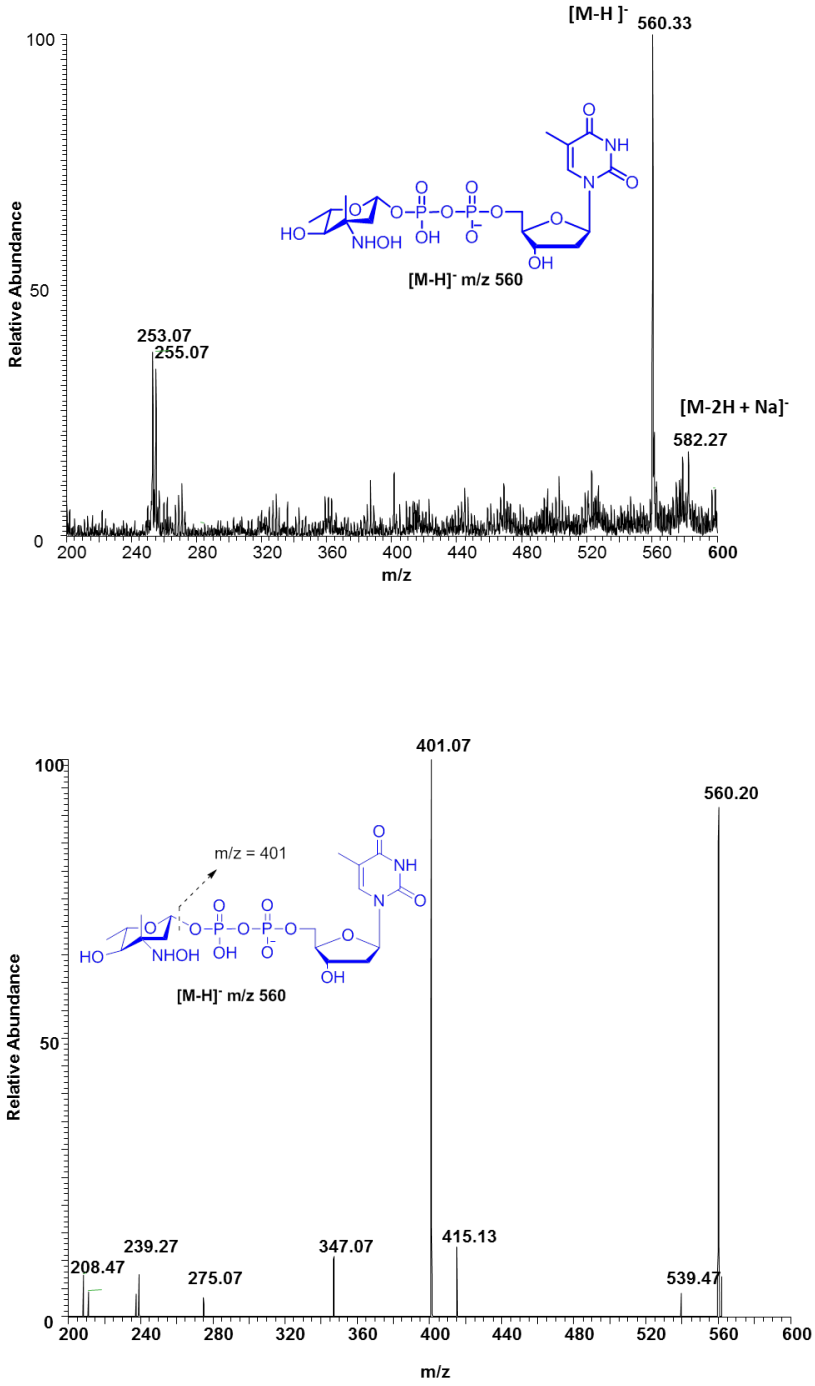

Figure A12. MS and Tandem MS of product ions for ORF36 catalyzed reactions. Shown spectra are MS (above) and MS/MS (below) of the hydroxylamine intermediate TDP-L-*epi*- vancoshydroxylamine.

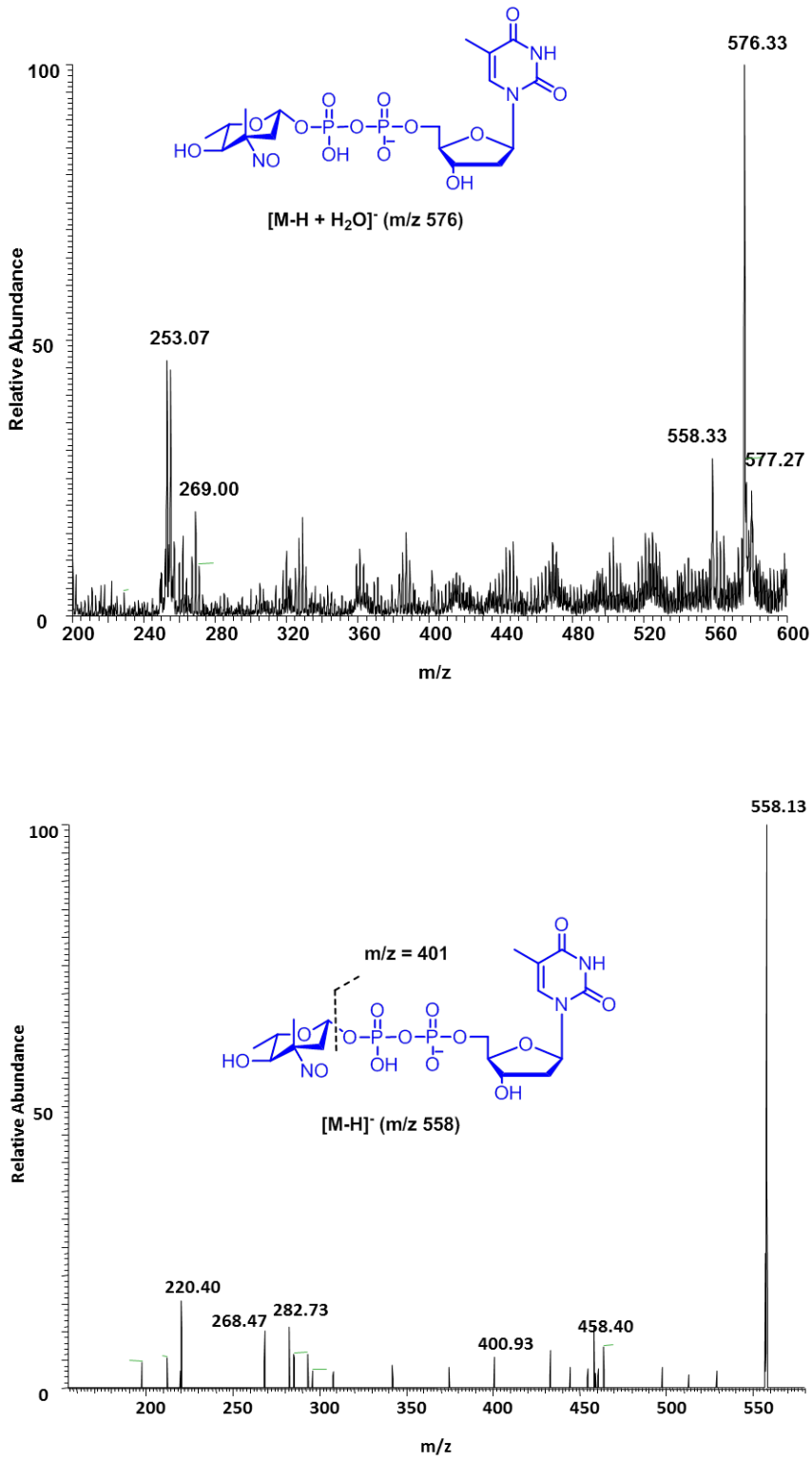

Figure A13. MS and Tandem MS of product ions for ORF36 catalyzed reactions. Shown spectra are MS (above) and MS/MS (below) of TDP-L-*epi*-vanconitrose oxidation product (m/z 558).

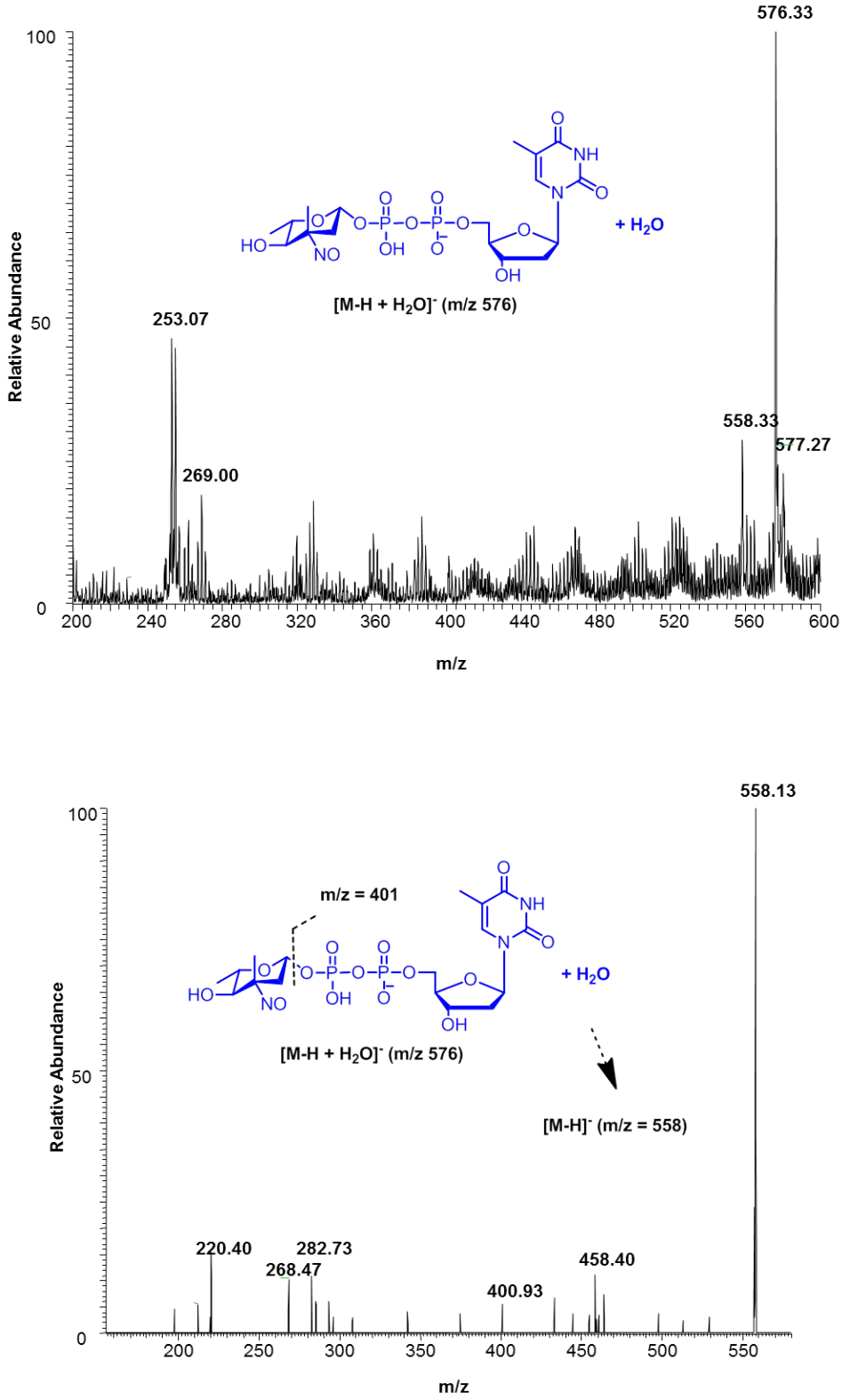

Figure A14. MS and Tandem MS of product ions for ORF36 catalyzed reactions. Shown spectra are MS (above) and MS/MS (below) of the hydrated TDP-L-*epi*-vanconitrose oxidation product (m/z 576).

GTGGCGGCGGATCTTCGCGCGCCGCTCACGCCGGCGGGGCGCACGGTGGTCG
ACCTGCTTGCCGGCGTGATCCCGAGAATCAGTGCGGAGGCCGCCGACCGGGA
CCGCACCGGCACCTTCCCGGTGGAGGCGTTCGAGCAGTTCGCGAAGCTCGGGT
TGATGGGCGCCACCGTTCCCGCCGAGCTGGGCGGCCTGGGGTTGACCCGGCT
GTACGACGTGGCGACCGCGCTGATGCGGCTGGCCGAGGCCGACGCGTCCACC
GCGCTGGCCTGGCACGTGCAGCTCAGCCGGGGCCTCACCCTCACCTACGAGTG
GCAGCACGGCACGCCGCCGGTGCGCGCGATGGCGGAGCGGCTGCTGCGGGC
GATGGCGGAGGGCGAGGCCGCCGTCTGCGGCGCGCTCAAGGACGCCCCCGG
CGTGGTCACCGAGCTGCATTCCGACGGCGCCGGCGGCTGGCTGCTGTCGGGC
CGCAAGGTGCTGGTCAGCATGGCGCCCATCGCGACCCACTTCTTCGTGCACGC
CCAGCGGCGCGACGACGACGGCTCGGTGTTCCTCGCCGTGCCGGTCGTGCAC
CGCGACGCCCCCGGGCTCACGGTGCTGGACAACTGGGACGGCCTGGGAATGC
GTGCCTCGGGGACGCTGGAGGTGGTCTTCGACCGGTGCCCGGTCCGGGCCGA
CGAGCTGCTGGAGCGCGGCCCGGTCGGGGCCCGGCGGGACGCCGTGCTGGC
CGGGCAGACGGTCAGCTCGATCACCATGCTCGGCATCTACGCCGGCATCGCCC
AGGCGGCCCGGGACATCGCGGTCGGTTTCTGCGCGGGGCGCGGCGGCGAGC
CACGGGCCGGTGCCCGGGCGCTGGTCGCCGGGCTGGACACCCGGCTCTACGC
GCTACGCACCACGGTCGGCGCGGCGTTGACCAACGCCGACGCGGCGTCGGTC
GACCTGTCCGGCGACCCGGACGAACGCGGCCGACGGATGATGACCCCGTTCCA
GTACGCGAAGATGACCGTCAACGAGCTGGCCCCGGCGGTGGTGGACGACTGC
CTCAGCCTGGTCGGCGGCCTCGCCTACACGGCCGGGCACCCACTCTCCCGGCT
CTATCGCGACGTGCGGGCCGGCGGGTTCATGCAGCCCTACAGCTACGTGGACG
CCGTCGACTACCTGAGCGGTCAGGCACTTGGACTCGACCGGGACAACGACTAC
ATGAGCGTGCGCGCGCTCCGCTCCCGGACCTCGGCGTAG

Figure A15. ***Orf36*** **DNA sequence from** ***Micromonospora carbonacea*** **var** ***africana*** **(NRRL 15099) (Genbank locus accession: AX574199).**

VAADLRAPLTPAGRTVVDLLAGVIPRISAEAADRDRTGTFPVEAFEQFAKLGLMGATVP
AELGGLGLTRLYDVATALMRLAEADASTALAWHVQLSRGLTLTYEWQHGTPPVRAMA
ERLLRAMAEGEAAVCGALKDAPGVVTELHSDGAGGWLLSGRKVLVSMAPIATHFFVHA
QRRDDDGSVFLAVPVVHRDAPGLTVLDNWDGLGMRASGTLEVVFDRCPVRADELLER
GPVGARRDAVLAGQTVSSITMLGIYAGIAQAARDIAVGFCAGRGGEPRAGARALVAGL
DTRLYALRTTVGAALTNADAASVDLSGDPDERGRRMMTPFQYAKMTVNELAPAVVDD
CLSLVGGLAYTAGHPLSRLYRDVRAGGFMQPYSYVDAVDYLSGQALGLDRDNDYMSV
RALRSRTSA*

Figure A16. ORF36 amino acid sequence (does not include His6 tag).

ATGGAGACGGAACAGGCCCCCCGGCCGGCCGAGCCACCCGGCGACCTGACCACC
GCCATCACCGCGCCAGGTGAACAGCTGCTGACCCTCCTGGACCGGCACCTGCCCC
GGATACGCGCCCAGGCGGCGCCGAACGACCGGGACAGCACCTTCCCCGCCGCGA
CGTTCCACGGCTTCGCGCGCGACGGCGTGCTGGGCGCGACCGTGCCCGCCGAAC
TGGGAGGGATGGGCGTCAGCCGGCTTCACGACGTGGCGGTCGCGCTTTTGCGGG
TCGCCGAGGCGGACGCCTCGACCGCACTGGCCTTGCACGCCCAGTTCAGCCGGG
GAATCACCCTGACATACGAGTGGCTGCACGGCCCGCCGCCGACCCGGAAACTGG
CCGAGCGGCTGCTGCGCGCGATGGCCCGCGGCGAGGCGGTGATCGGCGGCGCG
GTGAAGGACCACGGACGAGAGACCACCCGGCTGCGCCCCGACGGCTCCGGTGGC
TGGCTGCTGTCCGGACGCAAGACTCTGGTGACGATGGCGCCGATCGCGACGCACT
TCGTCGTCTCCGCCCAGGCGCCGGCCGCCGGGGGAACAACGCTGCTGTACGCCC
CCATCGTGGCACGGGACACCCCGGGGCTCTCCATCGTCGACGGATGGACCGGCC
TGGGCATGCGGGCGTCCGGCACGCTCGACGTGGCGTTCGACGACTGCCCGGTGC
CCGCCGGAAACCTGCTGGCGCGTGGCAGCGTCGGCGCGCACAGCGACGCGGCC
CTCGCCGGGCAGGCGGTCAGCTCCGTCGCCATGCTCGGCATCTACGTCGGCGTC
GCCCAGGCCGCCCGCGACCTCGCGGTGGAGACCATGGCCCGGCGGTCGGCCAC
ACCGCCCGCGGCCTCACGCACCCTGGTCGCCGAGACCGAGGCGCGGCTGTACGC
GCTGCGGGCCACCGCATCGGCTGCGCTCGTCAACGTCGACGAACTGTCGCCACGT
CACGACATGGATCCCGATGAGCGCGGCCGGCGGATGATGACCCCGTTCCAGTGC
GCCAAAGTCATGGTCAACCAACTGGCGGCCGCGGTGGTCGACGACTGCCTCACCG
TGGTGGGCGGGGCCACCTACGCGGCGGAGCACCCGCTGGCCCGGCTGTCCCGG
GACGTGCGGGCCGGCCGGTTCATGCAGCCGTACACGTACGCCGACGGGGTCGAC
TACCTGAGCGCCCAGGCGCTCGGTTTGGAAAGAGACAACAACTACGTGAGCCTGC
GGGCCACCCGGCCGGTGGACAGCCGGTGA

Figure A17*. rubN8* DNA sequence from *Streptomyces achromogenese var. rubradiris* (NRRL3061) (Genbank locus accession: AJ871581).

METEQAPRPAEPPGDLTTAITAPGEQLLTLLDRHLPRIRAQAAPNDRDSTFPAATFHGF
ARDGVLGATVPAELGGMGVSRLHDVAVALLRVAEADASTALALHAQFSRGITLTYEWL
HGPPPTRKLAERLLRAMARGEAVIGGAVKDHGRETTRLRPDGSGGWLLSGRKTLVTM
APIATHFVVSAQAPAAGGTTLLYAPIVARDTPGLSIVDGWTGLGMRASGTLDVAFDDCP
VPAGNLLARGSVGAHSDAALAGQAVSSVAMLGIYVGVAQAARDLAVETMARRSATPP
AASRTLVAETEARLYALRATASAALVNVDELSPRHDMDPDERGRRMMTPFQCAKVMV
NQLAAAVVDDCLTVVGGATYAAEHPLARLSRDVRAGRFMQPYTYADGVDYLSAQALG
LERDNNYVSLRATRPVDSR*

Figure A18. RubN8 amino acid sequence (Genbank accession: CAI94696) (does not include His6 tag).

APPENDIX B

SUPPLEMENTARY FIGURES FROM CHAPTER III

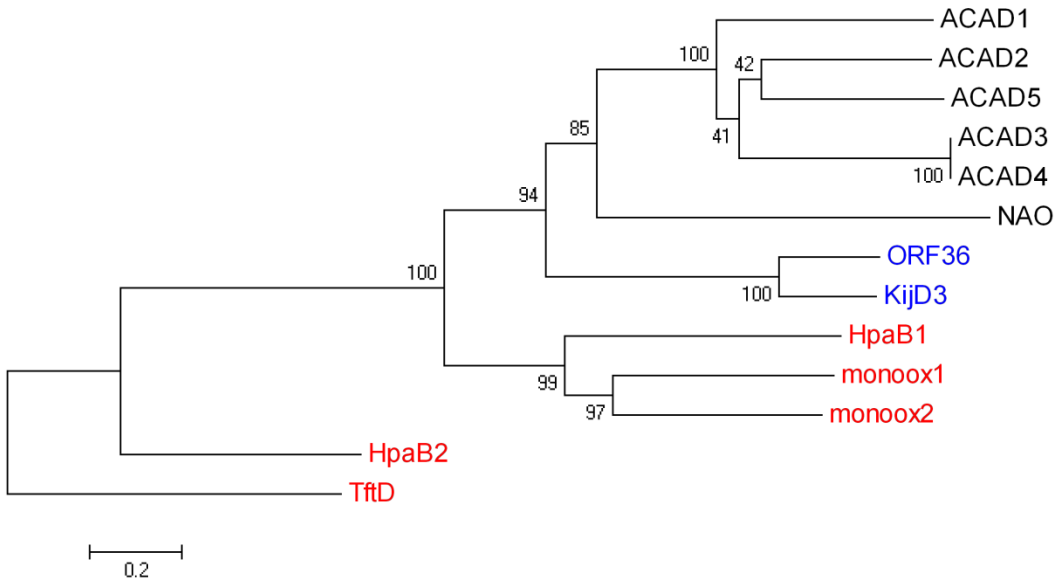

Figure B1. Evolutionary relationships of 13 taxa including nitrososynthases (ORF36 and KijD3), acyl-CoA dehydrogenases (ACADS), and flavincontaining monooxygenases. The evolutionary history was inferred using the Neighbor-Joining method.

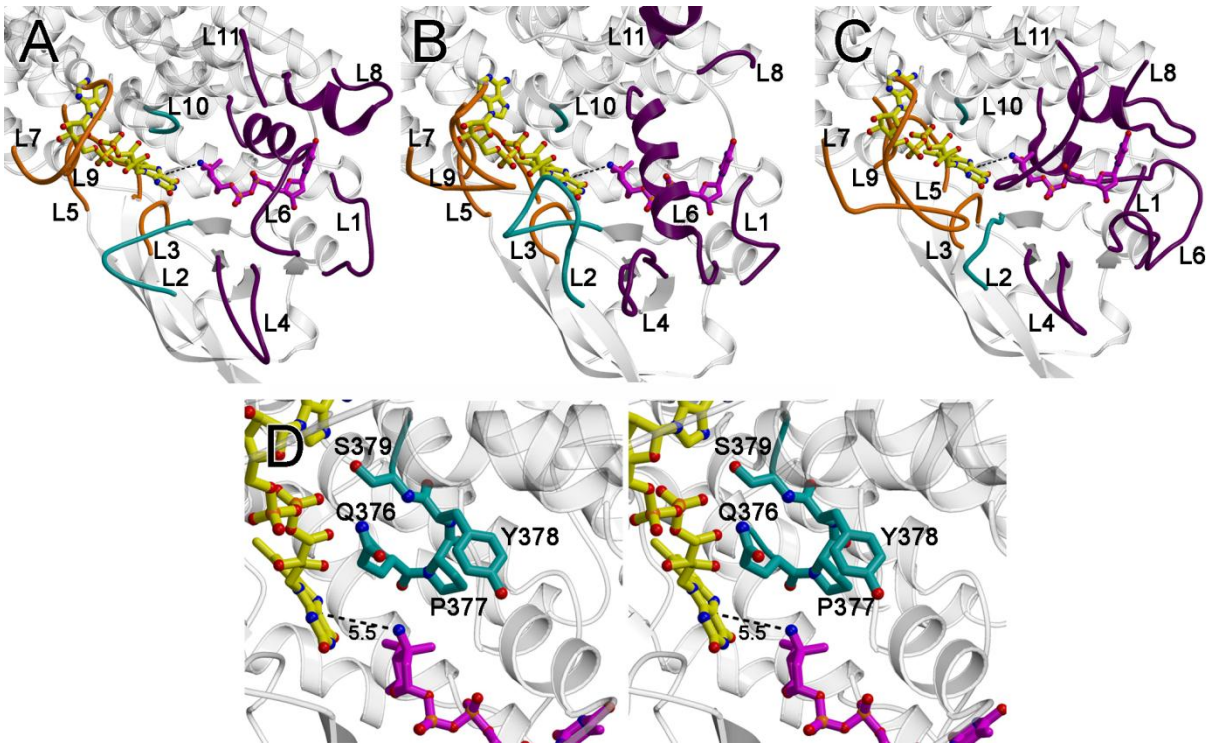

Figure B2. Active site loops. The loops that form the active site are as follows: the loops between α3 and α4 (loop L1; residues 106 – 109), β1 and β2 (loop L2; residues 134-142), β3 and β4 (loop L3, residues 158-164), β4 and β5 (loop L4; residues 178-180), β6 and β7 (loop L5; residues 201-213), β9 and α6 (loop L6; residues 248-253), α6' and α7' (where the ' indicates this is from an adjacent monomer; loop L7; residues 272-280), α7 and α8 (loop L8; residues 310-317), α8' and α9' (loop L9, residues 351-353), α9 and α10, (loop L10; residues 375-379) and at the C-terminus (loop L11; residues 390-412). (A) A ribbon diagram of ORF36 shown with modeled flavin (yellow carbons) and TDP-L-evernosamine (magenta carbons) as sticks. Active site loops L3, L5, L7, and L9, are predicted to interact with flavin and are colored orange, active site loops L1, L4, L6, L8, and L11 are predicted to interact with substrate and are colored purple, and active site loops L2 and L10 are predicted to interact with both substrate and cofactor and are colored teal. (B) A ribbon diagram of human short branched-chain acyl Co-A dehydrogenase (PDB entry 2JIF) (*1*), highlighting loops L1 to L11 colored are colored as in (A). (C) A ribbon diagram of *A. baumannii* 4-hydroxyphenylacetate monooxygenase (PDB entry 2JBT) highlighting loops L1 to L11 colored as in (A). (D) Stereoview of the ORF36 loop L10 containing a tandem cis-peptide. Loop L10 is shown in sticks with teal carbons. The Q376-P377 and P377-Y378 bonds both adopt a cis conformation. Modeled flavin and substrate are displayed as in (A).

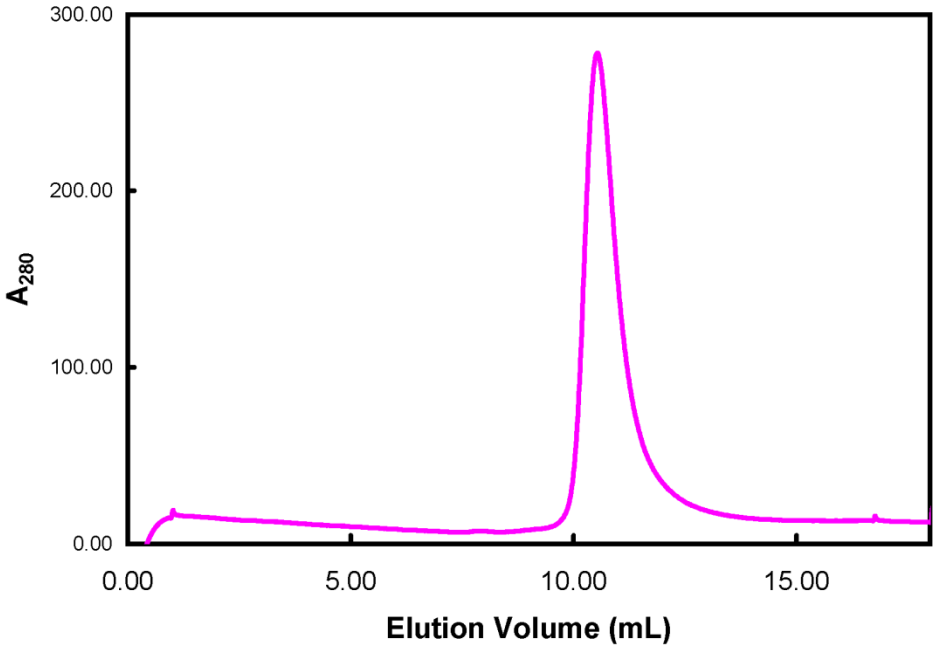

Figure B3. Size exclusion chromatogram of ORF36. Size exclusion chromatography of ORF36 on a Superdex S-200 column resulted in a single, monodisperse peak. The 10.8 mL elution volume corresponds to an approximate molecular weight of 185 kD, which is consistent with the 176 kD calculated for a tetramer.

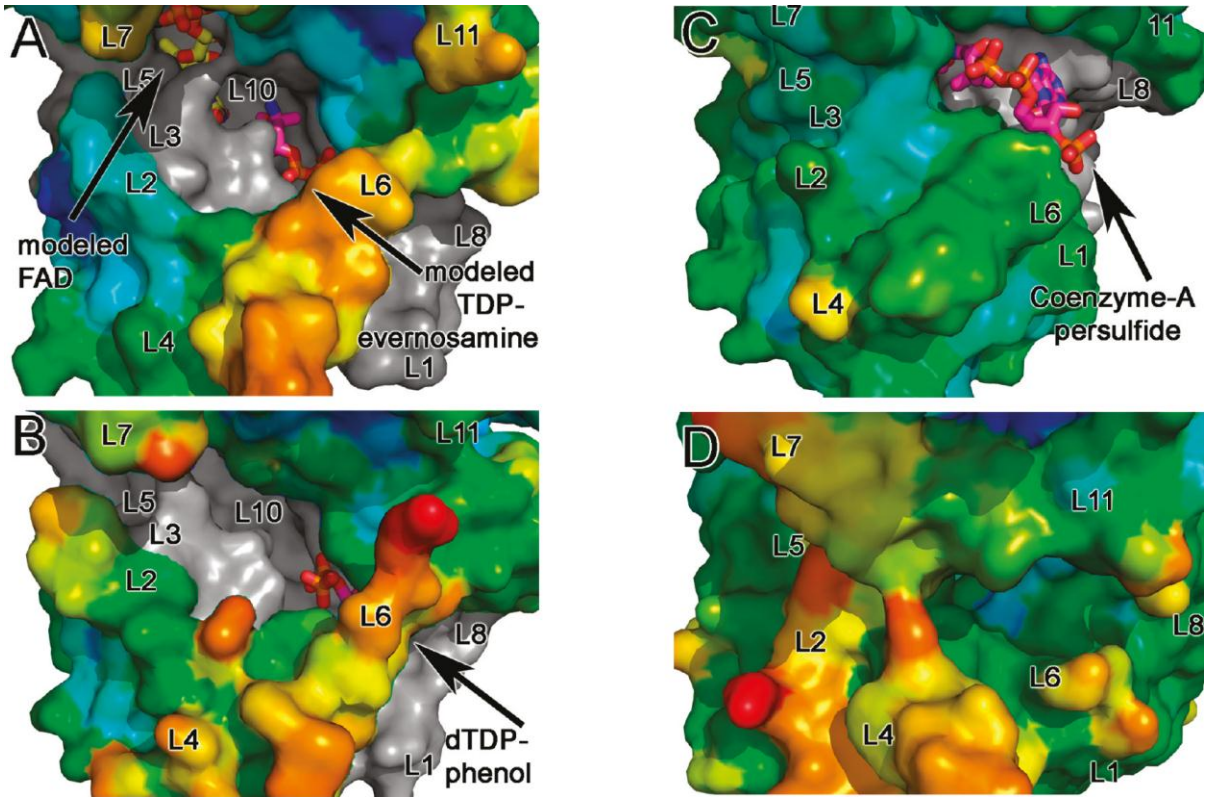

Figure B4. Surface representation of the active site clefts of nitrososynthases, acyl-CoA dehydrogenases, and flavin-containing monooxygenases are shown colored by B-factor. Active site loops are labeled L1-L11. Surfaces of each enzyme are shown colored using a rainbow color ramp in which red corresponds to the highest B-factor and blue corresponds to the low B-factor. Areas of the surface that form the base of the active site cleft are shown in grey. Substrates and co-factors are shown as sticks with atoms colored as follows: FAD: carbons, yellow, oxygen, red; nitrogen, blue; phosphate, orange; TDP-L-evernosamine, dTDP, CoenzymeA persulfide: carbons, magenta; oxygen, red; nitrogen, blue; phosphate, orange. (A) ORF36. Modeled FAD and TDP-L-evernosamine are displayed as sticks. In this orientation, loop L9 is concealed. The B factor color ramp gradient minimum and maximum values are 70 and 180 Å^2, respectively, and for this structure, the Wilson B is 111.2 Å^2 with an average protein B factor of 115.3 Å^2. (B) KijD3 (PDB entry 3M9V) with the dTDP of dTDP-phenol displayed as sticks. As in (A), loop L9 is concealed. The B factor color ramp minimum and maximum values for this panel are 10 and 80 Å^2, and the average protein B value is 27.6 Å^2. The Wilson B factor was not reported. (C) Human short/branched-chain acyl-CoA dehydrogenase (PDB entry 2JIF). The FAD molecule is concealed by the protein surface in this orientation, and coenzymeA persulfide is shown in stick representation. Loops L9 and 10 are concealed in this orientation. The B factor color ramp gradient has minimum and maximum values of 14 and 60 Å^2, the Wilson B is 25.84 Å^2 and the average protein B factor is 22.76 Å^2. (D) *A. baumannii* 4-hydroxyphenylacetate monooxygenase (PDB entry 2JBR). FMN, 4-hydroxyphenylacetate, and loops L3, L9 and L10 are concealed in this orientation. The B factor color ramp gradient minimum and maximum values are 40 and 90 Å^2, and the average protein B value is 56.77 Å^2. The Wilson B factor was not reported.

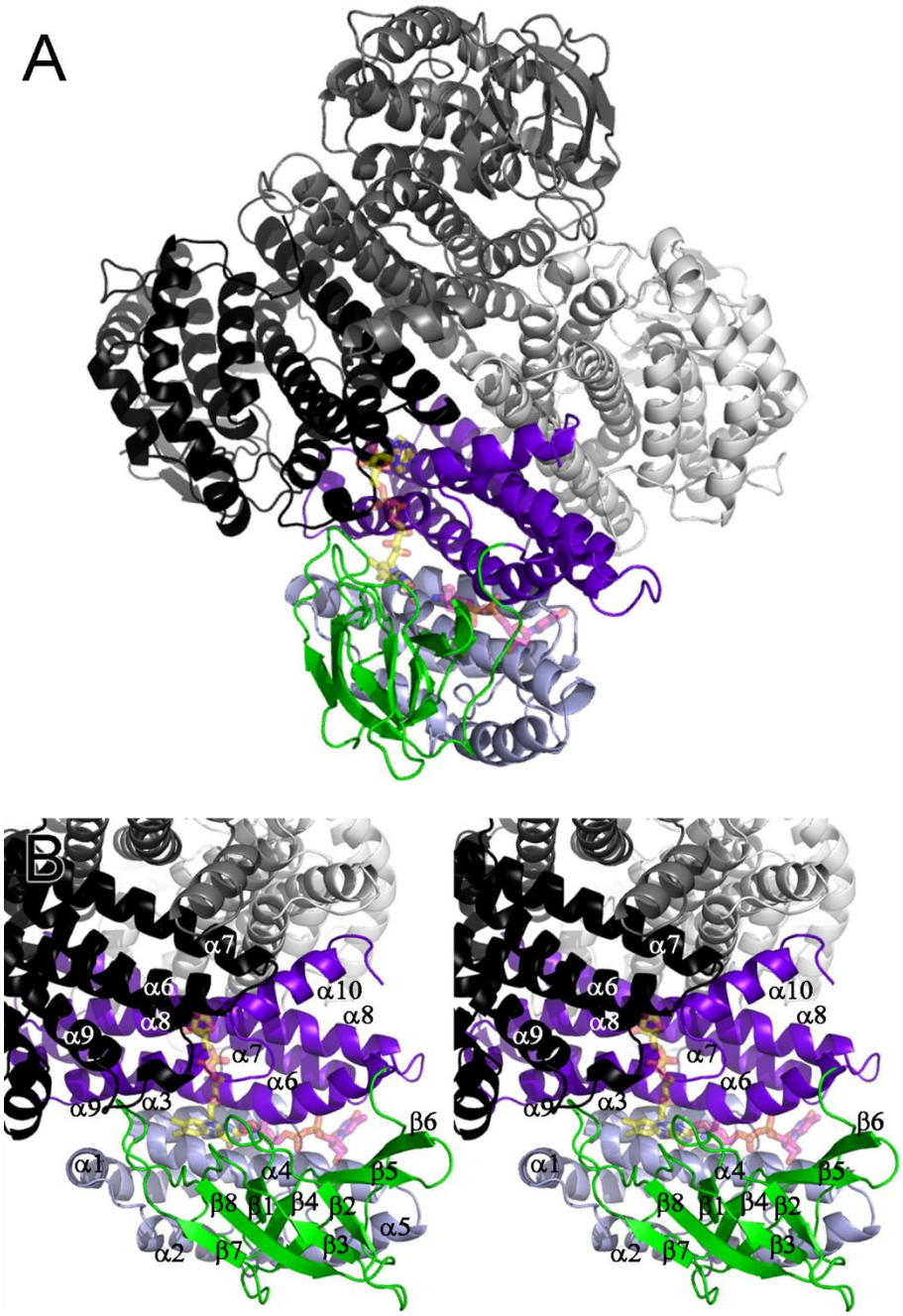

Figure B5. Location of the FAD and TDP-L-evernosamine molecules modeled within ORF36 active site. Chain A of ORF36 is shown colored by domain as in Figure III-2. Chains B, C and D are colored white, black and grey, respectively. The modeled small molecules (shown as transparent sticks) are colored as follows: FAD, yellow carbons, TDP-L-evernosamine, magenta carbons, oxygen, red; nitrogen, blue; sulfur, gold; phosphorus, orange. (A) The physiologically relevant tetramer, with modeled ligands shown at one active site. (B) A closer view of the labeled ORF36 monomer, shown in stereo. The monomer is shown in the same orientation as in Figure 5b, with the other three chains of the tetramer colored as in (A). Selected secondary structural elements from chain C are labeled in white text.

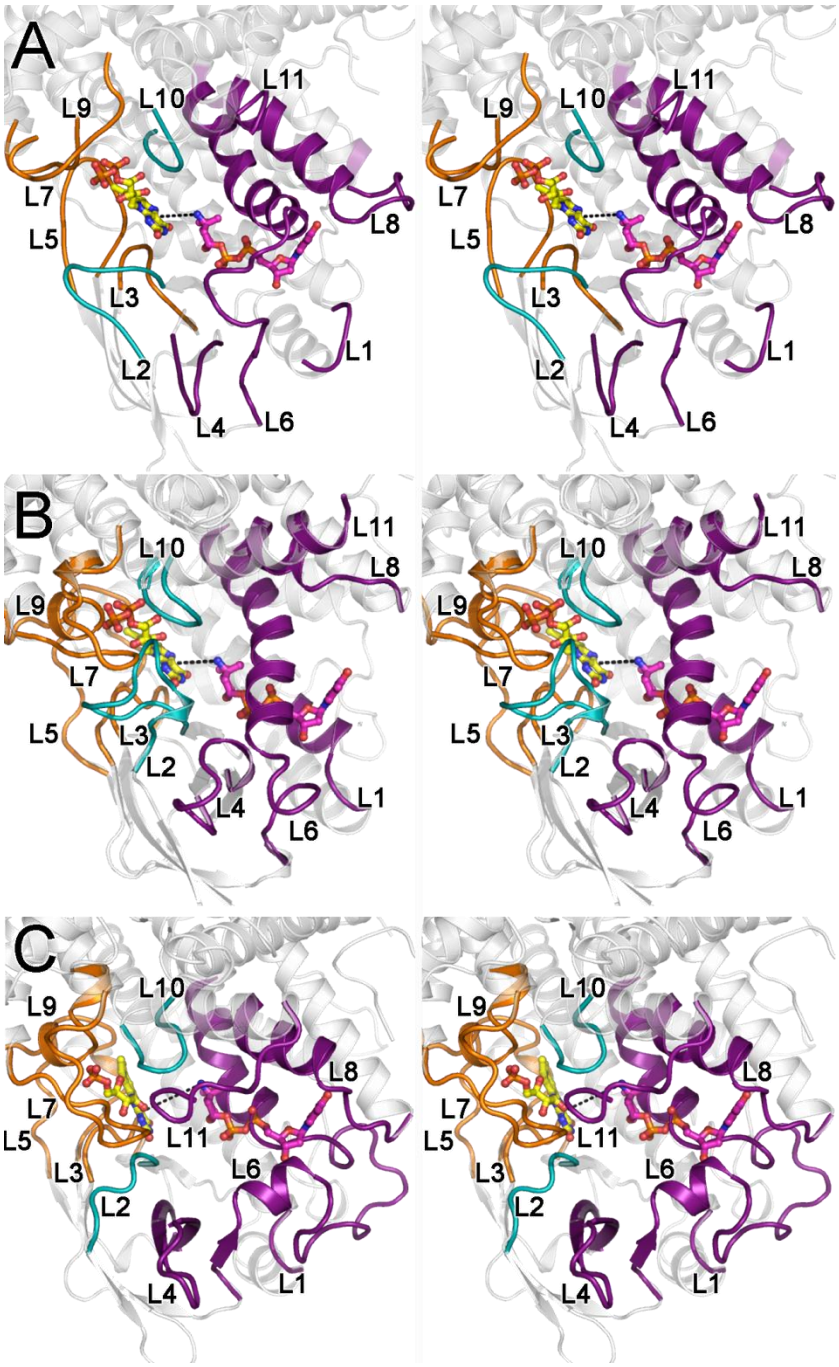

Figure B6. Stereoview diagrams depicting the active site loops. Panel (A) shows the ORF36 active site loops, displayed as in Figure 7a. (B) Human short branched-chain acyl Co-A dehydrogenase active site, displayed as in Figure B2b. (C) *A. baumannii* 4-hydroxyphenylacetate monooxygenase displayed as in Figure B2.

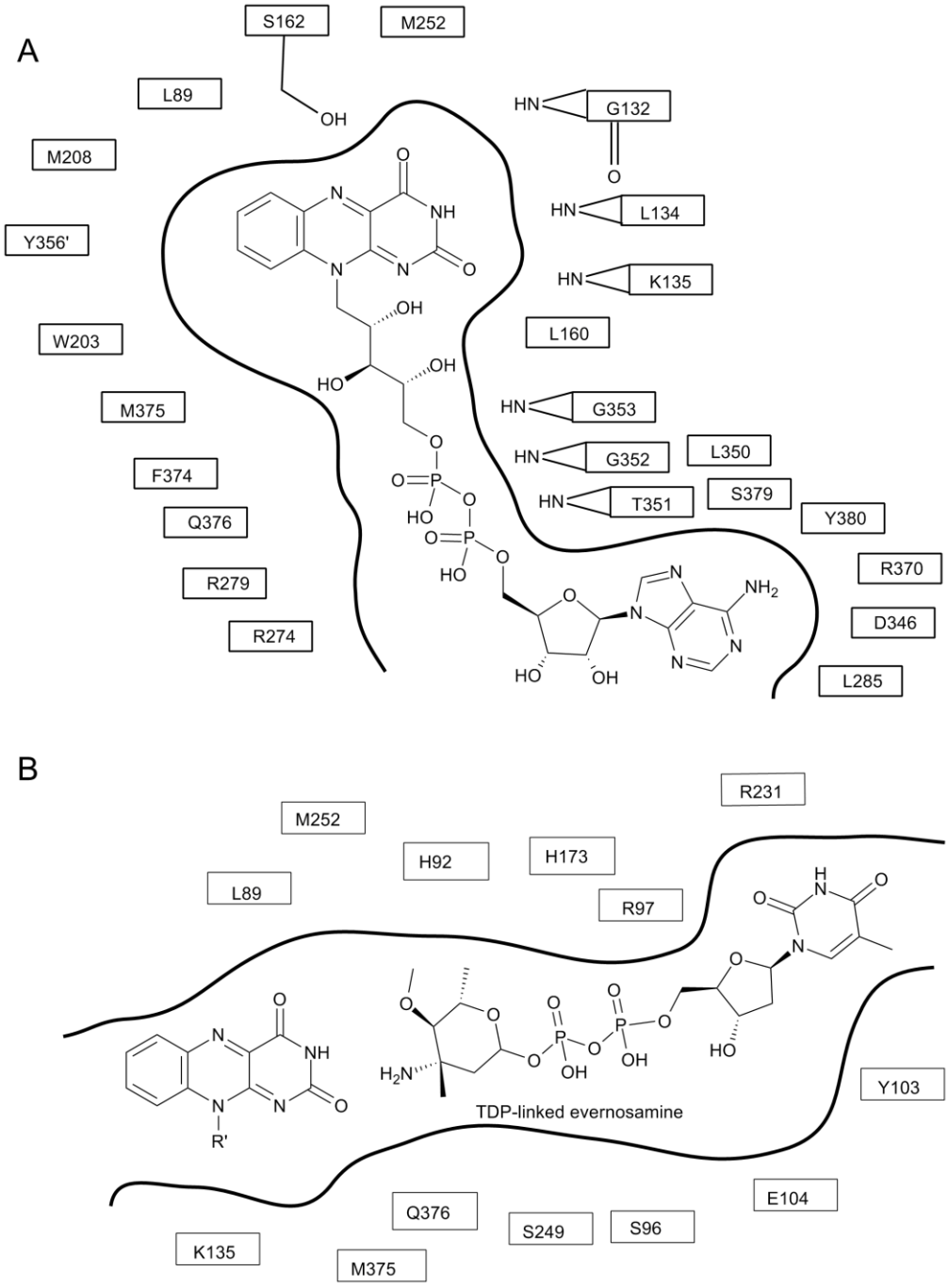

Figure B7. Schematic diagram of the active site. (A) Residues lining the putative FAD binding site are diagrammed. (B) Residues in the vicinity of the modeled FAD cofactor and TDP-L-evernosamine substrate are shown. R' = the ribityl diphosphonucleotide of the modeled FAD cofactor.

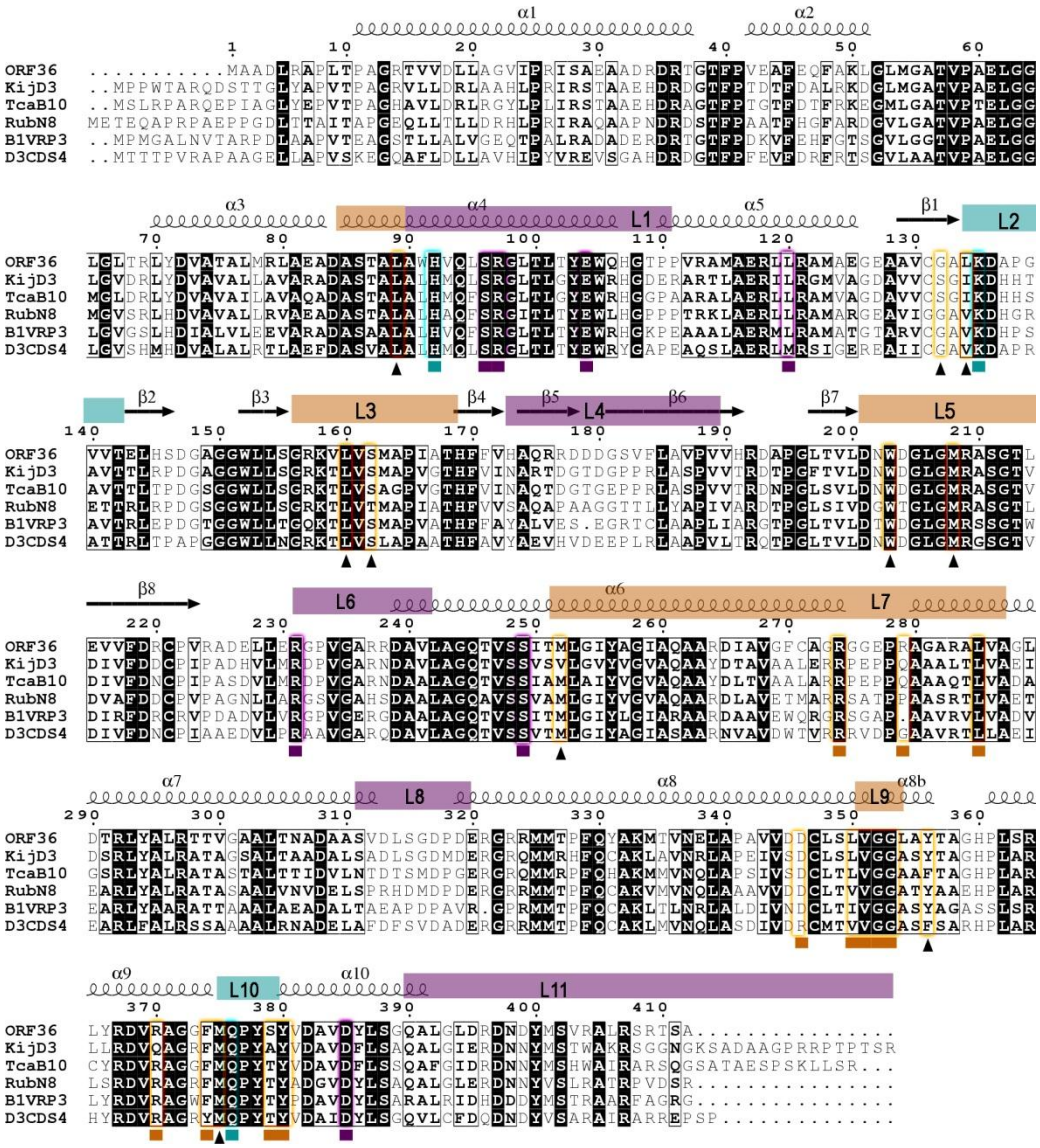

Figure B8. Sequence alignment of ORF36 and putative nitrososynthases. Strictly conserved residues are highlighted in black and residues with >70% similarity are boxed. Residues near the intersection of modeled isoalloxazine and TDP-L-evernosamine are boxed in teal and marked with a teal square; residues near the isoalloxazine of modeled FAD are boxed in orange and marked with black triangles; residues near the nucleotide of modeled FAD are boxed in orange and marked with orange squares; and residues near the modeled TDP-L-evernosamine are boxed in purple and marked with purple squares. Secondary structural elements and loops L1-L11 are marked above the alignment and highlighted orange (areas involved in flavin binding), purple (areas likely involved in substrate binding) or teal (areas located near the intersection of the putative flavin and substrate binding sites). Sequences aligned with ORF36 are: KijD3 (UniProtKB ID B3TMR1); TcaB10 from the tetrocarcin A biosynthetic pathway of *M. chalcea* (UniProtKB ID B5L6K4); RubN8 from the rubradirin biosynthetic pathway of (UniProtKB ID Q2PC69); B1VRP3, uncharacterized protein from *S. griseus*; D3CDS4, uncharacterized protein from *Micromonospora* sp. L5. These proteins were identified by a BLAST search of the ORF36 sequence (UniProtKB ID B5APQ9) and all had scores > 450 and E-values of less than $1x10^{-125}$. Sequences were aligned using ClustalW, and the figure was generated using ESPript.

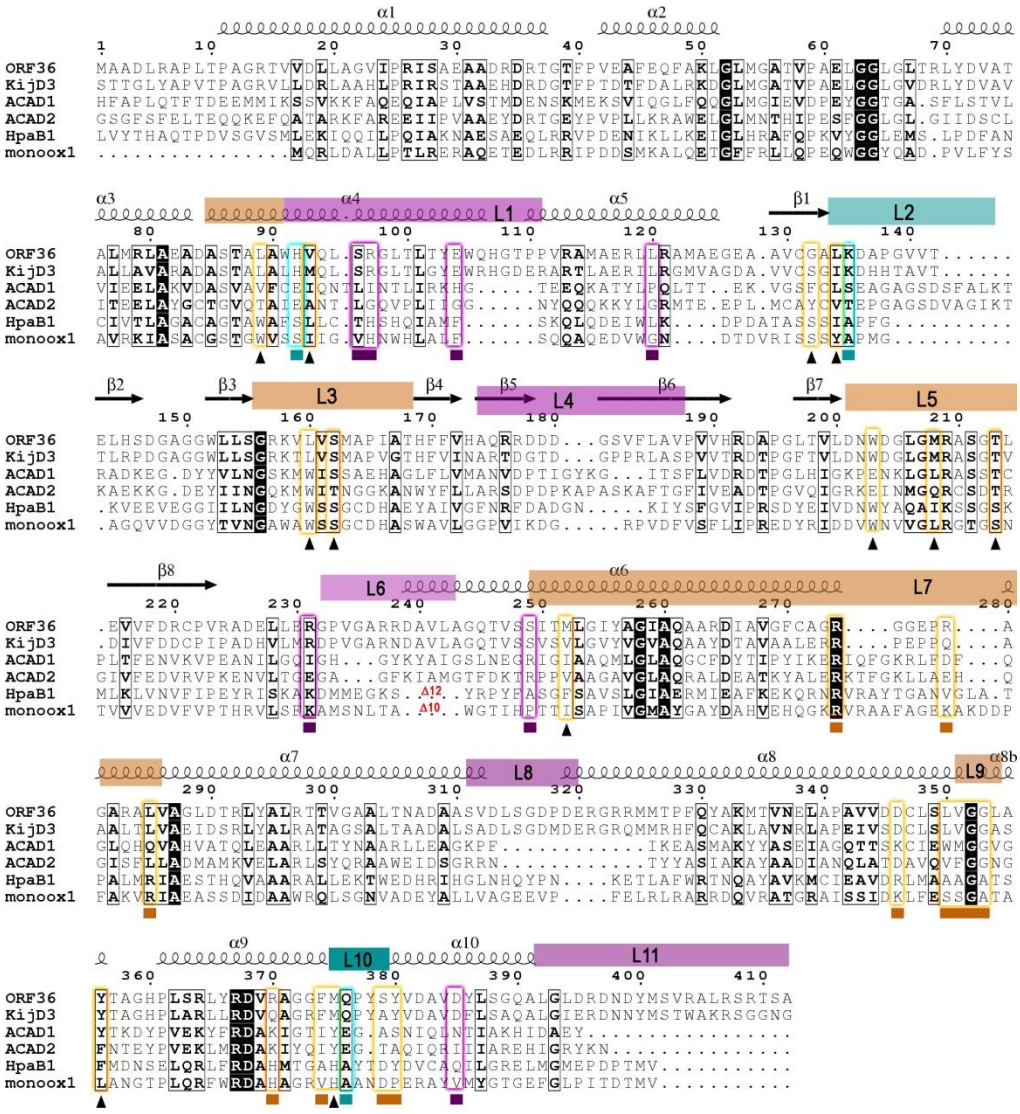

Figure B9. Sequence alignment of ORF36, KijD3, selected acyl-coA dehydrogenases, and selected Class D flavin monooxygenases. Loops and residues at the active site are highlighted as in Supplemental Figure S4. Of particular interest are the residues involved in the isoalloxazine binding site. For clarity, select divergent portions of individual sequences were truncated and are denoted with red lettering. Sequences aligned with ORF36 are: KijD3 (UniProtKB ID B3TMR1); ACAD1, short branched-chain acyl-coA dehydrogenase (*H. sapiens*), 2JIF; ACAD2, medium-chain acyl-coA dehydrogenase (*S. scrofa*), PDB entry 3MDE; HpaB1, 4-hydroxyphenylacetate monooxygenase (*A. baumannii*), PDB entry 2JBT; monoox1, 3-hydroxy-9,10-seco-nandrost-1,3,5(10)-triene-9,17-dione hydroxylase (*Rhodococcus* sp Rha1), PDB entry 2RFQ.

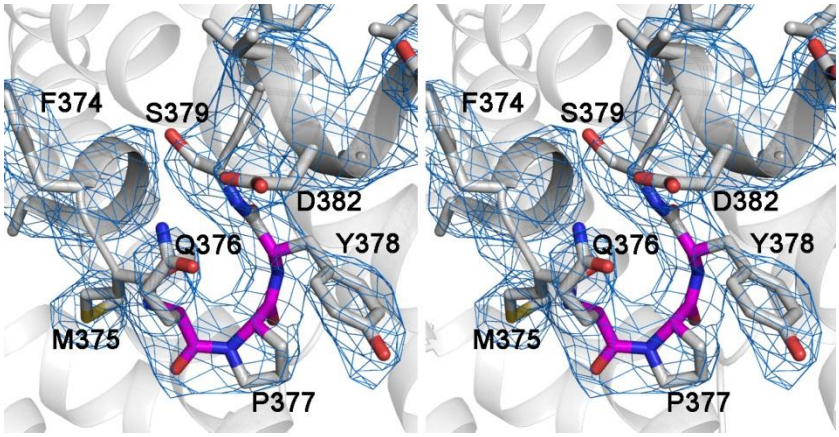

Figure B10. Stereoview of electron density for the tandem cis-peptide in L10 of ORF36. The protein chain is depicted as light grey cartoons. $2F_o$-F_c electron density is shown in blue for residues 372-389, which encompasses the two sequential cis-peptides between Gln376-Pro377 and Pro377-Tyr378. Those residues in loop L10 are shown in stick representation, and the main chain carbon atoms of the cis-peptides are highlighted in magenta.

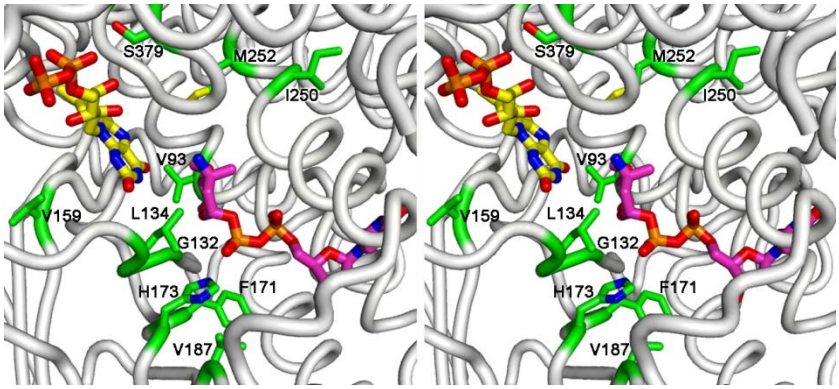

Figure B11. Stereoview of the ORF36 active site, with the protein shown in putty cartoon representation in the same orientation as Figure 7A. Modeled flavin and substrate are shown as thick sticks colored as in Figure 5. Selected residues within 5.5 Å of the flavin cofactor or L-evernosamine that are differ between ORF36 and KijD3 are colored with green carbons, shown in stick representation and labeled according to ORF36 numbering.

APPENDIX C

MS AND MS/MS SPECTRA FROM CHAPTER IV

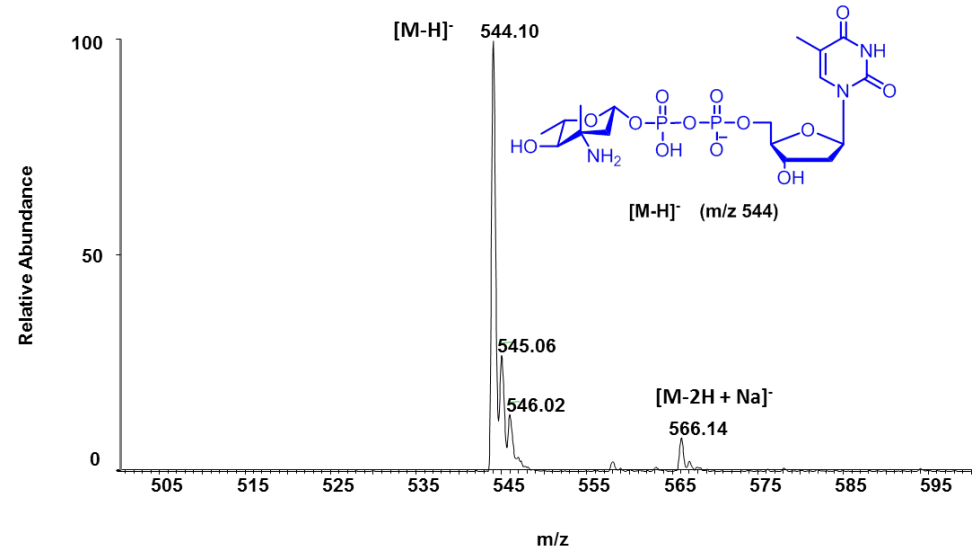

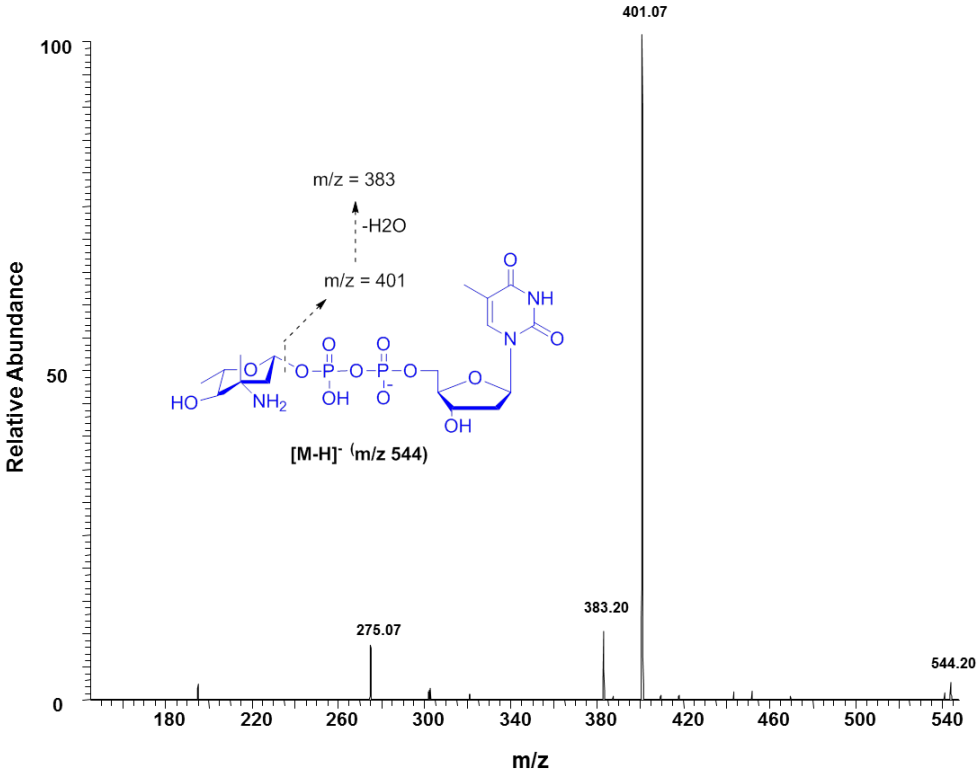

Figure C1. MS (above) and MS/MS (below) of the substrate (starting material) TDP-L-*epi*- vancosamine.

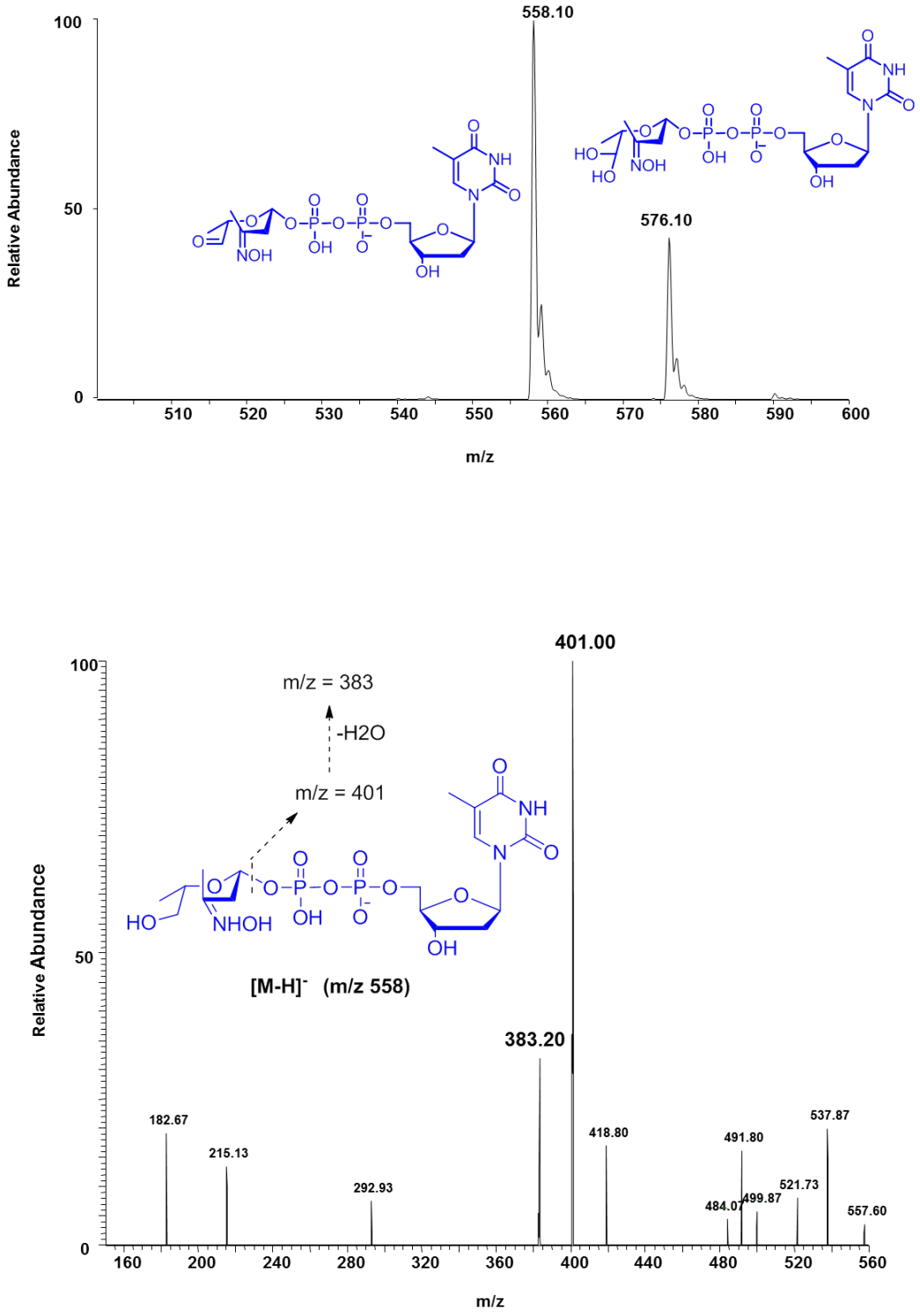

Figure C2. MS of the oxime-aldehyde species (m/z 558) and its hydrate (m/z 576) produced from the monooxygenation/retro-aldol activity of DnmZ with TDP-L-*epi*- vancosamine (above), and MS/MS of the oxime-aldehyde species (m/z 558) (below).

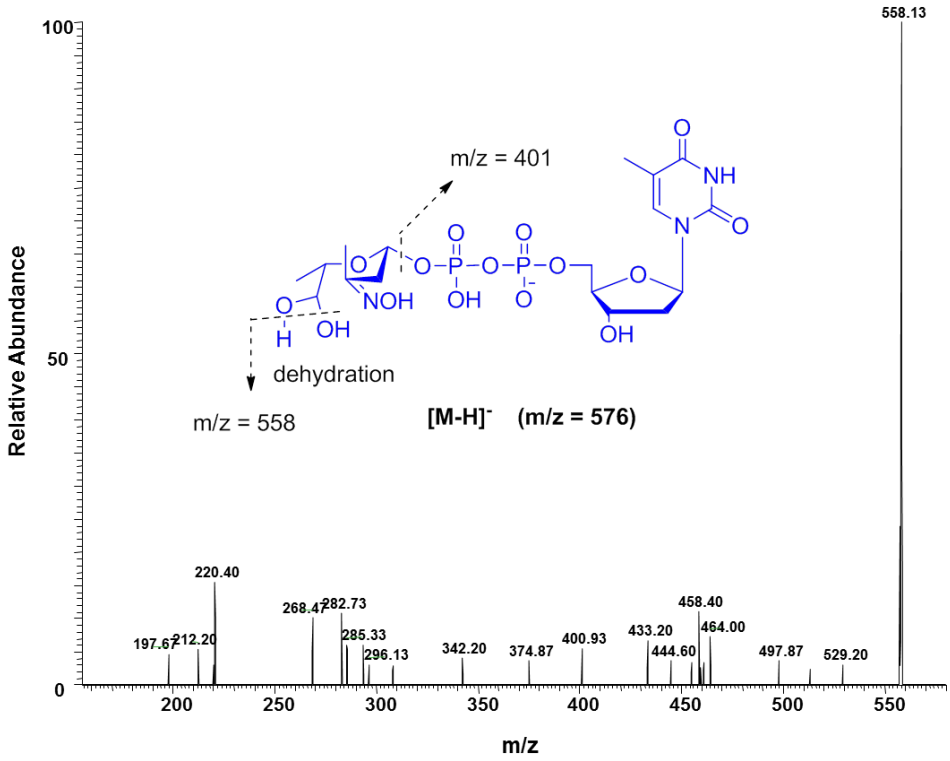

Figure C3. MS/MS of the oxime-aldehyde species (m/z 576) produced from the oxidation/retro-aldol activity of DnmZ withTDP-L-*epi*- vancosamine.

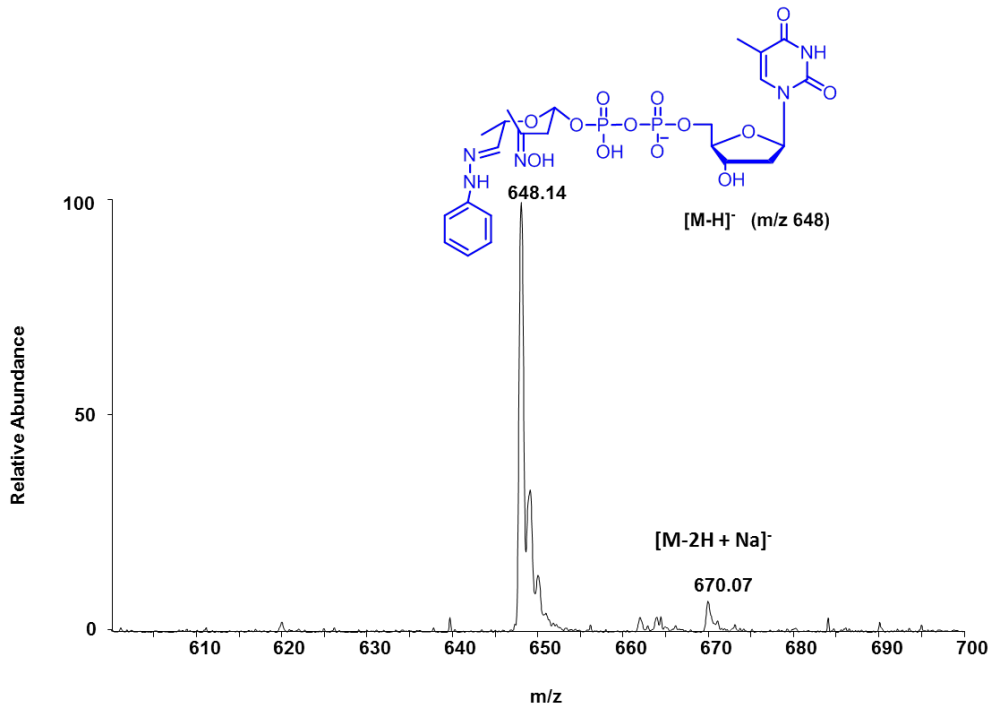

Figure C4. MS of the phenylhydrazone derivative (m/z 648) produced from the reaction of the corresponding oxime-aldehyde with phenylhydrazine.

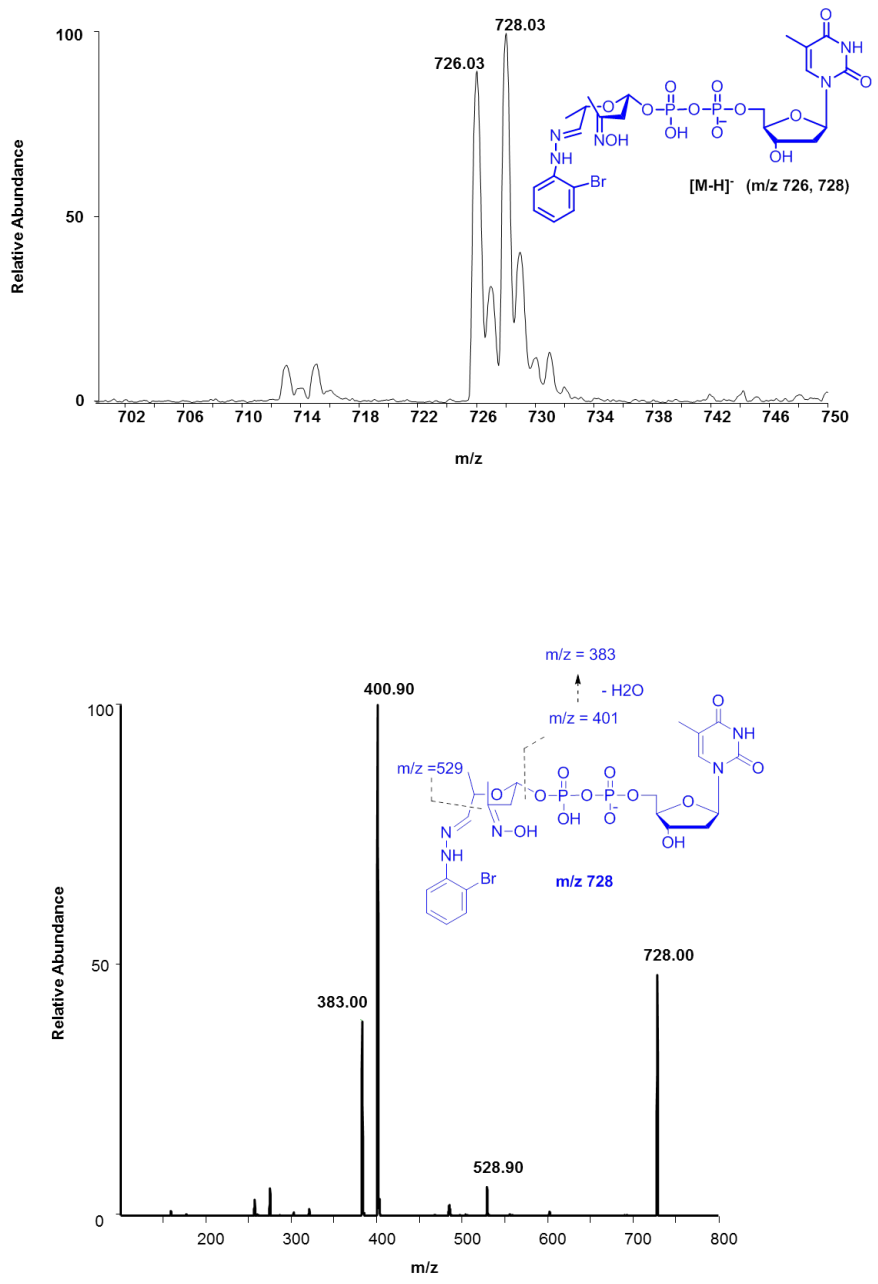

Figure C5. MS of the 2-bromophenylhydrazone derivative (m/z 726, 728) produced from the reaction of the corresponding oxime-aldehyde with 2-bromophenylhydrazine (above), and the MS/MS of the hydrazone species of m/z 728 (below).

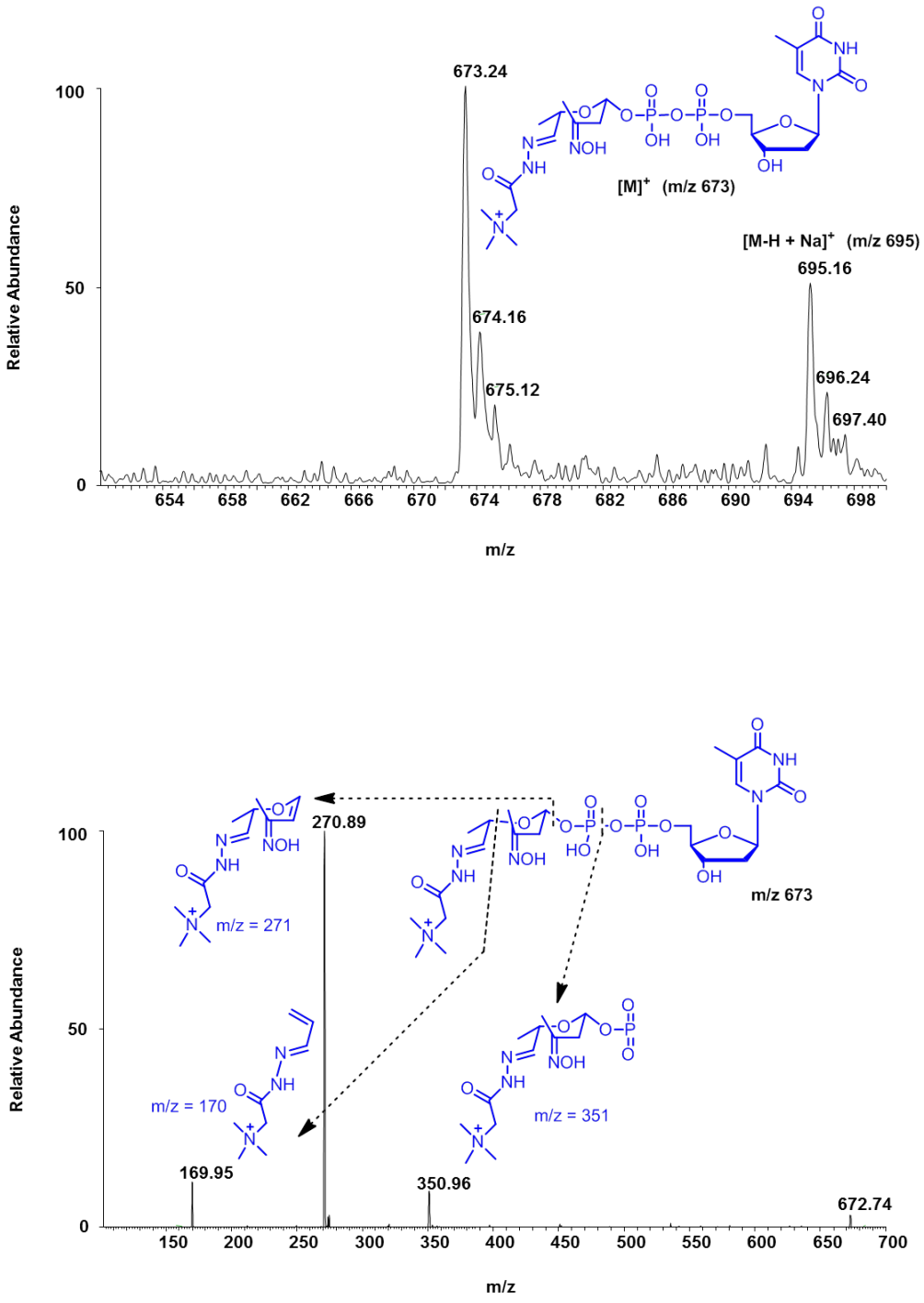

Figure C6. MS of the (Carboxymethyl)trimethylammonium (GirT) hydrazone derivative (m/z 673) produced from the reaction of the corresponding oxime-aldehyde with GirT hydrazine (above), and the MS/MS of the same species (below). Both analyses were performed in the positive mode.

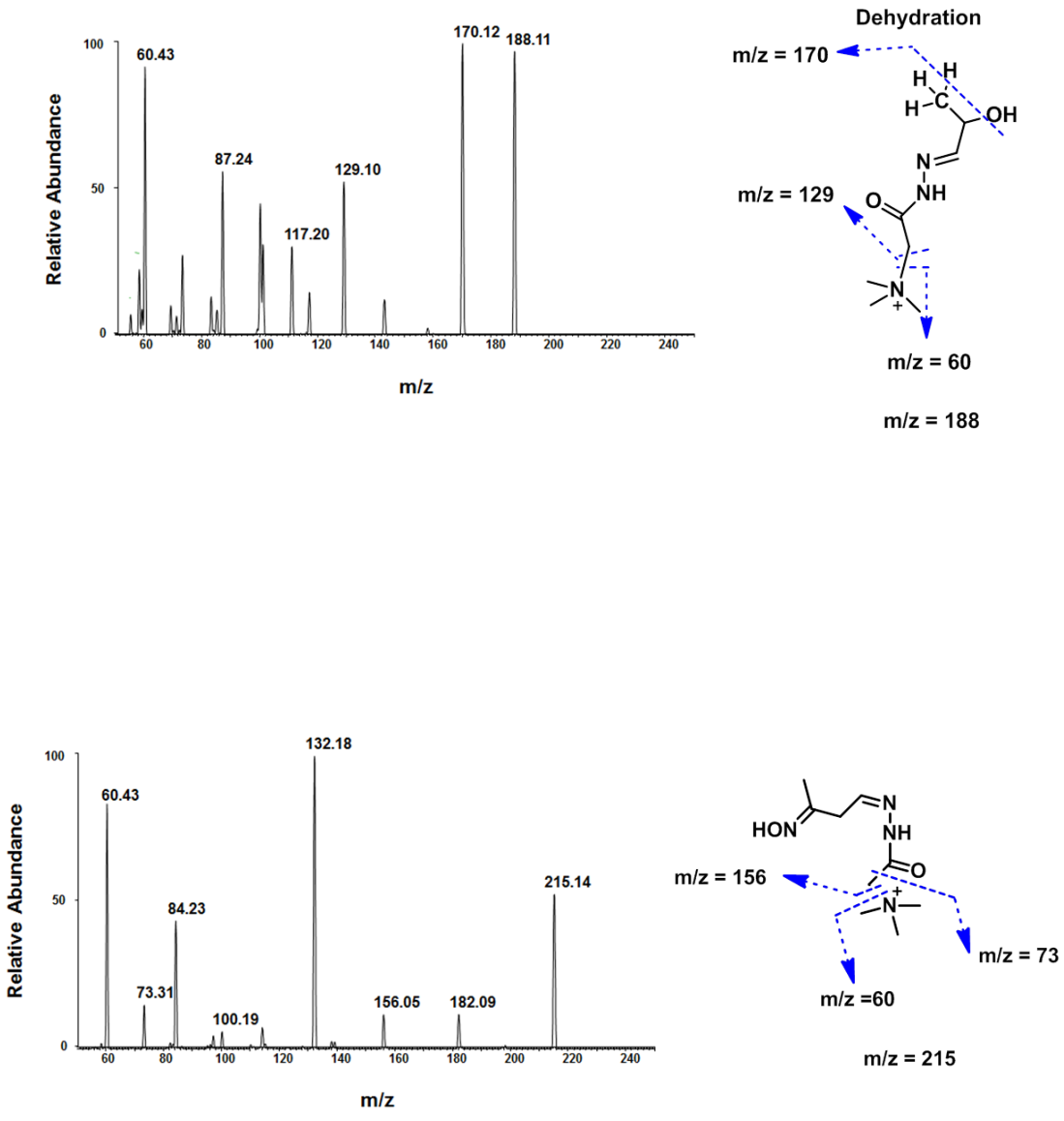

Figure C7. MS/MS of the acid hydrolysis fragments of m/z 188 (above), and m/z 215 (below) produced from the treatment of the (Carboxymethyl)trimethylammonium (GirT) hydrazone with HCl (1 M).